



International Symposium
on
Ligaments and Tendons-XV

Disney's Coronado Springs Resort

Orlando, FL

March 4, 2016

Edited by:

Zong-Ming Li, Ph.D. (Co-Chair)

Patrick Yung, M.D. (Co-Chair)

David T. Corr, Ph.D. (Program Chair)

Bruma Sai-Chuen Fu, Ph.D. (Special Session Chair)

Savio L-Y. Woo, Ph.D., D.Sc., D.Eng. (Honorary Chair)

Volume 15

ISL&T-XV Sponsors

We gratefully acknowledge our kind sponsors. They contribute to the greatness of the meeting.



Musculoskeletal
Research Center



Asian American Institute
for Research & Education



Rensselaer



香港中文大學
THE CHINESE UNIVERSITY OF HONG KONG

Volume 15

Table of Contents

Welcome by Drs. Zong-Ming Li and Patrick Yung.....	2
ISL&T-XV Committees.....	3
ISL&T-XV Awards.....	4
Instructions to Presenters.....	8
ISL&T-XV Program	
● Podium Sessions.....	9
● Poster Presentations.....	14
ISL&T-XV Abstracts	
● Savio L-Y. Woo Young Researcher Award Winners.....	15
● Podium Presentations.....	29
● Clinical Keynote Lecture.....	30
● Session I: Biomechanics I – Healing Ligament and Tendon/ In Vivo Assessment....	31
● Session II: Tendon Mechanobiology and Stem Cells.....	39
● Session III: Tissue Engineering in ACL Repair.....	44
● Session IV: Inflammation and Tendon Healing.....	47
● Special Session: Translational Tendon and Ligament Research – In Honor of Professor Kai-Ming Chan.....	51
● Session V: Biomechanics II – Theoretical and Computational Modeling.....	60
● Session VI: Rotator Cuff Injury and Repair.....	64
● Poster Presentations.....	68

WELCOME

TO THE MAGIC KINGDOM OF LIGAMENTS AND TENDONS

Zong-Ming Li, PhD, Co-Chair
Patrick Yung, MD, Co-Chair

We are delighted to welcome you to the Fifteenth International Symposium on Ligaments and Tendons (ISL&T-XV). This ISL&T gathering is very special because after 15 years, we return to this “magic” location where the inaugural ISL&T took place in Orlando, Florida, in 2000.

The prime goal of the ISL&T has been to promote ligament and tendon research by providing a forum for presenting the very best research in our field. The symposium series has placed an emphasis on bringing together bioengineers, biologists, and clinician scientists to stimulate thought-provoking discussions on current research and future collaborations. Throughout these years, ligament and tendon research continues to expand in quantity and improve in quality.

This year’s International Program Committee, led by Dr. David Corr of Rensselaer Polytechnic Institute, has put together what is sure to be an enriching day, full of outstanding scientific presentations. The research topics that will be covered include various 1) ligamentous/tendinous structures (e.g. ACL, rotator cuff, transverse carpal ligament), 2) approaches (e.g. biomechanics, mechanobiology, injury and healing mechanisms, tissue repair and engineering, cell therapy, surgical repair), and 3) models (e.g. cadaver, human, animal, computation). The program also features a special session on Translational Tendon and Ligament Research in honor of Professor Kai-Ming Chan of the Chinese University of Hong Kong. We anticipate active discussions among seasoned and junior investigators about the current hot topics and future challenging avenues of research. We also congratulate the outstanding young investigators on winning the Savio L-Y. Woo Young Researcher Awards and the other symposium awards.



Zong-Ming Li, Ph.D.



Patrick Yung, M.D.

We extend our gratitude to Professor Savio L-Y. Woo, Honorary Co-Chair of this 15th symposium, for establishing and fostering the ISL&T as an exceptional platform for investigators to share and discuss tendon and ligament research. We acknowledge the members of the International Advisory Committee and the International Program Committee for their contributions to the success of ISL&T. We appreciate the sponsorship from individuals, corporations, and institutions; this symposium and its many functions are made possible by their generosity. A special thank-you goes to our hard-working support team for superb organization of this event.

We hope our symposium here in Orlando continues to fuel your excitement on your paths to discoveries in ligament and tendon research, and wish you the best in finding your own “Keys to the Kingdom.”

Once again, welcome!

ISL&T-XV Committees

CHAIRS

Zong-Ming Li, Ph.D. (Co-Chair)

Patrick Yung, M.D. (Co-Chair)

Savio L-Y. Woo, Ph.D., D.Sc., D.Eng. (Honorary Chair)

PROGRAM COMMITTEE CHAIR

David T. Corr, Ph.D.

SPECIAL SESSION CHAIR

Bruma Sai-Chuen Fu, Ph.D.

INTERNATIONAL PROGRAM COMMITTEE

Paul Ackermann, M.D., Ph.D. (Europe)

Alex Almarza, Ph.D. (North America)

Mahmut Nedim Doral, M.D. (Europe)

Matthew Fisher, Ph.D. (North America)

Braden Fleming, Ph.D. (North America)

Bruma Sai-Chuen Fu, Ph.D. (Asia)

Kevin Hildebrand, M.D. (North America)

Wei-Hsiu Hsu, M.D. (Asia)

Alice Huang, Ph.D. (North America)

Catherine Kuo, Ph.D. (North America)

Michael Lavagnino, Ph.D. (North America)

Thay Q. Lee, Ph.D. (North America)

Guoan Li, Ph.D. (North America)

Helen Lu, Ph.D. (North America)

Joo Han Oh, M.D. (Asia)

Hong-Wei Ouyang, M.D., Ph.D. (Asia)

Scott Rodeo, M.D. (North America)

Hazel Screen, Ph.D. (Europe)

Jason Shearn, Ph.D. (North America)

Roger Smith, Ph.D. (Europe)

Lou Soslowsky, Ph.D. (North America)

Stavros Thomopoulos, Ph.D. (North America)

Ray Vanderby, Jr, Ph.D. (North America)

James Wang, Ph.D. (North America)

Ed Wojtys, M.D. (North America)

Chunfeng Zhao, M.D. (North America)

INTERNATIONAL ADVISORY COMMITTEE

Savio L-Y. Woo, Ph.D., D.Sc., D.Eng. (North America) - Chair

Tom Andriacchi, Ph.D. (North America)

Steven Arnoczky, D.V.M. (North America)

Albert Banes, Ph.D. (North America)

David Butler, Ph.D. (North America)

Giuliano Cerulli, M.D. (Europe)

Kai-Ming Chan, M.D., Ph.D. (Asia)

Chih-Hwa Chen, M.D. (Asia)

David T. Corr, Ph.D. (North America)

Mahmut Nedim Doral, M.D. (Europe)

James Goh, Ph.D. (Asia)

Catherine Kuo, Ph.D. (North America)

Thay Q. Lee, Ph.D. (North America)

Guoan Li, Ph.D. (North America)

Zong-Ming Li, Ph.D. (North America)

Helen Lu, Ph.D. (North America)

Christos Papageorgiou, M.D., Ph.D. (Europe)

Per Renstrom, M.D. (Europe)

Louis Soslowsky, Ph.D. (North America)

Stavros Thomopoulos, Ph.D. (North America)

Ray Vanderby, Jr., Ph.D. (North America)

James Wang, Ph.D. (North America)

Jennifer Wayne, Ph.D. (North America)

ADMINISTRATIVE SUPPORT

Ms. Diann DeCenzo

Ms. Jonquil R. Mau

Dr. Kathryn Farraro

Ms. Wancy Lo

Ms. Tamara Marquardt

Ms. Gina Wong

ISL&T-XV Awards

We established awards to stimulate high quality scientific research by investigators in the study of ligaments and tendons. The awardees are selected by members of the program committee/moderators based on the quality of the abstract and presentation as well as the overall merit of the study.

Savio L-Y. Woo Young Researcher Award

Award: up to \$1,000 (USD) and Certificate (up to 4)

Purpose: Professor Savio L-Y. Woo founded the International Symposium on Ligaments and Tendons (ISL&T) to promote awareness of the field, the exchange of information, and collaboration both nationally and internationally. The ISL&T has been a venue for lively discussion of current topics in connective tissue research and clinical applications. In addition to his leadership and significant scientific contributions to our field, Professor Woo has been an internationally recognized intellectual ambassador for training, mentoring, and for inspiring students in the field of biomedical engineering and orthopaedic surgery. We are honored to present the Savio L-Y. Woo Young Researcher Award to individuals who perform the best research in three major areas: biomechanical, biological and translational/clinical and have submitted their work to the ISL&T meeting.

The Award is intended to provide partial support (up to \$1,000) towards the applicant's research or for travel expenses to attend the ISL&T-XV meeting. Up to four awards will be given.

Eligibility: Open to graduate students and post-doctoral fellows. Applicant must be the first and presenting author of the abstract and be present at the ISL&T meeting and banquet to accept the award. Advisor's verification of eligibility letter is required.

Award Committee

Albert Banes, Ph.D. (Chair)

Thay Q. Lee, Ph.D.

Per Renstrom, M.D.

Stavros Thomopoulos, Ph.D.

Patrick Yung, M.D.

Jonquil R. Mau, M.S. (Assistant)

Acknowledgements: Sponsored by Flexcell International Corporation

Past Recipients of the Savio L-Y. Woo Young Researcher Award

ISL&T-X, Hong Kong, China (2010 Inaugural Year)



Biological Research

Xiao Chen, Ph.D.

Advisor: H-W. Ouyang
Zhejiang University
Zhejiang, China



Clinical Research

Saira Chaudhry, Ph.D.

Advisor: D. Morrissey
Queen Mary University of London
London, United Kingdom

ISL&T-XI, Irvine, CA (2011)



Biomechanical Research

Joo H. Oh, M.D., Ph.D.

Advisor: T.Q. Lee
VA Long Beach Healthcare System
University of California
Irvine, CA



Biological Research

Jeffrey P. Brown, Ph.D.

Advisor: C.K. Kuo
Tufts University
Medford, MA

ISL&T-XII, San Francisco, CA (2012)



Biological Research

Jonathan P. Gumucio, B.S.

Advisor: C.L. Mendias
University of Michigan
Ann Arbor, MI

ISL&T-XIII, Arezzo, Italy (2013)



Biomechanical Research

Chauvanne T. Thorpe, Ph.D.

Advisor: H.R. Screen
Queen Mary University of London
London, United Kingdom

ISL&T-XIV, Las Vegas, NV (2015)



Biological Research

Sarah Rooney, MSE

Advisor: L.J. Soslowsky
University of Pennsylvania
Philadelphia, PA

Savio L-Y. Woo Young Researcher Award Winners

ISL&T-XV, Orlando, FL (2016)



Biomechanical Research

Kuwabo Mubyana, Ph.D.

Advisor: David T. Corr, Ph.D.

Rensselaer Polytechnic Institute

Troy, NY

Abstract Title: Cyclic Mechanical Loading Improves Tensile and Failure Properties of Scaffold-Free Engineered Tendon Fibers



Translational Research

Thomas Teh, Ph.D.

Advisor: James C.H. Goh, Ph.D.

National University of Singapore

Singapore

Abstract Title: Augmentation of Tendon Graft Anterior Cruciate Ligament Reconstruction Outcome Using a Silk Based Osteoconductive Sheath



Biological Research

Michael Kuenzler, M.D.

Advisor: Matthias Zumstein, M.D.

University of Bern

Bern, Switzerland

Abstract Title: Reduced Muscle Degeneration and Decreased Fatty Infiltration after Rotator Cuff Tear in a PARP-1 Knock-Out Mouse Model

Best Student Paper Award

Award: Up to USD\$200 and Certificate

Eligibility: Open to current graduate students. Applicant must be the first author of the abstract and be present at the ISL&T meeting/banquet to accept the award. Applicant must indicate his/her intention to be considered for the award at the time of abstract submission and the advisor's verification of eligibility is required.

Selection Criteria and Process: Submitted abstracts will be reviewed by the Program Committee through the regular evaluation process based on scientific merit and research quality. The Award Committee will select the best paper during the international meeting. Award winner will be announced at the banquet.

Best Research Fellow Paper Award

Award: Up to USD\$200 and Certificate

Eligibility: Open to clinical fellows or post-doctoral research fellows. Applicant must be the first author of the abstract and be present at the ISL&T meeting/banquet to accept the award. Applicant must indicate his/her intention to be considered for this award at the time of abstract submission.

Selection Criteria and Process: Submitted abstracts will be reviewed by the Program Committee through the regular evaluation process based on scientific merit and research quality. The Award Committee will select the best paper during the international meeting. Award winner will be announced at the banquet.

Best Poster Award

Award: Up to USD\$200 and Certificate

Eligibility: Open to all participants of the poster presentations. Applicant must be the first author of the abstract and be present at the ISL&T meeting/banquet to accept the award. Applicant must indicate his/her intention to be considered for this award at the time of abstract submission.

Selection Criteria and Process: Submitted abstracts will be reviewed by the Program Committee through the regular evaluation process based on scientific merit and research quality. The Award Committee will select the best poster during the international meeting. Award winner will be announced at the banquet.

Acknowledgements: Awards sponsored by Flexcell International Corporation and the Asian♦American Institute for Research and Education (ASIAM):

Instructions to Presenters

Podium Presenters

The time for presentations has been limited, in favor of discussion. Please see the presentation formats listed below. Your moderators have been asked to adhere to the time allotted for your presentation as well as the number of slides.

An Important Note on Slides

All speakers must be prepared to present their research using PowerPoint format.

Podium Presentation Requirements

Keynote Presentations

- 10 min. presentations each immediately followed by a 5 min. discussion.
- Maximum 10 PowerPoint slides for computer presentation.

Regular Presentations

- 5 min. presentations followed by a 10-15 min. group discussion of 4-5 abstracts.
- Maximum 5 PowerPoint slides for computer presentation.

Important: All speakers are asked to check-in with the session moderators 15 minutes before the session in which they will present to meet the projectionist and the moderator.

Poster Presenters

Poster should be limited to 45 inches by 45 inches (114 cm x 114 cm).

Poster boards will be available in the meeting room. Please set up your poster between 7:30 am - 8:00 am and leave the posters up throughout the day. Posters are to be taken down by 6:00 pm.

Note: An opportunity has been provided for you to present your posters during different breaks as well as a one minute presentation during the Flash Presentation by Poster Presenters. Please be sure to attend to your poster at the assigned times.

Program

Podium Sessions

<u>Time</u>	<u>Topic</u>	<u>Speaker</u>
7:30	Registration and Light Breakfast	
8:00	Welcome	Zong-Ming Li, Ph.D. David T. Corr, Ph.D.
8:15	<i>Clinical Keynote Lecture: Innovation in Hip Arthroscopy Over the Past 10 Years</i> (pg. 30)	Marc Philippon, M.D.
	Podium Session I: Biomechanics I: Healing Ligament and Tendon / In Vivo Assessment (pg. 31-38)	Moderators: Louis Soslowky, Ph.D. Chunfeng Zhao, M.D.
8:30	<i>Keynote Lecture: Timing Of Post-Operative Mechanical Loading Effects Healing Following Anterior Cruciate Ligament Reconstruction</i>	Christopher L. Camp, M.D.
8:40	<i>Discussion</i>	
8:45	Detection of Osteoclastic Activity in a Murine Model of Anterior Cruciate Ligament Reconstruction using Optical Near-Infrared Imaging and Cathepsin K Probe	Amir Lebaschi, M.D.
8:50	Contrasting Effects of Re-injury on the Structural and Material Properties of the Rabbit Medial Collateral Ligament	Johnathan L. Sevick, M.Sc.
8:55	The LG/J Murine Strain Exhibits Near-Normal Tendon Biomechanical Properties Following A Full-Length Central PT Defect	Jason T. Shearn, Ph.D.
9:00	Impact of Incremental Flexor Retinaculum Release on Carpal Tunnel Compliance	Rubina Ratnaparkhi, B.S.
9:05	<i>Discussion</i>	
9:20	Kinematics of ACL-Deficient and Healthy Knees During Stair Descent: An Application of a Clinician-Friendly Motion Capture System	Kam-Ming Mok, M.Phil.
9:25	Transverse Carpal Ligament and Tendon Interaction in the Carpal Tunnel	Tamara L. Marquardt, B.S.

9:30	Orientation and Size Changes in the Porcine Anterior Cruciate Ligament Throughout Skeletal Growth	Stephanie Cone, B.S.
9:35	<i>Discussion</i>	
9:50	Coffee Break/ Poster Session I (even numbers)	
	Podium Session II: Tendon Mechanobiology & Stem Cell (pg. 39-43)	Moderators: Alice Huang, Ph.D. Lisa Larkin, Ph.D.
10:20	<i>Savio L-Y. Woo Young Researcher Award - Biomechanical Cyclic Mechanical Loading Improves Tensile and Failure Properties of Scaffold-Free Engineered Tendon Fibers (pg. 16)</i>	Kuwabo Mubyana, Ph.D.
10:30	<i>Discussion</i>	
10:35	The Role of SPARC in Mechanosensing Function of Tendon	Tao Wang, Ph.D.
10:40	Origin of Cells that Contribute to Murine Rotator Cuff Tendon Healing	Ryu Yoshida, M.D.
10:45	<i>Discussion</i>	
10:55	Stem/Progenitor Cell Recruitment to Deteriorating Tendons in Mice with Conditional Deletion of TGF-Beta Type II Receptor	Guak-Kim Tan, Ph.D.
11:00	A Comparison of Adipose- and Bone Marrow- Derived Mesenchymal Stem Cell Behavior on Micro-Photopatterned Surfaces	Sean Meehan, M.S.
11:05	Tendon Tissue Derived Extracellular Matrix Enhances Tenogenic Response to TGF-Beta of Mesenchymal Stem Cells via Smad Complex Signaling	Guang Yang, Ph.D.
11:10	<i>Discussion</i>	
	Podium Session III: Tissue Engineering in ACL Repair (pg. 44-46)	Moderators: Christos Papageorgiou, M.D., Ph.D. Jason Shearn, Ph.D.
11:25	<i>Keynote Lecture: Fresh and Frozen Tissue Engineered 3D Bone-Ligament-Bone Constructs for Sheep ACL Repair Following Two-Year Implantation</i>	Vasu Mahalingam, M.S.
11:35	<i>Discussion</i>	

11:40	Savio L-Y. Woo Young Researcher Award - Translational Augmentation of Tendon Graft Anterior Cruciate Ligament Reconstruction Outcome Using a Silk Based Osteoconductive Sheath (pg. 19)	Thomas K.H. Teh, Ph.D.
11:50	<i>Discussion</i>	
11:55	Effect Of Tripeptide Copper Complex GHK-Cu On Cultured Healing Cells Derived From Tendon Graft In Anterior Cruciate Ligament Reconstruction	Yau-Chuk Cheuk, M.Phil.
12:00	A Novel Magnesium Ring Device Combined with ECM Bioscaffolds Improves ACL Healing Compared to ECM Treatment Alone	Kathryn Farraro, Ph.D.
12:05	<i>Discussion</i>	
12:15	Flash Presentation by Poster Presenters (pg. 68-78)	Moderators: Connie Chamberlain, Ph.D. Michael Lavagnino, Ph.D. Johnna Temenoff, Ph.D.
12:30	Lunch (Group Photo and Poster Viewing)	
	Podium Session IV: Inflammation and Tendon Healing (pg. 47- 50)	Moderators: Paul Ackermann, M.D., Ph.D. Stavros Thomopoulos, Ph.D.
13:30	Keynote Lecture: The Immunomodulation of Ligament Healing	Connie S. Chamberlain, Ph.D.
13:40	<i>Discussion</i>	
13:45	Curcumin: Does it Decrease Inflammation in Tendon Healing?	Diana Zhu, B.S.
13:50	The Differential Effects of Protease-Activated Receptors 1 and 4 in Human Platelet Activation and Inflammation	Jianying Zhang, Ph.D.
13:55	The Role of Interleukin-13 in Tendinopathy	Moed Akbar, Ph.D.
14:00	<i>Discussion</i>	

	<i>Special Session: Translational Tendon and Ligament Research - In Honor of Professor Kai-Ming Chan (pg. 51-59)</i>	Moderator: Bruma Sai-Chuen Fu, Ph.D. Patrick Yung, M.D.
14:15	Research in Orthopaedics-What Have I Learned in 40 Years	Kai-Ming Chan, M.D., Ph.D.
14:35	What Do Orthopaedic Surgeons Need For Research?	Mahmut Doral, M.D.
14:40	Cell Therapies for Tendon Surgery	Minghao Zheng, M.D., Ph.D.
14:45	Learn from Tendon Stem Cells-Potential Clinical Use	Hongwei Ouyang, M.D., Ph.D.
14:50	<i>Discussion</i>	
15:05	Out of Academics: Product Development from Concept, Patent Process, R&D, Prototyping, Testing, to the Market	Albert Banes, Ph.D.
15:10	PRP Myths	Ramon Cugat, M.D.
15:15	Is There Any Substance in the PRP Treatment of Tendinopathy?	James Wang, Ph.D.
15:20	<i>Discussion</i>	
15:35	Healing and Regeneration After Anterior Cruciate Ligament Injury	Chih-Hwa Chen, M.D.
15:40	Biomechanics and Kinematic Studies of the ACL	Guoan Li, Ph.D.
15:45	<i>Discussion</i>	
15:55	Coffee Break/Poster Session II (odd numbers)	
	Podium Session V: Biomechanics II: Theoretical and Computational Modeling (pg. 60 – 63)	Moderators: Ray Vanderby Jr., Ph.D. Guoan Li, Ph.D.
16:25	Predicting Tendon ECM Composition from Tenocyte Strain and Fiber Damage	Arash Mehdizadeh, Ph.D.
16:30	Development and Validation of a Computational Foot and Ankle Model to Investigate Lateral Ligamentous Strain	Sophia Chui-Wai Ha, M.A.
16:35	Adaptive Remodeling of Achilles Tendon: A Multi-scale Computational Model	Stuart Young, B.E.

16:40	Histology-Inspired Mechanical Analysis of Anterior Cruciate Ligament Injury	Callan Luetkemeyer, B.S.
16:45	<i>Discussion</i>	
	Podium Session VI: Rotator Cuff Injury and Repair (pg. 64 – 67)	Moderators: Dianne Little, D.V.M., Ph.D. Roger Smith, Ph.D.
17:00	<i>Savio L-Y. Woo Young Researcher Award - Biological Reduced Muscle Degeneration and Decreased Fatty Infiltration After Rotator Cuff Tear in a Parp-1 Knock-Out Mouse Model (pg. 23)</i>	Michael Kuenzler, M.D.
17:10	<i>Discussion</i>	
17:15	Pre-Operative Intramuscular Fat Fractions are Significantly Higher in Patients with Eventual Failed Rotator Cuff Repair	Drew Lansdown, M.D.
17:20	Micro-CT Evaluation of Cartilage Degeneration on Two Rat Models of Shoulder Injury	Jennifer McFaline-Figueroa, B.S.
17:25	Effect of Hypercholesterolemia on Fatty Infiltration and Rotator Cuff Healing in a Chronic Rotator Cuff Tear Model of Rabbit	Seok Won Chung, Ph.D.
17:30	Tissue Engineered Tendon Constructs for Rotator Cuff Repair in a Sheep Model	Stoyna S. Novakova, B.S.
17:35	<i>Discussion</i>	
17:50	Closing Remarks for ISL&T - XV	Patrick Yung, M.D. Savio L-Y. Woo, Ph.D., D.Sc., D.Eng.
18:00	<i>Proceed to Banquet Venue (Transportation Provided)</i>	
18:30	Banquet and Award Ceremony Ming Court Restaurant 9188 International Drive	

Poster Presentations

**Moderators: Connie Chamberlain, Ph.D., Michael Lavagnino, Ph.D.,
and Johnna Temenoff, Ph.D.**

(pg. 68 - 78)

<u>Poster Number</u>	<u>Title</u>	<u>Presenter</u>
1	Hypoxia Inhibits Primary Cilia Formation and Reduces Cell-Mediated Contraction in Stress-Deprived Rat Tail Tendon Fascicles	Anna Oslapas
2	Hyperelastic and Viscoelastic Characterization of Anterior Cruciate Ligament Biomechanics	Kaitlyn Mallett, B.S.
3	Inhibition of Retinoic Acid Signaling and Stimulation of Wnt Signaling Allows Efficient Paraxial Mesoderm Formation from Human Embryonic Stem Cells	Ryan P. Russell, M.A.
4	High throughput, multi-image cryohistology of joint tissues	Nathaniel Dymont, Ph.D.
5	Dysfunction of CFTR Impairs Tendon Differentiation through Activation of pERK1/2 in Mice	Gang Li, Ph.D.
6	Procollagen Biomarkers of Healing in Microdialysate Predict Patient-reported Outcome after Achilles Tendon Rupture	Simon Svedman
7	Recovery of Viscoelastic Properties of Achilles Tendon Following Rupture	Jennifer Zellers, D.P.T
8	Comparison of the Cellular Composition and Cytokine-Release Kinetics of Various Platelet-rich Plasma (PRP) Preparations	Young Hak Roh, M.D., Ph.D.
9	Heat shock induces the expression of pro-inflammatory cytokines in human tenocytes	Alessio D'Addona, M.D.
10	Adverse Effects of Synovial Fluid on Internal Tendon Cells – Implications for Intrasynovial Tendon Repair	Roger Smith, Ph.D.

SAVIO L-Y. WOO YOUNG RESEARCHER AWARD
WINNERS
EXTENDED ABSTRACTS

CYCLIC MECHANICAL LOADING IMPROVES TENSILE AND FAILURE PROPERTIES OF SCAFFOLD-FREE ENGINEERED TENDON FIBERS

K. Mubyana and D. T. Corr

Department of Biomedical Engineering, Rensselaer Polytechnic Institute, Troy, NY

INTRODUCTION

The treatment of compromised tendon is a growing clinical and financial burden, because of high injury occurrence and frequent re-rupture. Engineering scaffold-based tendon replacement grafts, while increasingly common, still carries a potential risk of immune rejection. Moreover, there are significant challenges to overcome in order to optimize scaffold-based tendon grafts, including creating an implantable graft that is biocompatible, emulates the mechanical properties of native tendon, and in the case of bioresorbable scaffolds, degrades at a rate that matches the rate of cellular matrix deposition. A relatively new area of research explores a promising alternative to this: scaffold-free tissue engineering to create tendon replacement grafts.

Our laboratory recently created a scaffold-free approach to engineer single tendon-like fibers to study the influence of biophysical stimuli on fiber formation and structural/functional maturation^{1,2}. This approach is inspired by embryonic tendon development, and mimics some key aspects of tenogenesis, which include high initial cell density, direct cell-cell contact and fiber formation by cellular self assembly¹. The **objective** of this study was to examine the effect of mechanical stimulation, specifically intermittent periods of cyclic uniaxial tensile strain, on the mechanical and failure properties of these tendon fibers. It was **hypothesized** that cyclic uniaxial strain would improve the tensile and failure properties of the engineered scaffold-free tendon fibers within seven days, increasing Elastic modulus, toughness, failure stress and failure strain. The findings of this study will provide unique insight into the role of mechanical stimulation on tendon development and tissue formation.

METHODS

Growth Channel Fabrication and Cell Seeding: Tendon fibers were synthesized using previously outlined methods². In brief, u-shaped growth channels (150 μm -wide, 300 μm -deep, and 17.5 mm-long) were molded using a custom-fabricated Aluminum 6061-T6 micro-mold (Precision MicroFab, Curtis Bay, MD) and 2-wt% gel, made from electrophoresis-grade agarose powder and Dulbecco's Modified Eagle's Medium (DMEM). To create a differentially-adherent surface within the growth channel, the agarose was UV-crosslinked, and human fibronectin (0.375 $\mu\text{g}/\text{mL}$, Corning, MA) was wicked through the growth channel and allowed to dry for 50 minutes.

Human dermal fibroblasts (CCD-1065sk, ATCC) were seeded in growth channels at very high density (1.5×10^7 cells/mL), and allowed 10 minutes to selectively adhere to the channel, prior to fully immersing the entire agarose growth channel in growth medium (DMEM, supplemented with 10% fetal bovine serum, 0.5% penicillin-streptomycin, and 50 $\mu\text{g}/\text{mL}$ L-ascorbic acid). Seeded growth channels were then incubated (37 $^{\circ}\text{C}$, 5% CO_2 , 95% RH) for 18 h, at static strain. This static strain period was selected to facilitate initial fiber formation, and was sufficient for fibers to develop adequate tissue integrity to withstand the mechanical stimulation.

Mechanical Loading: Approximately 18 h post-seeding, the fibers were mounted onto a modified pneumatic FlexCell[®] Tissue Train[®] system (Flexcell International Corp., Burlington, NC), and subjected to intermittent cyclic uniaxial strain for 1 ($n = 7$), 3 ($n = 9$), and 7 ($n = 7$) days. The loading protocol was 8 h of 0.7% sinusoidal strain at 0.1 Hz, alternating with 8 h rest periods of 0% static strain, as illustrated in **Fig. 1**. Additionally, three unloaded control groups were cultured under static strain for 1 ($n = 6$), 3 and 7 days.

Mechanical Characterization: Loaded fibers, and unloaded controls, were dissected from the growth channel and transferred to phosphate-buffered saline (PBS), where they were each transected into two or three material testing segments, and T-clipped (**Fig. 2a**). Given the scale of the fibers ($< 150 \mu\text{m}$ -wide), a mechanical tensile tester of high sensitivity was imperative. Fibers were tested on a custom ADMET single fiber BioTense bioreactor (Admet Inc., Norwood, MA) (**Fig. 2c**). To mount a fiber for mechanical characterization, the T-clips on each end of the fiber segment were mounted onto two stainless-steel wire hooks; one attached to a uniaxial servo-controlled force actuator

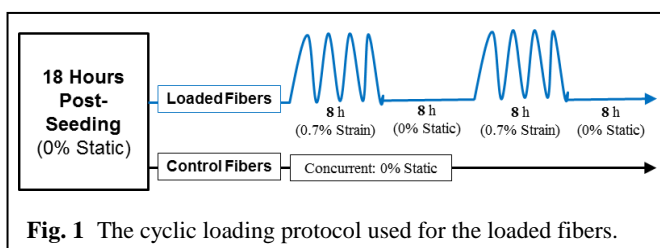


Fig. 1 The cyclic loading protocol used for the loaded fibers.

with an integrated displacement transducer (2.0 cm maximum stroke, with 0.0046 μm displacement resolution), and the other hook attached to a Kronex AE-800 series sensor element force gauge (SensorOne Technologies Co., Sausalito, CA), permitting mN-scale force measurements at 50 μN resolution. Mounted test specimens were imaged using Leica Application Suite (Leica Microsystems, Switzerland), as shown in **Fig. 2c inset**, and fiber length, diameter and cross-section area were acquired in ImageJ³. To test, fibers were elongated to failure at a constant rate of 0.08 mm/s, and force, displacement and time data were recorded at 50 Hz. Load-displacement data were normalized to specimen geometry to calculate stress-strain, and used to calculate the Elastic modulus (slope of linear elastic range), toughness, and the stress and strain at failure. **Statistical data analyses** were conducted in R statistical software, using Kruskal-Wallis Rank Sum Tests.

RESULTS

Within the first 12 hours after seeding, fibroblast cells densely packed into the growth channel and self-aligned to the channel's long axis, forming fibers. Within 24 h of loading, fibers lost all lateral adhesion to the channel walls (**Fig. 2b**). All tested fibers exhibited a characteristic tendon mechanical response: a clear toe-in region, followed by a linear elastic region, and brief softening prior to fiber failure (**Fig. 3**). In the loaded groups, there was no significant difference in modulus, peak stress or toughness between days 1 and 3, however all of these properties increased significantly at 7 days. Conversely, failure strain was similar in all loaded groups, regardless of loading duration.

Unloaded control fibers formed within 24 h of seeding, but failed inside their growth channels after 42 h. This permitted 1-day controls to be mechanically characterized, but prevented testable control fibers at days 3 or 7. Additionally, all the surviving unloaded fibers retained lateral adhesions to the channel walls.

Elastic modulus was clearly influenced by cyclic strain loading, with loaded fibers displaying more than a six-fold increase in modulus compared to unloaded controls. Similarly, the failure stress and toughness were markedly lower in unloaded 1-day fibers than corresponding loaded fibers (**Table 1**).

DISCUSSION

Mechanical stimulation plays a pivotal role in matrix deposition and incipient growth of embryonic tendon⁴. In fact, in the embryonic development of chicks, movement is detected as early as 3 days, prior to the development of skeletal muscles. Over following days, cyclic loading not only continues, but increases in magnitude⁵. The exact magnitudes of loading that the tendon experiences at that stage of development are not known. As a result, in this study, a strain of 0.7% was selected because it is within a physiologically-relevant range⁶.

The results herein indicate that mechanical stimulation, specifically applied uniaxial cyclic strain, increases modulus, failure stress, and toughness, thereby suggesting the promotion of matrix deposition and tendon maturation.

Two additional findings indicated that these tensile and failure properties were heavily influenced by intermittent cyclic strain. First, without cyclic strain, unloaded control fibers could not be maintained past the 1 day point, showing that loading was critical for fiber maturation beyond that point. Secondly, lateral adhesions to the growth channel persisted in unloaded fibers, preventing

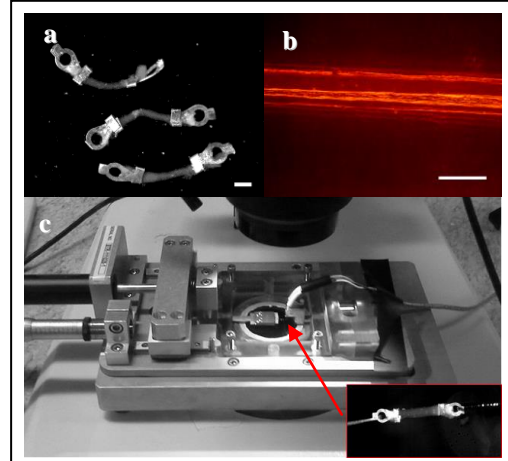


Fig. 2 a) 7-day loaded fibers, T-clipped in solution for mechanical testing. b) Fiber inside growth channel, 24 h post-loading (scale bars = 250 μm). c) For testing, fibers were mounted onto the wire hooks (inset) of a custom Admet BioTense bioreactor.

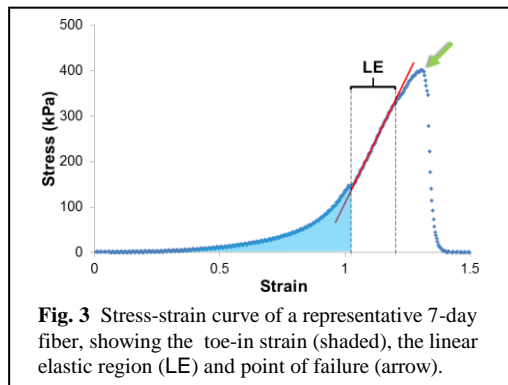


Fig. 3 Stress-strain curve of a representative 7-day fiber, showing the toe-in strain (shaded), the linear elastic region (LE) and point of failure (arrow).

Table 1 Mechanical properties of the engineered fibers (mean \pm standard deviations). * denotes statistical difference from the control. ^Δ and [†] denote statistical difference from 1-day loaded and 3-day loaded fibers, respectively.

	Controls		Loaded Fibers	
	1-day	1-day	3-day	7-day
Failure Stress (kPa)	19.0 \pm 2.0	80.2 \pm 16.0*	103.6 \pm 33.3	314.4 \pm 36.1 ^{Δ†}
Failure Strain	1.7 \pm 0.6	1.4 \pm 0.1	1.4 \pm 0.1	1.5 \pm 0.1
Modulus (kPa)	26.8 \pm 3.6	178.8 \pm 34.4*	344.0 \pm 144.3	789.1 \pm 9.3 ^{Δ†}
Toughness (kJ·m⁻³)	9.3 \pm 4.3	23.6 \pm 6.4*	30.8 \pm 7.1	80.2 \pm 11.2 ^{Δ†}

pure uniaxial loading, and possibly interfering with aligned matrix deposition. During cell seeding, cells form focal adhesions to the walls of the growth channel. In this highly dense environment, there is a substantial amount of direct cell-to-cell contact, and the cells receive cues from multiple directions. The findings of this study strongly suggest that the uniaxial cyclic strain establishes a primary direction in which these cells orient, inducing a release of focal adhesions from the growth channel walls, and forming a fiber that is round in cross section. This is consistent with previous studies, which have shown that cells respond to uniaxial stretching by undergoing reorientation of actin stress fibers in the cytoskeleton, a gradual process that is mediated at the focal adhesions⁷. Within hours of cyclic stretching, Tenascin-C expression has been shown to increase, and Tenascin-C is known to disrupt attachment of cells to fibronectin⁸ (the ECM protein used to coat the walls of the growth channels).

Contrary to our hypothesis, this study found that failure strain was not influenced by cyclic uniaxial strain. However, mechanical stimulation produced tendon fiber constructs with higher Elastic modulus, thus increased linear-range stiffness.

In addition to the linear region, another important tensile property is the tendon fiber toe-in, i.e., the initial region of non-linearity in the stress-strain curve. The non-linear strain-stiffening behavior displayed in the toe-in region is typically attributed to the progressive recruitment and realignment of crimped collagen fibrils, as the tendon is stretched. Understanding the mechanics of the toe-in region, or at least, the changes in toe-in duration, is important because the toe-in region dominates the normal physiological range within which tendon functions⁹. Our most recent findings, in a separate follow-on study, examined the low-load behavior of these engineered scaffold-free tendon fiber constructs using two methods to compute toe-in duration. First, we determined the toe-in limit strain by extrapolating the linear elastic slope to the strain axis. We also directly quantified the toe-in strain by determining the lowest strain value at which the 1st derivative of the stress-strain curve equals the Elastic modulus, i.e., the point at which the stress-strain response becomes linear, as illustrated in **Fig. 3**. Both methods revealed that toe-in duration was not influenced by intermittent uniaxial cyclic strain¹⁰. Taken together with our modulus and failure strain results, these findings suggest that mechanical stimulation promotes matrix deposition in a manner that increases the resistance to stretch, yet does not affect the ultimate extensibility of the fiber.

Numerous studies have demonstrated the use of mechanical cues to promote tenogenesis or repair of cellularized scaffold-based engineering grafts^{11–15}. However, this study demonstrates the influence of cyclic strain on the mechanical properties of engineered tendon fibers, using a scaffold-free method that mimics key aspects of embryonic tendon development (e.g., high cell density, direct cell-cell contact, absence of provisional matrix/structure). As such, these findings provide unique insight into the role of mechanical stimulation on fiber formation, maturation, and matrix deposition, which may prove pivotal for future regenerative strategies to create/repair tendon. We are currently running a parallel study, utilizing immunohistochemistry, to examine matrix deposition, structure, and composition in response to cyclic tensile strain.

ACKNOWLEDGEMENTS

This study was supported, in part, by the NSF CAREER Award CBET-0954990 (DTC).

REFERENCES

1. Schiele, N.R. *et al. Tissue Eng. Part A* 19, 1223–32 (2013).
2. Mubyana, K. and Corr, D.T. *Proc of IEEE NEBEC* (2015).
3. Rasband, W.S. ImageJ, U.S. National Institutes of Health.
4. Glass, Z.A. *et al. J. Biomech.* 47, 1964–8 (2014).
5. Wu, K.C. *et al. J. Exp. Zool.* 291, 186–94 (2001).
6. Cohen, S. *et al. Tissue Eng. Part A* 16, 3119–37 (2010).
7. Yoshigi, M. *et al. J. Cell Biol.* 171, 209–15 (2005).
8. Chiquet, M. *et al. Matrix Biol.* 22, 73–80 (2003).
9. Hansen, K.A. *et al. J. Biomech. Eng.* 124, 72 (2002).
10. Mubyana, K. and Corr, D.T. *Proc of ORS 2016 Annual Meeting* (Submitted) (2016).
11. Saber, S. *et al. Tissue Eng. Part A* 16, 2085–90 (2010).
12. Scott, A. *et al. J. Musculoskelet. Neuronal Interact.* 11, 124–32 (2011).
13. Juncosa-Melvin, N. *et al. Tissue Eng.* 12, 2291–300 (2006).
14. Nirmalanandhan, V. S. *et al. J. Biomech.* 41, 822–828 (2008).
15. Lin, T. W. *et al. J. Biomech.* 37, 865–77 (2004).

Biological Research

**AUGMENTATION OF TENDON GRAFT ANTERIOR CRUCIATE LIGAMENT RECONSTRUCTION
OUTCOME USING A SILK BASED OSTEOCONDUCTIVE SHEATH**

T.K.H. Teh 1, P. Shi 1, 3, S.N. Png 1, X. Ren 2, J.H.P. Hui 2, J. Li 1, 3 and J.C.H. Goh 1, 2

1 Department of Biomedical Engineering, National University of Singapore, Singapore

2 Department of Orthopedic Surgery, National University of Singapore, Singapore

3 Institute of Materials Research and Engineering, Agency for Science, Technology and Research, Singapore

INTRODUCTION

With increased longevity in the global aging population, joint health remains critical as the quality of life is increasingly associated with human mobility. Coupled with the growing focus on an active lifestyle, intervention procedures performed on the knee have been gaining popularity, particularly the Anterior Cruciate Ligament (ACL) reconstruction. Such surgical intervention often involves the use of tendon autografts, with semitendinosus and gracilis tendons being popular choices. Nevertheless, less than optimal healing of the tendon graft within the surgically created bone tunnel remains a fundamental problem in this procedure. The proposed solution involves the application of a novel silk fibroin (SF) based sheath, embedded with nanoparticles of low crystallinity hydroxyapatite (nHA), to complement the use of tendon autografts and promote entheses formation. This SF-nHA sheath configuration was tested against SF sheaths with incorporation of bone morphogenetic protein 2 (BMP-2) only (SF-BMP2), a blend of BMP-2 and nHA (SF-BMP2-nHA) and pure silk sheaths (pure SF) to evaluate their potential in osteointegration of tendon grafts. The optimal sheath type was subsequently put through an in depth assessment for biocompatibility and also *in vivo* study in small and large animal models for up to 9 months to evaluate the efficacy of the sheath in promoting osteointegration of tendon grafts.

METHODS

Knitted SF scaffolds (240 fibroins, L30 × Ø5 mm) were first fabricated from raw *Bombyx mori* silk (Chul Thai Silk Co. Ltd) and subsequently degummed. The nHA precipitates were synthesized by a co-participation method of aqueous (NH₄)₂HPO₄ with aqueous Ca(NO₃)₂. Hydrothermal treatment of the precipitates' aqueous solution was carried out at 140 °C under a pressure 0.3 MPa for 2 h in an autoclave to form the nanograde rod HA crystals. SF sponges, made from a blend of aqueous SF solution (2% w/v) and synthesized nHA (12.9 mg/ml), were incorporated to the knitted structures via a lyophilization process in a customized mould. This SF-nHA group was compared with pure SF, SF-BMP2 (19.3 µg/ml BMP-2) and SF-BMP2-nHA (19.3 µg/ml BMP-2 and 12.9 mg/ml nHA) via static culture of 10 × 10 mm specimens (Fig. 1A) with seeded porcine bone marrow derived MSCs (P2, 0.5 × 10⁶/scaffold) over 28 days. *Ex vivo* static culture of the four groups of SF sheaths with tendon autografts (porcine Flexor Digitorum Profundus sections, L10 × Ø5 mm, Fig. 1B) and porcine bone marrow derived MSCs (P2, 2 × 10⁶/scaffold) was then conducted over 28 days. In these assessments, the cellular viability, proliferation, gene expression, collagen deposition levels, scanning electron microscopy (SEM) and histological analyses were performed (n = 3). Consequently, the most efficacious group for osteointegration of tendon grafts was selected for the in depth biocompatibility assessments and *in vivo* tests.

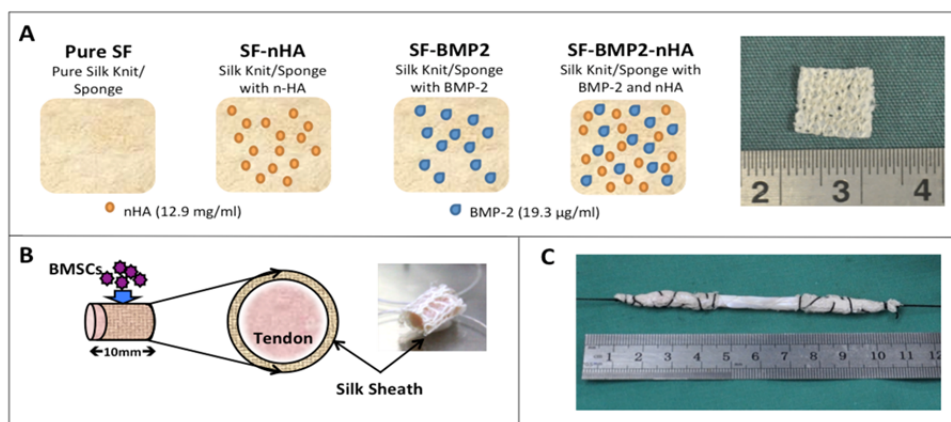


Fig. 1. (A) Scaffold groups tested *in vitro* for effects of nHA, BMP-2 and their combination, on osteogenic differentiation of porcine bone marrow derived mesenchymal stem cells (MSCs). (B) *Ex vivo* static culture of porcine tendon graft sleeved with porcine MSCs seeded SF sheaths. (C) SF sheath secured onto both ends of porcine tendon autografts prior to ACL reconstruction in a porcine model.

The complete optimized sheath was then tested through a series of biocompatibility assessment for cytotoxicity, sensitization, intracutaneous reactivity, acute systemic and 14 days sub-chronic repeated dose toxicity, genotoxicity (Ames test, chromosome aberration assay, mouse lymphoma assay) and 12-weeks implantation in rabbit femur. A preclinical trial was conducted in the porcine ACL reconstruction model using tendon autograft harvested from the flexor digitorum profundus and SF-based sheath sutured onto both ends of the graft (Fig. 1C). Graft integration in the presence of SF-based sheaths within the bone tunnels and tendon integrity within the intra-articular space were assessed via imaging (CT and MRI), histomorphometrical and histopathological methods at 1, 3, 6 and 9 months time points. All animal experiments were approved by the respective institutional IACUC.

RESULTS

The SF sheaths were observed to be porous with interconnected pores. nHA and BMP-2 were observed to be securely incorporated in the lyophilized SF sponges. BMP-2 bioactivity was ascertained after the fabrication process and was shown to be eluting with an initial burst release, followed by a lowered sustained release.

MSCs were observed to be viable and proliferative in all four groups of the *in vitro* study. Increased proliferations were observed in SF-nHA, SF-BMP2 and SF-BMP2-nHA at the early phase (days 1-7) with an accelerated differentiation phase beginning from day 14. Consequently, there was an upregulation of osteogenic related genes (Collagen I (Coll I), Collagen III (Coll III), osteonectin (ON) and osteopontin (OPN)) (Fig. 2), leading to a significantly increased deposition of collagen by day 21. However, it was further noted that between SF-nHA, SF-BMP2, and SF-BMP2-nHA, the presence BMP-2 did not improve upon a persistent (beyond 21 days) upregulation of osteogenic genes and increase in collagen production.

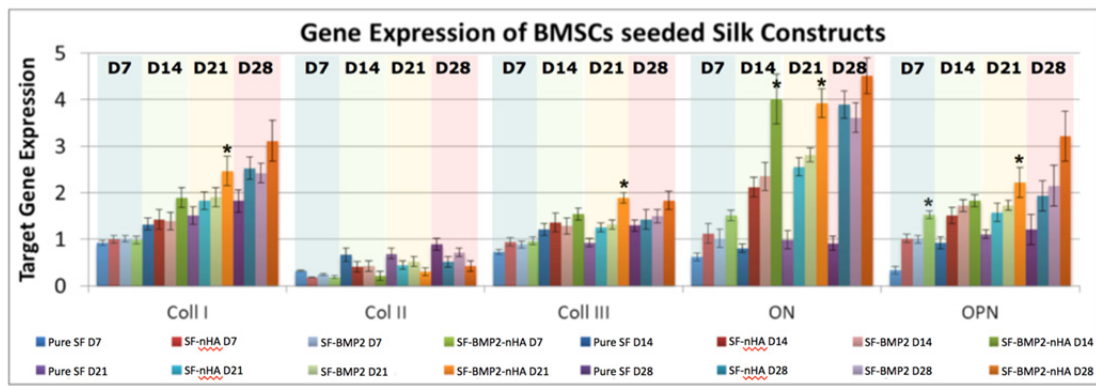


Fig. 2. Gene expressions for osteogenic ECM components were up-regulated in SF-BMP2-nHA group compared to the other groups by day 21 (* $p < 0.05$), which did not persist beyond. Levels were normalized to the housekeeping gene, GAPDH.

When cultured with excised tendon sections, it was observed that cells from within the tendon tend not to participate in interfacial tissue regeneration, while seeded MSCs were viable and produced ECM for bridging the tendon-scaffold interface after 2 weeks in SF-nHA, SF-BMP2, and SF-BMP2-nHA (Fig. 3A-H) as observed via SEM and H&E staining images. SF sheaths with nHA stimulated osteogenesis from seeded MSCs as observed by the presence of calcium deposits in SF-nHA and SF-BMP2-nHA via alizarin red staining (Fig. 3I-P). Ossification was thus observed with the presence of nHA, with or without the presence of BMP-2.

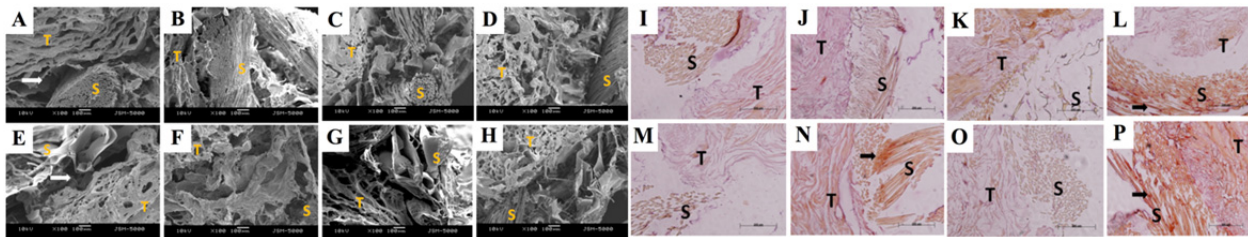


Fig. 3. (A-H) SEM images of tendon-scaffold interface after 2 (A-D) and 4 (E-H) weeks of static culture, scale bar: 100 μm . Arrows point to the gap between SF sheath and tendon graft. New tissues formed in the gaps between the SF sheaths and tendons of SF-nHA, SF-BMP2 and SF-nHA-BMP2 groups. (I-P) Alizarin Red staining images of tendon-scaffold interface after 2 (I-L) and 4 (M-P) weeks of static culture, scale bar: 200 μm . Arrows point to positive staining for matrix mineralization in SF-nHA and SF-BMP2-nHA samples. Pure SF (A, E, I, M), SF-nHA (B, F, J, N), SF-BMP2 (C, G, K, O), SF-BMP2-nHA (D, H, L, P). T: tendon, S: Silk.

Consequently, the SF-nHA sheath configuration was selected for further biocompatibility assessment and *in vivo* testing. The SF-nHA sheath was found to induce discrete intracytoplasmic granules with no cell lysis or reduction in cell growth in the tested mouse connective tissue cell line (NCTC clone 929), indicating non-cytotoxicity. Sensitization tests indicated limited erythema and oedema at challenged skin site over the 48 hours. There were also no significant biological reactivity findings compared to the respective negative control groups in the acute systemic and sub-chronic repeated dose toxicity assessments. Genotoxicity (Ames test) showed that the sheath was non mutagenic in the tested bacterial strains of *Salmonella typhimurium* and *Escherichia coli*, while *in vitro* chromosome aberration test indicated that the sheath did not induce structural chromosome aberration in the cultured mammalian somatic cells. Histopathological assessments of the extracted femurs of the 12 weeks implantation study indicated absence of inflammatory cells with presence of neovascularization and bone ingrowth.

At 1 month post ACL reconstruction using the SF-based sheath with tendon autografts in the preclinical porcine model, the reconstructed ACL became taut, when initially the tendon graft was implanted slack. This indicated that there was simultaneous growth and graft remodeling during this period. Regenerated epiligament was also formed, which provided

vascularization to the graft (Fig. 4A). It should be noted that the cartilage of the ACL reconstructed knee remained pristine and clear of cartilage erosion, which was indicative of accelerated and enhanced joint stability soon after the ACL reconstruction. The enhancement in osteointegration of tendon autograft was evident as multiple small foci of mineralization were identified within the femoral and tibial ends of the graft from as early as one month post ACL reconstruction (Fig. 4B). By 3 months, bone tissue infiltration into the interfacial space was evident from the increase in bone mineralization and vascularized neotissue formation, indicating improved graft to bone integration comparing to control (tendon autograft ACL reconstruction without SF-based sheath).

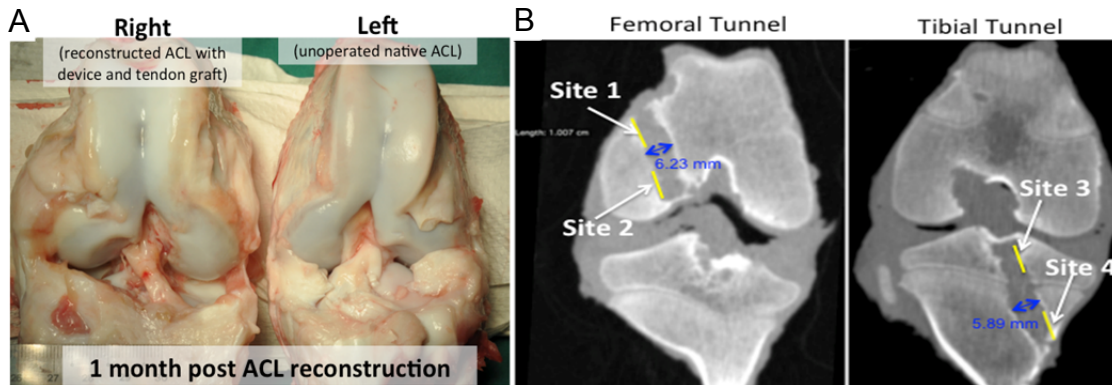


Fig. 4: Gross observation (A) and dorsal reconstruction CT images (B) of excised porcine knee joints at 1 month post-ACL reconstruction.

DISCUSSION

Prompt osteointegration of the tendon graft within the bone tunnel post ACL reconstruction is difficult with conventional therapies due to the lack of biochemical precursors. These precursors are provided by the SF-based sheath, which also includes a temporary scaffolding material that helps to provide a snug fit to the bone interface. It will prevent micromotion, which is often the cause of early inflammatory reactions and subsequent onset of fibrosis. The sheath will also serve as delivery platform for cellular and bioactive components. Progenitor cells, either seeded or attracted from the host into the porous sheath, will reconstitute the native cellular environment of the enthesis by differentiating into chondrocytes and osteoblasts. They will not only deposit the necessary ECM but also cytokines that elicit regenerative responses at the integration site. The delivery of osteogenic factors via the SF-based sheath will accelerate tissue restoration by triggering a migration of host reparative cells. These bioactive agents will also induce cellular differentiation required for the formation of fibrocartilage and bony tissue at the anchorage sites.

Results from the *in vitro* study indicated that although BMP-2 led to earlier upregulation of osteogenic genes, the expression of Coll I and ON were not significantly higher in SF-BMP2-nHA by day 28 when compared with SF-nHA. In terms of protein production, collagen synthesis between SF-nHA and SF-BMP2-nHA were not significant throughout the study, indicating that even though SF-BMP2-nHA might have stimulated the targeted genotypic behavior, the phenotypic outcome was not significantly improved. This was further substantiated when the silk sheaths were cultured with excised porcine tendons, whereby mineralized ECM could be found after 4 weeks of culture in SF-nHA and SF-BMP2-nHA.

Balancing clinical needs with our *in vitro* and *ex vivo* findings, the SF-nHA sheath was selected for further development. It was found that nHA stimulated tissue infiltration of host bone tissue, resulting in bone tunnel narrowing with new mineralized tissues observed in both the small and large animal models. Consequently, there is enhanced graft-to-host integration progressively over the 9 months implantation period, which can potentially result in overall mechanical properties closer to that of the native bone-ACL-bone construct. Based on our knowledge, this study is the first to investigate a SF-based device to augment ACL reconstruction with tendon autografts. With minimal disruption to current surgical practice, the SF-based sheath exhibits clinical potential in accelerating healing to allow earlier and more aggressive rehabilitation.

Translational Research

REDUCED MUSCLE DEGENERATION AND DECREASED FATTY INFILTRATION AFTER ROTATOR CUFF TEAR IN A PARP-1 KNOCK-OUT MOUSE MODEL

Michael B. Kuenzler, MD^{1,2}, Katja Nuss, DVM², Agnieszka Karol, DVM², Michael O. Schaer, MD¹, Michael O Hottiger, DVM, PhD³, Sumit Raniga, MD¹, David Kenkel⁴, Brigitte von Rechenberg, DVM, ECVS^{2,3}
Matthias A. Zumstein, MD¹

INTRODUCTION

Rotator cuff tears (RCT) cause profound and potentially irreversible structural alterations in the affected muscle. There is significant migration of inflammatory cells within the first few days of a tear and the muscle fibers undergo apoptosis⁶. In the ensuing weeks to months, this early response leads to muscular retraction, degeneration and atrophy, which are subsequently followed by fatty infiltration. The degree of fatty infiltration in a chronically torn rotator cuff is a negative predictor for a successful surgical outcome¹¹.

The complex interplay of molecular and cellular mechanisms, which leads to potentially irreversible structural alterations in skeletal muscle, is well described⁴. However, a single upstream regulator may orchestrate this molecular cascade. The discovery of such a regulator could potentially provide a future target for therapeutic interventions at the molecular level that may enhance the recovery of rotator cuff muscles post surgical repair.

Poly (ADP-ribose) polymerase-1 (PARP-1), also known as ADP-ribosyltransferase (ARTD1), is a key transcription factor involved in the maintenance of cellular homeostasis⁸. It activates NF-κB transcription during the inflammatory response which not only induces apoptosis and muscular atrophy, but also inhibits muscle regeneration¹⁰; it promotes apoptosis²; it has a role in adipogenesis and may induce fatty infiltration of the muscle¹; it also induces muscular atrophy and fibrosis whilst depressing regenerative pathways⁹. Hence, PARP-1 may be the upstream regulator that orchestrates the molecular and cellular mechanisms that leads to potentially irreversible structural alterations after RCT.

We therefore hypothesized that the absence of PARP-1 would lead to a reduction in muscular architectural damage, early inflammation, atrophy and fatty infiltration subsequent to combined tenotomy and neurectomy in an established PARP-1 knock-out mouse model^{3,5}. The aim of this study was to investigate the role of PARP-1 in regulating the potentially irreversible structural alterations after RCT utilizing macroscopic, histological, molecular, and radiological techniques.

METHODS

A total of 42 PARP-1 KO and 42 WT mice were included in the study. In both groups the animals were randomly assigned to three time points. These were then further subdivided for histological (Histology group), gene expression (PCR group) or MRI (MRI group, 12 week time point only) analysis (n=6 each). The surgery was carried out on the left shoulder and the contralateral shoulder served as an uninjured control. A 2 cm long skin incision was made over the shoulder joint and the deltoid muscle split parallel to its fibers to expose the underlying rotator cuff insertion and the tendons of the SSP and ISP were sharply detached from the humeral head. The suprascapular nerve was identified in the suprascapular notch and a 2 mm segment was resected. At the specified time points post surgery, the mice were euthanized and the muscles harvested.

For routine histology muscle cross-sections and longitudinal sections were stained with H&E and Picrosirius Red. To visualize intramuscular fat deposition, the SSP cross-sections were stained with an antibody against Fabp4. Fatty infiltration was graded from 0 to 5 (0= no intramuscular fat except around the main vessel; 1= Single intramuscular fat cells or fat cells that penetrate from the vessel into the muscle; 2= Streaks of fat cells into the muscle; 3=Fatty streaks in 2 of 4 quadrants of the muscle; 4=fat cells in all quadrants; 5=severe fatty infiltration). The pennation angle was measured in the longitudinal sections of the ISP muscle in the Picrosirius Red stained sections.

The samples for Real Time qPCR (RTqPCR) were stored in RNAlater at -20°C until RNA extraction. The TrizolPlus Kit (Life Technologies) was utilized for RNA extraction. RTqPCR was performed on a 7500 Fast Real-Time PCR system (Applied Biosystems) using TaqMan probes with Fast Advanced Mastermix for the expression of inflammatory (NF-κB, IL1-β, TNFα, IL-6), apoptotic (Caspase3, AIF), atrophic (FOXO1, MuRF, Atrogin1, Ube2b, Ube3a), regenerative (AKT, MyoD₁, Myf-5), fibrotic (TGFB₁ and MSTN) and fatty infiltration (PPARγ, Fabp4) genes. GAPDH serves as the housekeeping gene and relative levels of gene expression are measured with the ΔCt method.

We acquired T1 weighted images using a RARE sequence (Rapid Acquisition with Relaxation Enhancement) for the anatomic depiction. For the fat quantification in-phase and out-of-phase sequences were performed⁷. A linear polarized hydrogen whole-body mouse radiofrequency coil was used. With the acquired data a region of interest (ROI) analysis was done using in house Matlab routines (The MathWorks, Natick, MA) for the fat quantification.

Statistical analysis included analysis of variance (ANOVA) and post Hoc tests to reveal differences between the subgroups.

RESULTS

Retraction was quantified on MRI scans (**Table I**) at the 12 week time point. Both tendon and muscle retraction was significantly lower in the PARP-1 KO mice compared to the WT mice ($p = 0.012$ and $p = 0.081$ at 6 and 12 weeks respectively). The wet weight (**Table I**) of the SSP muscle decreased significantly in both the PARP-1 KO and in the WT mice (difference $p = 0.001$) in the first 6 weeks post surgery compared to the uninjured contralateral side ($p < 0.0001$). At 12 weeks the wet weight of the SSP in PARP-1 KO mice was almost normal whilst it remained significantly lower in the WT mice (difference $p < 0.0001$).

In comparison to the uninjured contralateral side of all animals, there was a statistically significant increase in pennation angle in the WT mice (**Fig. 1E**). Conversely, after an initial increase in the pennation angle in the PARP-1 KO mice it remained unchanged at the 6 and 12 weeks time points and did not reach statistical significance when compared to the controls (**Fig. 1E**). H&E staining of the SSP cross sections showed a higher inflammatory cell infiltrate at 1 week post injury in the WT mice. This was followed by an increase in degenerative changes in both groups, with muscle fibers undergoing degradation and atrophy at 6 weeks. PARP-1 KO mice had a higher number of regenerating fibers at this time point. After 12 weeks almost no degenerative changes were observed in either group. Muscles of the PARP-1 KO group had less fibrosis and better muscle architecture compared to the WT group. Fatty infiltration was present in both groups at 6 weeks (difference: $p = 0.578$, **Fig. 1B** and **C**). This decreased in the PARP-1 KO mice at 12 weeks post surgery, which was significantly lower than in the WT mice (difference $p = 0.043$). Intramuscular fat was also quantified in the in-phase and out-of-phase sequences of the MR scans. The relative amount of intramuscular fat was significantly lower in the PARP-1 KO group compared to the WT group (difference $p = 0.027$, **Fig. 1B**).

Gene expression analysis (**Fig. 2**) of various *inflammatory* genes revealed that TNF α mRNA was upregulated at 1 and 12 weeks after injury in both PARP-1 KO and WT mice without reaching statistical significance. IL1- β expression was upregulated at 1 and 6 weeks post surgery in the WT group without reaching statistical significance when compared to the PARP-1 KO mice. There was a significant upregulation of NF- κ B and the *proapoptotic* factor AIF at the 1-week time point in the WT group (**Fig. 2A**). The mRNA of the *proliferative factors* TGF β_1 and MSTN were also significantly upregulated in the WT group at 1 week (**Fig. 2B**). The *muscle atrophy* related Ubiquitin ligases MuRF1 and Atrogin-1 were present at significantly higher levels in the WT group consistent with the higher levels of Ubiquitin ligase Ube3a mRNA at the 1-week time point. The mRNA level of regulatory protein FOXO1 was also significantly upregulated in the WT mice at 6 weeks (**Fig. 2C**). The main regulator of *muscle regeneration* AKT was equally upregulated in the PARP-1 KO and WT group at 1 and 12 weeks. Both MyoD and Myf-5 mRNA were upregulated at week 1 and week 6 post surgery in both groups (**Fig. 2C**). The upregulation of both factors was significantly higher at week 1 in the WT group compared to the PARP-1 KO group. The mRNA levels of genes regulating *fatty infiltration* were significantly upregulated at 6 weeks in the WT group (**Fig. 2D**).

DISCUSSION

Disturbed muscular architecture, complete atrophy and fatty infiltration remain irreversible in chronic rotator cuff tears even after repair. The complex interplay of molecular and cellular mechanisms, which leads to potentially irreversible structural alterations in skeletal muscle has been described⁴. PARP-1 has shown to be a key regulator of inflammation, apoptosis, muscle atrophy, muscle regeneration and adipocyte development^{1;9}. Our study is the first to show that the absence of PARP-1 leads to a reduction in muscular architectural damage, early inflammation, apoptosis, atrophy and fatty infiltration after combined tenotomy and neurectomy of the rotator cuff muscle. PARP-1 is one of the upstream regulators that orchestrates the molecular and cellular mechanisms that leads to potentially irreversible structural alterations after RCT. It plays an important role in modulating the muscles reaction to RCT by promoting the immediate inflammatory response. This inflammatory response leads to apoptosis and damage to the muscle fibers and initiates muscular degeneration and atrophy. Architectural changes and loss of myocytes hinders the muscles ability to regenerate and ultimately leads to fatty infiltration.

There are limitations in this study. It could be suggested the differences observed in our study were due to reinnervation. Another possible criticism could be that we analyzed gene expression and not effective protein levels and their activity. The first time point of 1 week may be perceived as a bit delayed to assess inflammation.

It can be concluded that in the absence of PARP-1, the initial inflammatory response is dampened leading to less myocyte degeneration. Although the macroscopic muscles reaction to injury is similar in the first 6 weeks, its ability to regenerate is much greater in the PARP-1 KO group leading to a near normalization of the muscle substance and muscle weight, less retraction, and less fatty infiltration after 12 weeks. We conclude that PARP1 is a molecular regulator of muscular deterioration after RCT.

REFERENCES

1. Erener S, Hesse M, Kostadinova R, Hottiger MO. Poly(ADP-ribose)polymerase-1 (PARP1) controls adipogenic gene expression and adipocyte function. *Mol Endocrinol* 2012; 26:79-86. doi:10.1210/me.2011-1163 [pii] 10.1210/me.2011-1163.
2. Hong SJ, Dawson TM, Dawson VL. Nuclear and mitochondrial conversations in cell death: PARP-1 and AIF signaling. *Trends in pharmacological sciences* 2004; 25:259-64. doi:10.1016/j.tips.2004.03.005.
3. Kim HM, Galatz LM, Lim C, Havlioglu N, Thomopoulos S. The effect of tear size and nerve injury on rotator cuff muscle fatty degeneration in a rodent animal model. *J Shoulder Elbow Surg* 2012; 21:847-58. doi:10.1016/j.jse.2011.05.004.
4. Laron D, Samagh SP, Liu X, Kim HT, Feeley BT. Muscle degeneration in rotator cuff tears. *J Shoulder Elbow Surg* 2012; 21:164-74. doi:10.1016/j.jse.2011.09.027.
5. Liu X, Laron D, Natsuhara K, Manzano G, Kim HT, Feeley BT. A mouse model of massive rotator cuff tears. *The Journal of bone and joint surgery. American volume* 2012; 94:e41. doi:10.2106/JBJS.K.00620.
6. Lundgreen K, Lian OB, Engebretsen L, Scott A. Tenocyte apoptosis in the torn rotator cuff: a primary or secondary pathological event? *British journal of sports medicine* 2011; 45:1035-9. doi:10.1136/bjism.2010.083188.
7. Nozaki T, Tasaki A, Horiuchi S, Osakabe C, Ohde S, Saida Y et al. Quantification of Fatty Degeneration Within the Supraspinatus Muscle by Using a 2-Point Dixon Method on 3-T MRI. *AJR. American journal of roentgenology* 2015; 205:116-22. doi:10.2214/AJR.14.13518.
8. Pirinen E, Cantó C, Jo YS, Morato L, Zhang H, Menzies KJ et al. Pharmacological Inhibition of poly(ADP-ribose) polymerases improves fitness and mitochondrial function in skeletal muscle. *Cell Metab* 2014; 19:1034-41. doi:10.1016/j.cmet.2014.04.002.
9. Sakamaki J-i, Daitoku H, Yoshimochi K, Miwa M, Fukamizu A. Regulation of FOXO1-mediated transcription and cell proliferation by PARP-1. *Biochemical and biophysical research communications* 2009; 382:497-502. doi:10.1016/j.bbrc.2009.03.022.
10. Sishi BJ, Engelbrecht AM. Tumor necrosis factor alpha (TNF-alpha) inactivates the PI3-kinase/PKB pathway and induces atrophy and apoptosis in L6 myotubes. *Cytokine* 2011; 54:173-84. doi:10.1016/j.cyto.2011.01.009.
11. Zumstein MA, Jost B, Hempel J, Hodler J, Gerber C. The clinical and structural long-term results of open repair of massive tears of the rotator cuff. *The Journal of bone and joint surgery. American volume* 2008; 90:2423-31. doi:10.2106/JBJS.G.00677.

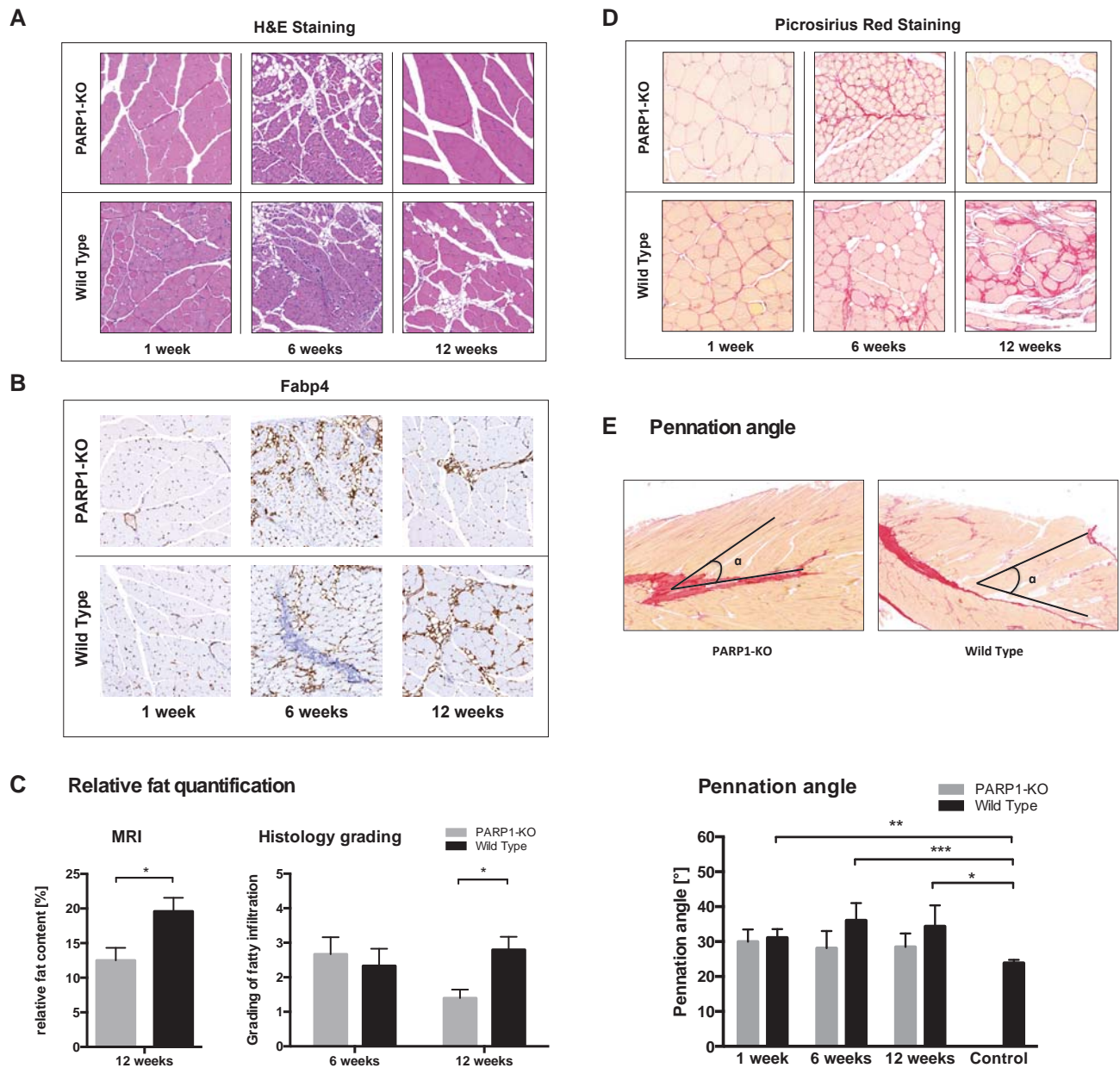
Table 1**TABLE I**

COMPARISON OF RETRACTION, MUSCLE WEIGHT AND PENNATION ANGLE BETWEEN PARP-1 KNOCK OUT AND WILD TYPE MICE

	PARP-1 Knock Out	Wild Type	P value
Retraction in MRI: *			
Tendon [mm]	2.2 ± 0.21	3.4 ± 0.41	0.012
Muscle [mm]	0.4 ± 0.23	1.8 ± 0.41	0.008
Muscle wet weight: †			
6 weeks	37 ± 3.4%	48 ± 3.2%	0.008
12 weeks	85 ± 1.7%	58 ± 2.1%	< 0.0001

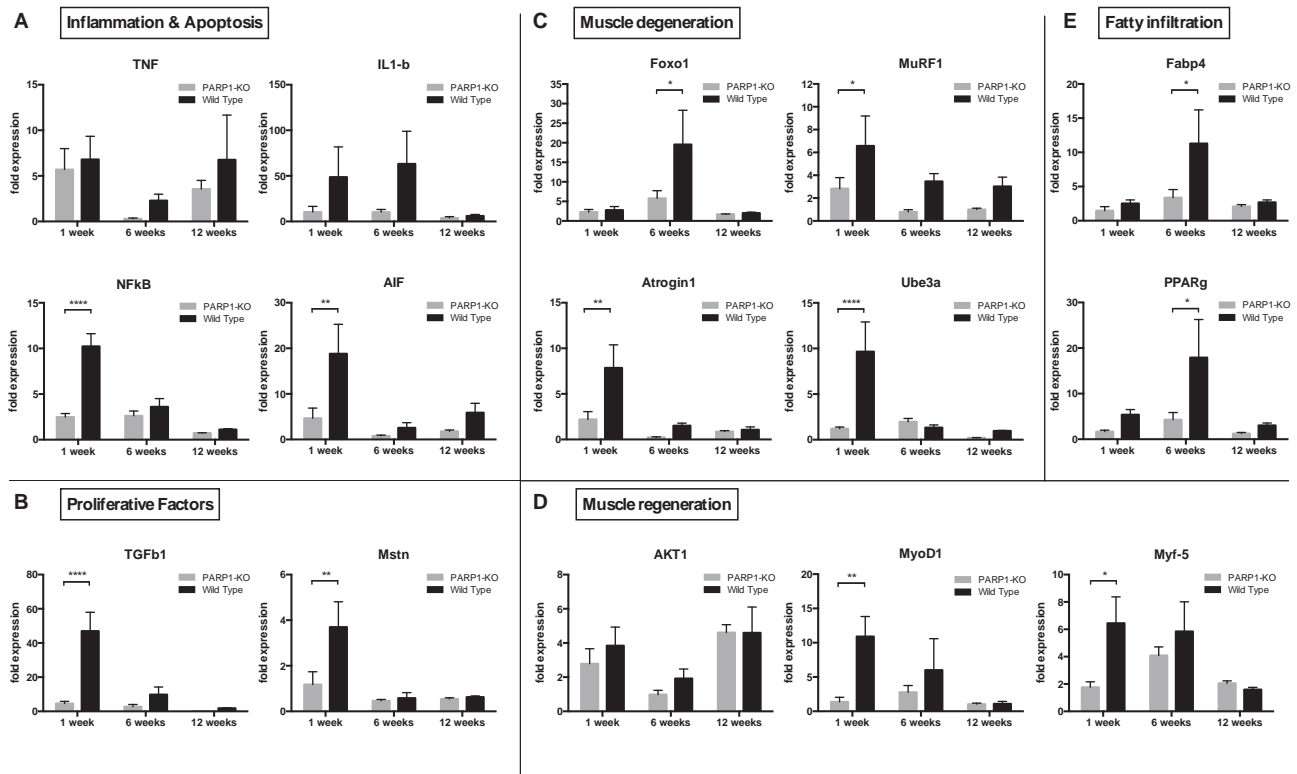
* Retraction was measured in the MR scans after 12 weeks † Muscle weight values are relative to the contralateral uninjured side. Statistical significant differences are shown. Values are mean ± SEM

Figure 1



Representative histological slides and results of the fat quantification and pennation angle measurement. A: Representative histological cross sections of the SSP stained with H&E after 1, 6 and 12 weeks. B: Representative histological cross sections stained with an antibody against Fabp4. C: Fat quantification in the SSP muscles. Relative fat quantification in the MR scans with a 2-Point Dixon Method on a 4.7T small animal MRI scanner and histological grading of the endo- and perimysial fat content in the cross sections of the SSP muscles stained with Fabp4. D: Representative histological cross sections of the SSP stained with Picrosirius Red to visualize the connective tissue. E: Pennation angle measurements in the Picrosirius Red stained longitudinal sections of the ISP muscles of PARP-1 KO and WT mice and bar graphs indicating the degree of the angle. The contralateral side of both groups acted as an uninjured control measurement. Statistical significant differences are shown * $p < 0.05$, ** $p < 0.01$ and *** $p < 0.001$.

Figure 2



Results of the gene expression analysis with real time RT-PCR. The increase of mRNA levels is shown as fold expression compared to the uninjured contralateral side with the Δ Ct method. A: Genes of the inflammatory cascade (TNF α , IL-1 β and NF- κ B) and apoptosis (AIF). B: Proliferative factors of the TGF β superfamily represented by TGF β 1 and Myostatin. C: Genes involved in the degeneration of muscle fibers. Foxo1 is the upstream regulator of the Ubiquitin-Ligases MuRF1 and Atrogin-1, which bind to Ube3a. D: Genes for muscular regeneration. AKT is the upstream regulator of the MRFs here represented by MyoD1 and Myf-5. E: Genes regulating fatty infiltration (PPAR γ) and binding of fatty acids (Fabp4). Statistical significant differences are shown * $p < 0.05$, ** $p < 0.01$ and **** $p < 0.0001$.

PODIUM PRESENTATION ABSTRACTS

INNOVATION IN HIP ARTHROSCOPY OVER THE PAST 10 YEARS

Marc J. Philippon, MD

The Steadman Clinic and Steadman Philippon Research Institute, Vail, CO

The hip is the second most common area for injury in collegiate athletes and may account for two to five percent of all sports injuries. Hip injuries are commonly seen in hockey, American football, soccer, dancers, golf, baseball and basketball. Hip injuries can be caused by repetitive motion, trauma, and use of the hip in extreme ranges of motion. In the last 10 years, femoroacetabular impingement (FAI) has been recognized as a the common cause of intra-articular damage and hip pain. Although FAI was first reported over 30 years ago, it has only become a focus in the hip. In cam impingement, an osseous bump located in the femoral head-neck junction is forced into the joint, most commonly in a flexed and adducted position with internal rotation, causing displacement of the labrum with eventual labral tear and detachment of the acetabular cartilage due to increased loads, friction and shear forces. For pincer impingement, the conflict consists of an abutment of the femoral neck against a retroverted or deep acetabulum causing compression of the hip labrum and subluxation of the joint with a usually postero-medial countercoup chondral lesion, in what is called the pincer impingement. Labral damage is almost always associated with FAI. Over the last 10 years, the diagnosis and treatment of FAI have significantly evolved. More is known about the anatomy and biomechanics of the hip and FAI. In addition, outcomes studies have shown predictors of superior results, which has led to specific treatment algorithms. In 2016, hip arthroscopy has more science supporting it and research continues.

TIMING OF POST-OPERATIVE MECHANICAL LOADING EFFECTS HEALING FOLLOWING ANTERIOR CRUCIATE LIGAMENT RECONSTRUCTION

CL Camp, AH Lebaschi, GT Cong, Z Album, C Carballo, L Ying, XH Deng, SA Rodeo
Tissue Engineering, Repair and Regeneration Program, Hospital for Special Surgery, New York, NY

INTRODUCTION

Robust healing of the bone-tendon interface is prerequisite for successful outcomes following anterior cruciate ligament reconstruction (ACL) with soft tissue grafts. Although the rate and strength of integration is dependent upon a multitude of factors, one of the most critical is the mechanical load the tissues are exposed to during the healing phase. The purpose of this work was to determine the effect of delayed onset mechanical loading on tendon-to-bone healing.

METHODS

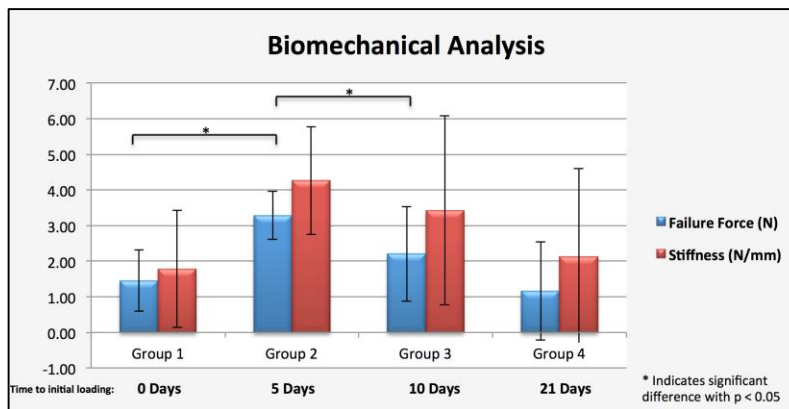
Using a flexor tendon autograft, ACL reconstruction was performed on 44 mice that were evenly randomized to four groups with differing times to initiation of post-operative mechanical load: 1) immediate, 2) five days, 3) ten days, or 4) twenty-one days. An external fixator (ex-fix) was placed across the knee at the time of surgery and removed when mechanical loading was scheduled to commence. Following ex-fix removal, animals were permitted full weight bearing and free, unrestricted cage activity. All mice were euthanized on postoperative day twenty-eight and bone-to-tendon healing was assessed by biomechanical testing, histological analysis, and micro-computerized tomography (micro-CT).

RESULTS

The mean failure force (\pm Standard Deviation [SD]) of the reconstructed ACL at the time of sacrifice for groups 1-4 was 1.46 ± 0.86 N, 3.29 ± 0.68 N, 2.21 ± 1.33 N, and 1.17 ± 1.38 N respectively ($p=0.008$). The greatest failure force was noted for Group 2 (six days immobilization) and post hoc pairwise comparisons revealed a mean difference (MD) of 1.84 N (95% CI 0.93 to 2.73; $p<0.001$) between groups 1 and 2; 1.08 N (95% CI -0.15 to 2.31; $p=0.08$) between groups 2 and 3; and 2.12 N (95% CI 0.83 to 3.41; $p=0.0041$) between groups 2 and 4. The mean stiffness (\pm SD) of groups 1 through 4 was 1.79 ± 1.64 N, 4.27 ± 1.51 N, 3.42 ± 2.65 N, and 2.13 ± 2.47 N respectively ($p=0.137$).

DISCUSSION

Following ACL reconstruction, a defined period of immobilization without weight bearing appears to improve biomechanical strength of the healing tendon to bone interface while prolonged periods without mechanical load and motion decrease the ultimate load to failure and stiffness in this murine model. Accordingly, patients may benefit from a brief period of immobilization and restricted weight bearing after ACL reconstruction; however, additional study in this clinical population is warranted.



DETECTION OF OSTEOCLASTIC ACTIVITY IN A MURINE MODEL OF ANTERIOR CRUCIATE LIGAMENT RECONSTRUCTION USING OPTICAL NEAR-INFRARED IMAGING AND CATHEPSIN K PROBE

AH Lebaschi, CL Camp, GT Cong, CB Carballo, Z Album, L Ying, J Zong, XH Deng, SA Rodeo
Tissue Engineering, Repair and Regeneration Program, Hospital for Special Surgery, New York, NY

INTRODUCTION

Reconstruction of the anterior cruciate ligament (ACL) using a tendon graft requires creation of bone tunnels in the femur and tibia. Healing of the graft-to-bone junction requires bone ingrowth into the tendon, and thus osteoblastic and osteoclastic activity is critical for the tendon-to-bone healing process. The aim of this study is to detect and profile osteoclastic activity in a murine ACL reconstruction model using a cathepsin K molecular probe, which has previously been used for in-vivo, non-invasive optical imaging to follow osteoclastic activity.

METHODS

Twenty-four C57BL/6 inbred wild-type mice underwent right ACL reconstruction and external fixation according to our established model. The mice were randomly allocated to six groups based on the day of imaging: 1) 3 days, 2) 6 days, 3) 10 days, 4) 14 days, 5) 21 days, and 6) 28 days. External fixator was left in place throughout the study. In each group, three mice received 2 nmol of cathepsin K probe (Cat K 680 FAST, PerkinElmer) via tail vein injection (study mice). One mouse in each group served as control and did not receive the probe (control mouse). All mice in each group received the probe via tail vein injection at 8 AM and underwent optical imaging (LICOR Pearl Impulse) six hours later. Imaging was performed using the 700nm channel. For analysis of signal intensity, background signal intensity in each mouse was defined as the signal detected in the area corresponding to the location of the contralateral knee.

RESULTS

Imaging revealed that mean signal intensity in study mice increased in magnitude from day #3 to reach a peak at day #14. This was followed by a gradual decline in signal intensity to reach baseline values at four weeks. Signal intensity in control mice did not show a specific pattern, although mean maximal signal intensity was observed on day #6 (Figure 1 & 2).

DISCUSSION

Osteoclastic activity, as reflected by cathepsin K probe signal intensity, reaches a peak at two weeks in immobilized knees following ACL reconstruction in mice and returns to baseline levels in four weeks. Nonspecific background signal also showed increased activity, although the detected signal was of lower intensity. This study provides insight into the temporal profile of osteoclastic activity following ACL reconstruction and could assist in timing therapeutic interventions to enhance graft-to-bone healing.

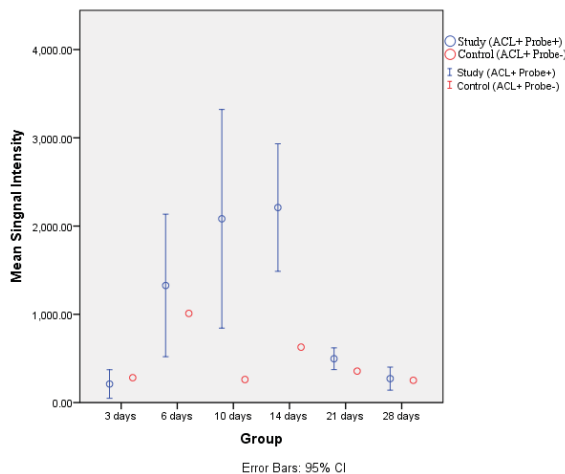


Figure 1. Image of a study mouse on day 14.

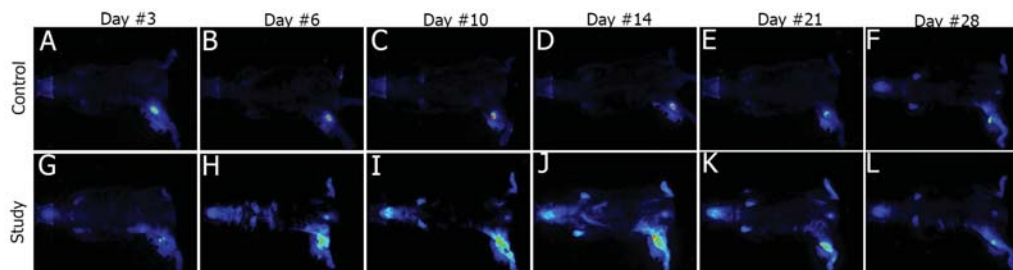


Figure 2. Signal intensity in study (G, H, I, J, K, and L) and control (A, B, C, D, E, and F) mice at different time points. Second row shows one study mouse from each group.

CONTRASTING EFFECTS OF RE-INJURY ON THE STRUCTURAL AND MATERIAL PROPERTIES OF THE RABBIT MEDIAL COLLATERAL LIGAMENT

Johnathan L. Sevick^{1,3}, Bryan J. Heard³, Ian K.Y. Lo³, Cyril B. Frank³, Nigel G. Shrive^{2,3}, Gail M. Thornton^{2,3}

¹Biomedical Engineering Graduate Program; ²Civil Engineering, Schulich School of Engineering;

³McCaig Institute for Bone and Joint Health; University of Calgary, Calgary, Alberta

INTRODUCTION

Athletes often re-injure ligaments in their knee when they return to activity [1]. The healing process in ligaments subject to a single injury has been the topic of substantial enquiry, as has the mechanical (structural and material) behaviour of such ligaments. To our knowledge, however, the effects of re-injury have not been well studied. Thus, we compared the structural and material properties of injured and re-injured ligaments in the same animal, using equivalence/non-inferiority evaluation with the null hypothesis that re-injured ligaments would be inferior, structurally and materially, to their contralateral singly injured counterparts.

METHODS

The medial collateral ligaments (MCLs) of 2 rabbit groups (each n=4) were used. For both groups, the MCLs of right hindlimbs were transected surgically and left hindlimbs underwent sham surgery. One week after this first surgery, the left MCLs in both groups were transected, the right MCLs in the transection re-injury group were transected a second time, and the right MCLs in the gap re-injury group underwent gap surgery. After 5-6 weeks of healing, ligaments underwent mechanical testing. Two compression-tension cycles (-5 N to +2 N) to evaluate MCL laxity preceded the measurement of MCL length and cross-sectional area (CSA). Cyclic creep testing (3600 cycles at 1Hz between +0.1 N and +20 N) was followed by recovery and elongation to failure at 20 mm/min.

Equivalence/non-inferiority tests comparing re-injured to injured MCLs (difference between right and left) were performed to establish the effect of re-injury on geometric (CSA), structural (failure load, stiffness, MCL laxity) and material (failure stress, cyclic creep strain) properties. The equivalence margins were based on published data [2].

RESULTS

Structural properties (failure load, stiffness, MCL laxity) of ligaments in both groups were statistically equivalent (Figure 1). Non-inferiority was established in the transection re-injury group, comparing transection re-injury to transection injury, for material properties (failure stress, cyclic creep strain) and CSA (Figure 1). Comparing gap re-injury to transection injury, material properties and CSA were shown to be potentially inferior (Figure 1).

DISCUSSION

For the specific transection re-injury model studied, re-injured MCLs were structurally equivalent and not materially inferior to their singly injured counterparts. Gap re-injured MCLs, on the other hand, were structurally equivalent and potentially materially inferior. These results appear to indicate different healing strategies depending on the severity of re-injury while achieving, early on, a similar level of structural performance.

The initial healing resulting from the first transection injury may not have been eliminated by the second transection re-injury, giving these ligaments the resources to heal at least as effectively as those being transected for the first time. A lack of in-situ tension in the injured ligaments [3] could have further benefitted transection re-injured ligament healing by lessening the distance to be bridged between ligament ends, conceivably approaching contact. Conversely, gap surgery likely eliminated a significant portion of the initial healing products in re-injured ligaments and, despite a lack of in-situ tension, left a relatively larger gap to be bridged between ligament ends. As a result, the healing capacity of gap re-injured ligaments may have been diminished, accounting for the potential material inferiority observed.

Accordingly, the material quality of transection re-injured ligaments is such that less material is required to attain the same structural characteristics of a transection injured ligament, whereas the material quality of a gap re-injured ligament may not be. The findings of our study suggest that there is a severity of re-injury below which there is no further detriment to the healing process, mechanical function and subsequent potential for re-injury. However, additional biological and mechanical exploration is required to fully explain the outcomes observed.

REFERENCES

- [1] Price, RJ et al., Br J Sports Med 2004, 38:466–471. [2] Majima, T et al., J Orthop Sci 2006, 11:272–277. [3] Frank, C et al., J Orthop Res 1983, 1:179-188.

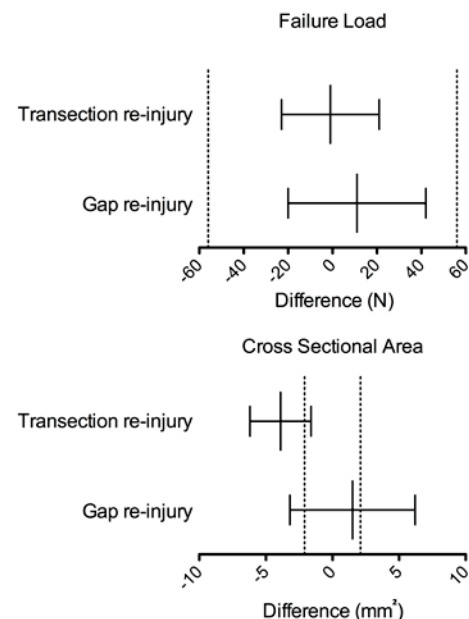


Fig. 1 (Top) Failure load (N) equivalence/non-inferiority test. (Bottom) Cross-Sectional Area (mm²) equivalence/non-inferiority test. Difference between right (re-injured) and left (injured) shown on the x-axis. Data are shown as mean +/- 90% confidence interval. Dashed lines indicate the equivalence margins.

THE LG/J MURINE STRAIN EXHIBITS NEAR-NORMAL TENDON BIOMECHANICAL PROPERTIES FOLLOWING A FULL-LENGTH CENTRAL PT DEFECT

J. R. Arble and J. T. Shearn

Biomedical Engineering Department, University of Cincinnati, Cincinnati, Ohio

INTRODUCTION

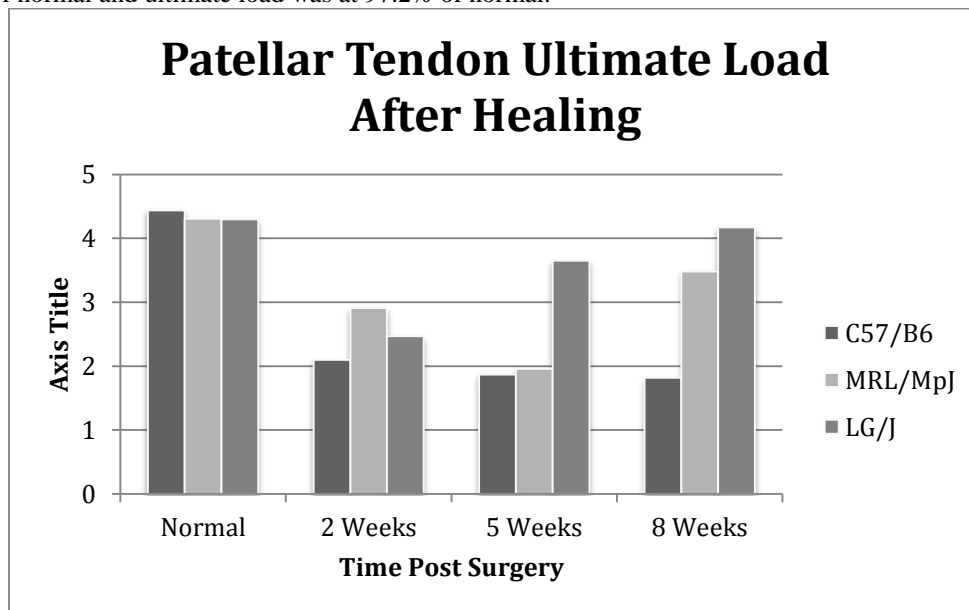
Musculoskeletal injuries are common in the United States, with injuries to tendons accounting for 30% of reported injuries.¹ Injuries to tendons are difficult to repair and usually do not heal to normal properties, resulting in a high risk of rerupture and often a need for further medical intervention. Understanding how tendons heal after injury is a vital part of creating successful strategies to improve healing outcomes. We have previously evaluated the tendon healing of the MRL/MpJ murine strain, which is known for regenerative healing. In this study, we evaluate the healing of the LG/J murine strain, which comprises 75% of the MRL/MpJ strain, to determine if the LG/J strain exhibits improved healing.

METHODS

A full-length central patellar tendon defect was introduced at 16 weeks of age. Mechanical properties and histology were assessed at 2, 5, and 8 weeks post surgery. Tissue stain markers were placed on the tendon and photographed throughout the tensile test to allow for calculations of regional strain. Tendons were loaded into grips and preloaded to a value of 0.02 N, at which point the tendons were photographed for cross-sectional area optical measurements. Tendons were tested in 37°C PBS, preconditioned from 0 to 1% strain for 25 cycles, and then ramped to failure at 0.1% of length/second.

RESULTS

Average LG/J structural properties improved to near-native values at 8 weeks, with normal tendons displayed an average ultimate load of 4.29 ± 1.5 N and stiffness of 10.88 ± 2.34 N/mm. Tendons after healing displayed an ultimate load of 4.17 ± 1.2 N and stiffness of 10.52 ± 3.40 N/mm. At 8 weeks, stiffness was at 96.7% of normal and ultimate load was at 97.2% of normal.



DISCUSSION

The LG/J strain returns to normal structural properties by 8 weeks, with a steady increase in properties at each time point. Future studies will focus on analyzing the transcriptome and the proteome to understand the healing process employed by the LG/J strain.

1. Kaux JF, Forthomme B, Le Goff C, et al. 2011. Current opinions on tendinopathy. J Sports Sci Med 10:238-253.

IMPACT OF INCREMENTAL FLEXOR RETINACULUM RELEASE ON CARPAL TUNNEL COMPLIANCE

Rubina Ratnaparkhi, Kaihua Xiu, Xin Guo, Zong-Ming Li

Hand Research Laboratory, Departments of Biomedical Engineering, Orthopaedic Surgery, and Physical Medicine & Rehabilitation, Cleveland Clinic, Cleveland, OH, USA

INTRODUCTION

The flexor retinaculum (FR) forms the roof of the carpal tunnel and consists of three segments known as the antebrachial fascia (AF), transverse carpal ligament (TCL), and distal aponeurosis (DA). FR release is the primary surgical treatment for carpal tunnel syndrome used to relieve median nerve compression in the carpal tunnel. *In vitro* studies have shown that FR release drastically impacts carpal tunnel biomechanics.^{1,2} However, it remains unclear how different amounts of FR release, including DA and AF release, alter the compliance of the carpal arch at both the proximal and distal levels. The purpose of this study was to investigate the effect of sequential FR release on carpal tunnel compliance (CTC). We hypothesized that CTC would increase with incremental FR release and that the impact of FR release would differ between the proximal and distal levels.

METHODS

Paired outward 10 N forces were applied to the insertion sites of the TCL at the distal (hamate-trapezium) and proximal (pisiform-scaphoid) levels of the carpal tunnel in nine fresh frozen cadaver hands. The FR was released incrementally with sequential transection of 25%, 50%, 75%, and 100% of the TCL, followed by DA release and then AF release. CTC was calculated at each level from the change in carpal arch width normalized to the 10 N force. Two-way repeated measures ANOVA was performed with post-hoc Tukey's test for pairwise comparisons.

RESULTS

With FR intact, CTC was 13.6 times greater at the proximal level (0.696 ± 0.128 mm/N) as compared to the distal level (0.056 ± 0.020 mm/N) (Fig. 1). At the distal level, a 100% TCL release was required to increase CTC significantly relative to the intact FR condition ($p < 0.001$). DA release yielded some gain in CTC beyond that with 100% TCL release, though this did not reach the level of statistical significance ($p = 0.052$). At the proximal level, a significant increase in CTC relative to CTC with FR intact was seen with 50% TCL release ($p < 0.001$). 75% TCL release increased CTC beyond the gain with 50% TCL release, and 100% TCL release further significantly increased CTC relative to CTC with 75% TCL release ($p < 0.05$). DA release had minimal effect on CTC versus 100% TCL release at the proximal level ($p = 0.987$). Complete FR release provided further gain in CTC relative to 100% TCL release at both levels ($p < 0.05$). The distal carpal tunnel was more rigid than the proximal level regardless of FR status, though FR release reduced the difference in CTC across levels. Overall, complete FR release increased CTC relative to CTC with FR intact by 0.166 ± 0.041 mm/N (293%) at the distal level and by 0.365 ± 0.137 mm/N (52%) at the proximal level.

DISCUSSION

We demonstrated that FR release increases carpal tunnel compliance and that the impact of FR release steps on CTC is dependent on extent of FR release and location in the carpal tunnel. We showed that 100% TCL release was required to increase CTC at the distal level and significantly augmented CTC relative to 50% or 75% TCL release at the proximal level. Moreover, complete release of the FR, including the DA and AF, further enhanced CTC relative to the increase seen with 100% TCL release alone. This suggests that incomplete FR release limit potential gains in carpal tunnel structural flexibility. FR release increased local compliance to a greater extent at the distal carpal tunnel relative to the proximal level, which is of interest given its greater inflexibility and its significance as a common site of median nerve entrapment. In conclusion, the increase in CTC with FR release helps explain the benefit of carpal tunnel release surgery for median nerve decompression in carpal tunnel syndrome. Complete FR release is important to increase compliance effectively, particularly at the more rigid distal carpal tunnel.

REFERENCES

1. Tengrootenhuysen et al. (2009) *Acta Orthop Belg* 75:467-471. 2. Xiu et al. (2010) *Clin Biomech* 25:776-780.

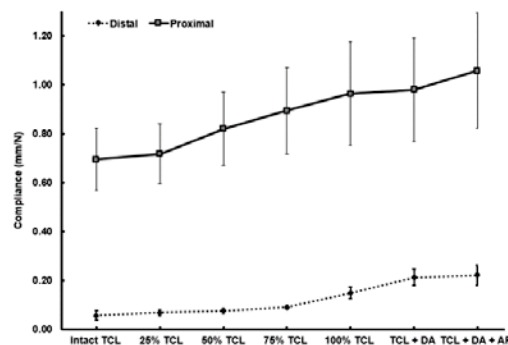


Fig. 1. Carpal tunnel compliance (CTC) as a function of FR transection

KINEMATICS OF ACL-DEFICIENT AND HEALTHY KNEES DURING STAIR DESCENT: AN APPLICATION OF A CLINICIAN-FRIENDLY MOTION CAPTURE SYSTEM

K.M. Mok, E. Chua, M.Y. Yeung, S.C. Fu, P.S.H. Yung, K.M. Chan

Department of Orthopaedics and Traumatology, Faculty of Medicine, The Chinese University of Hong Kong

INTRODUCTION

The anterior cruciate ligament (ACL) is important in stabilizing the human knee joint, not only restricting the anterior translation but also the axial and frontal plane movement of the knee. Stair descending is common daily ambulatory task which demands knee stability¹. A previous study reported that ACL deficiency knees exhibited less flexion / extension range of motion (ROM), less internal rotation and less valgus². In this study, a clinician-friendly motion capture system, which enables efficient collection of knee kinematic data within a limited space, was used to evaluate altered kinematics in ACL-deficient patients, with comparison made to healthy controls. We hypothesized that ACL deficient knees would show less movement compared to the healthy knees.

METHODS

A total of 12 healthy subjects, and 12 ACL-deficient patients, with or without concomitant meniscal injury were recruited in this study. Tibiofemoral joint kinematics was measured using an optoelectronic motion capture system (Opti-Knee®, Shanghai Innomotion Inc., China). A total of 8 reflective markers were attached on the lateral side of the lower limb, with 4 on the thigh and the remaining on the calf. Each of the testing subjects performed the stair descending task from a 2-steps platform with an 80Hz beat rhythm. Each step was 20 cm high. Three successful trials were acquired for each of the subjects. Knee kinematics was calculated at each frame during the motion task by the geometric relationships between the reflective markers under the established femur and tibia coordinate systems upon calibration. The knee kinematics between foot strikes was regarded as a complete gait cycle. Measures of selected kinematic variables were compared between the 2 limbs within each groups using paired t-tests, and on the side-to-side difference between the 2 subject groups using independent t-tests. Statistical significance was denoted at an alpha level of 0.05.

RESULTS

Among all selected kinematics variables, only the side to side difference of the internal rotation reached statistical significance between ACL deficient patients and healthy controls, as showed in table 1. Among all 12 ACL deficient patients, half of them were having a higher knee internal rotation on the injured side.

Table1. Selected knee joint kinematic variables during stair descent.

	Healthy controls		ACL deficient patients		Side to side difference	
	Dominant	Non-dominant	Injured	Non-injured	Healthy	ACL deficient
Flexion (°)	90.0 (7.2)	89.9 (5.2)	90.4 (6.9)	89.0 (7.0)	5.2 (3.0)	5.3 (4.2)
Flexion / Extension ROM (°)	88.7 (7.0)	87.3 (5.1)	88.9 (7.0)	88.3 (7.5)	5.0 (3.6)	6.2 (4.0)
Valgus (°)	21.6 (10.6)	16.7 (6.4)	17.1 (7.7)	18.0 (4.8)	8.9 (10.5)	6.4 (7.2)
Valgus / Varus ROM (°)	21.6 (10.4)	17.4 (4.8)	18.0 (7.3)	17.8 (4.8)	7.8 (10.2)	5.9 (7.2)
External rotation (°)	5.5 (5.4)	3.8 (2.3)	6.3 (4.9)	7.0 (7.3)	3.7 (3.0)	6.5 (5.7)
Internal rotation (°)	9.0 (5.6)	11.6 (4.7)	9.7 (6.8)	9.6 (5.2)	3.7 (3.5)*	6.7 (3.1)*
Internal / External ROM (°)	14.3 (2.6)	15.3 (4.2)	16.0 (4.0)	16.6 (5.8)	3.0 (3.2)	4.2 (2.9)
Ant-posterior translation (cm)	2.4 (0.5)	2.5 (0.7)	2.8 (0.7)	2.8 (0.6)	0.5 (0.4)	0.8 (0.6)
Distal-proximal translation (cm)	1.8 (1.3)	1.7 (0.9)	1.6 (0.6)	1.6 (0.6)	0.5 (0.8)	0.6 (0.5)
Med-lateral translation (cm)	2.0 (0.6)	1.9 (0.4)	1.9 (0.3)	1.9 (0.5)	0.5 (0.3)	0.4 (0.3)

* Statistical difference between healthy subject and ACL deficient patients at level $p < 0.05$

DISCUSSION

Our study has shown that ACL deficient patients have significant alternation in limb symmetry of the knee internal rotation. The results have suggested the potential use of the current optoelectronic motion analysis system in clinical application. Further study will be using the current protocol to investigate the rehabilitation progress of ACL reconstructed patients, in order to determine the return-to-sport criteria.

REFERENCES

- 1) Kutzner et al., J Biomech. 2010, 43: 2164-2173.
- 2) Gao et al., Hum Mov Sci. 2012, 31: 222-235.

TRANSVERSE CARPAL LIGAMENT AND TENDON INTERACTION IN THE CARPAL TUNNEL

Tamara L. Marquardt, Joseph N. Gabra, Joshua L. Gordon, Zong-Ming Li
Hand Research Laboratory, Departments of Biomedical Engineering, Orthopaedic Surgery,
and Physical Medicine & Rehabilitation, Cleveland Clinic, Cleveland, OH, USA

INTRODUCTION

The transverse carpal ligament (TCL) arches over the carpal tunnel contents and serves many biomechanical functions, including resisting the volar displacement of the flexor tendons to prevent “bowstringing”. This function has been demonstrated *in vitro* for different wrist postures^{1,2}; however, the biomechanical interaction between the TCL and flexor tendons has not been examined *in vivo*. The purpose of this study was to investigate the *in vivo* biomechanical interaction between the TCL and flexor tendons during finger loading under various wrist postures. It was hypothesized that wrist flexion and loading would lead to increased biomechanical interaction between the TCL and index finger flexor tendons, indicated by an increase in TCL arch height.

METHODS

Eight (n = 8) healthy, female subjects (26.9 ± 7.1 years old) participated in this study. With a custom apparatus, the wrist was placed in 20° extension (-20°), neutral (0°), 20° flexion (+20°), or 40° flexion (+40°) while the index finger was isometrically loaded at the distal phalange (Fig. 1). Within each wrist posture, an ultrasound image at the distal level of the carpal tunnel was captured with the index finger 1) unloaded (0 N) and 2) after 5 seconds of 15 N of isometric loading. Three trials were collected for each subject with one minute of rest between trials. *ImageJ* was used to outline the TCL and select the most volar points of the hamate and trapezium in each ultrasound image. The coordinates obtained in *ImageJ* were transformed to a defined anatomical coordinate system using a custom *MATLAB* program (Fig. 2). The TCL arch height, defined as the maximum volar point of the TCL was found for each condition. A two-way (4x2) RMANOVA with factors of wrist posture (-20°, 0°, +20°, +40°) and load (0 N and 15 N) was performed with Tukey’s post-hoc tests for pairwise comparisons ($\alpha = 0.05$).

RESULTS

TCL arch height increased with wrist flexion, and this phenomenon was amplified with finger loading (Fig. 3). Wrist posture and load significantly affected TCL arch height ($p < 0.001$), and there was also a significant posture × load interaction ($p < 0.001$). For the unloaded condition, the posture of +40° had a significantly greater TCL arch height than postures of -20°, 0°, and +20° ($p < 0.05$). As wrist posture changed from 0° to +40°, TCL arch height increased by 0.97 ± 0.32 mm. When the index finger was loaded, there were significant increases in TCL arch height for the postures of +20° and +40° in comparison to 0° posture ($p < 0.05$). Within wrist postures, loading significantly increased TCL arch height by 0.56 ± 0.34 mm and 0.91 ± 0.44 mm for +20° and +40° postures, respectively ($p < 0.001$, Fig. 3). The greatest change in TCL arch height occurred between the (0°, 0 N) condition and the (+40°, 15 N) condition, where the arch height increased from 0.79 ± 0.56 mm to 2.67 ± 0.56 mm.

DISCUSSION

Ultrasonography was used to examine the *in vivo* changes of TCL arch height associated with wrist posture and finger loading. As expected, TCL arch height increased with wrist flexion and finger loading due to volar migration of the flexor tendons inducing a biomechanical interaction between the structures. The phenomenon of TCL arch height increase has been shown *in vitro* when a volarly directed force was applied to the TCL³. In this *in vivo* study, we found that a higher degree of wrist flexion resulted in an increased TCL arch height. Additionally, the combination of wrist flexion and finger loading intensified this ligament-tendon interaction as quantified by increased arch height. This study provides visual and quantitative evidence of the *in vivo* biomechanical interaction between the TCL and flexor tendons which may lead to undesirable compression of the median nerve as well as tissue remodeling of TCL and tendon hypertrophy.

REFERENCES

- 1) Kline et al. (1992) *J Bone Joint Surg Am* 74:1478-1485.
- 2) Armstrong & Chaffin (1978) *J Biomech* 11:119-128.
- 3) Li et al. (2009) *J Biomech Eng* 131:081011.

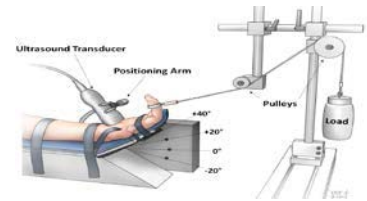


Fig 1. Experimental setup used to control wrist posture and index finger loading.

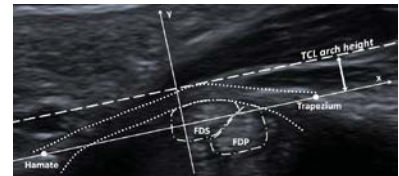


Fig 2. Representative ultrasound image with the hamate, trapezium, TCL, TCL arch height, and flexor tendons identified.

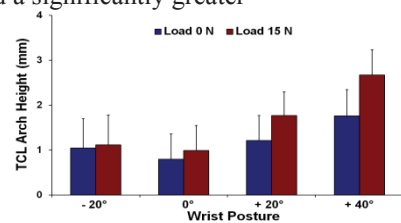


Fig 3. TCL arch heights at various wrist postures and loading conditions.

ORIENTATION AND SIZE CHANGES IN THE PORCINE ANTERIOR CRUCIATE LIGAMENT THROUGHOUT SKELETAL GROWTH

Stephanie Cone¹, Jeffrey Spang², Lynn Fordham³, Jorge Piedrahita⁴, Matthew Fisher^{1,2}.

¹Translational Orthopaedic Research Laboratory, Department of Biomedical Engineering, University of North Carolina – Chapel Hill and North Carolina State University, Raleigh, NC; ²Department of Orthopaedics, University of North Carolina – Chapel Hill, Chapel Hill, NC; ³Department of Radiology, University of North Carolina – Chapel Hill, Chapel Hill, NC; ⁴College of Veterinary Medicine, North Carolina State University, Raleigh, NC.

INTRODUCTION

Injuries to the anterior cruciate ligament (ACL) of the knee joint are common in the athletic population¹, and incidence rates among pediatric patients are rapidly increasing, likely due to increases in youth sports participation². Recently, changes in the orientation of the human ACL during skeletal growth have been reported, specifically an increase in the sagittal and coronal angles of the ligament relative to the tibial plateau³. As a step toward developing a large animal model to study pediatric ACL injuries, we hypothesized that similar changes in orientation are present in a common pre-clinical model. The objective of this study was to quantify changes in the orientation and size of the ACL in the porcine model during skeletal growth.

METHODS

Hind limbs were collected from female Yorkshire pigs from near-birth through late adolescence, specifically at 1.5 months (n=6), 3 months (n=6), 6 months (early adolescence, n=6) and 18 months (late adolescence, n=5), and the stifle (knee) joints were isolated. The joints were imaged using a 7.0 Tesla Magnetic Resonance Imaging (MRI) system (Siemens Magnetom) within the Biomedical Research Imaging Center at the University of North Carolina – Chapel Hill. Scans were performed using a double echo steady state (DESS, flip angle: 25°, TR: 17ms, TE: 6ms) sequence with a voxel size of 0.42x0.42x0.4 mm. Images were analyzed using commercial software (ScanIP, Simpleware) to measure the coronal and sagittal angles of the ACL relative to the tibial plateau as well as the total length of the ACL in the sagittal plane and cross-sectional area of the ACL in the midsubstance. Statistical analysis consisted of one-way analysis of variance with a Bonferroni post-hoc ($p < 0.05$).

RESULTS

The average sagittal angle of the ACL increased steadily by 32° from 1.5 months to 18 months of age, with statistically significant changes between each age group ($p < 0.05$, Fig. 1A). The average coronal angle of the ACL also increased by 27° from 1.5 months to 6 months of age ($p < 0.05$), with no further changes by 18 months of age ($p > 0.05$).

In terms of the overall size of the ACL, the anterior length of the ACL increased by 2.7 fold from 1.5 to 6 months ($p < 0.05$), with less dramatic increases by 18 months ($p < 0.05$). The posterior length of the ACL increased by 3.2 fold from 1.5 to 6 months ($p < 0.05$), with no further increases by 18 months ($p > 0.05$). Similarly, the cross-sectional area of the ACL increased by 6 fold from 1.5 to 6 months ($p < 0.05$) (Fig. 1B), with no further increases by 18 months ($p > 0.05$).

DISCUSSION

In support of our hypothesis, the coronal and sagittal angles of the porcine ACL relative to the tibial plateau increased during skeletal growth, similar to data reported in humans³. Interestingly, the sagittal angle continued to increase from early to late adolescence, while the coronal angle did not. The length and cross-sectional area of the ACL also increased rapidly until early adolescence, with little to no changes afterward. This data suggests that the porcine model may be useful to study ACL function, injury, and treatment during skeletal growth.

REFERENCES

¹Jung HJ+. *Sports Med Arthrosc Rehabil Ther Technol*. 1(9): 2009. ²Collins S+. *Pediatr Therapeut*. 4(2): 2014. ³Kim HK+. *Radiology*. 247(3): 2008.

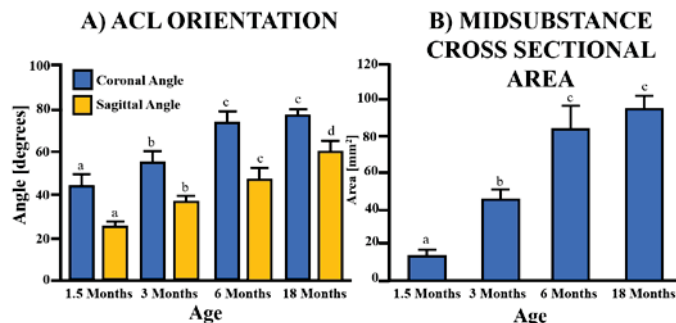


Figure 1. (A) ACL orientation and (B) midsubstance cross-sectional area during skeletal growth. Different letters indicate statistical significance between age groups ($p < 0.05$).

THE ROLE OF SPARC IN MECHANOSENSING FUNCTION OF TENDON

Tao Wang^{1,2}, Christine Thien¹, Kai Song¹, Aswin Beck¹, Qiujuan Zheng² and Minghao Zheng¹

1. Translational Orthopaedic Research Centre, The University of Western Australia, WA, Australia

2. Guangdong General Hospital & Guangdong Academy of Medical Sciences, Guangdong, China

INTRODUCTION

Secreted protein acidic and rich in cysteine (SPARC) is a matricellular collagen-binding glycoprotein that modulates the interaction of cells with the extracellular matrix (ECM) by regulating cell adhesion and matrix assembly. SPARC is widely expressed in bone and tendon, thus we investigated its role in tendon development by comparing wild-type (WT) and SPARC-deficient (KO) mice.

METHODS

Mouse tendons were examined histologically and their gene expression profile of differentiation markers compared by RT-qPCR. We isolated tendon derived stem cells (TDSCs) for stem cell differentiation assays and to generate tendon-like tissue which was then subjected to 6% cyclic tensile strain (0.25Hz, 8h/d for 6 days) in a bioreactor. Extracted proteins were examined by Western blotting. Mice were run on a treadmill (12m/min, 13° incline for 2hr/day for 16 days) to determine the effect on the Achilles tendon.

RESULTS

We found that adult SPARC^{-/-} mice exhibit hypoplastic tendons at load bearing regions throughout the body (Fig. 1A). The hypoplastic tendon phenotype developed between 10d and 3wk post-natally, when mice become increasingly mobile (Fig. 1B). Likewise, the Achilles tendon gene profiles were not significantly different at 10 days, whereas increased osteogenic and adipogenic markers and decreased tenogenic markers were detected in 3wk old SPARC^{-/-} mice compared to WT mice (Fig. 1C). TDSCs from SPARC^{-/-} mice showed increased proliferation rate, osteogenic and adipogenic differentiation potential but weaker chondrogenic differentiation potential (Fig. 2A,B). Importantly, SPARC^{-/-} TDSCs were still able to form tendon-like tissue but with much less ECM formation compared to WT (Fig. 2B). Mechanical loading activated the AKT and S6 Kinase pathways in WT tendon-like tissue, however pS6K was only slightly activated, and collagen type I production was strongly inhibited by mechanical stimulation of KO tendon-like tissue (Fig. 2B). The *in vitro* defects seen in the SPARC KO in response to mechanical stimulation was confirmed by the treadmill assay, where ruptured Achilles tendons were observed in SPARC^{-/-} mice but not in WT mice after 16 days (Fig. 2D).

DISCUSSION

Our data demonstrate SPARC plays a critical role in the development and mechanosensing function of tendon tissue. An absence of SPARC can inhibit signaling pathways and reduce the type I collagen production stimulated by mechanical stimulation resulting in impaired tendon development and compromised tendon remodeling.

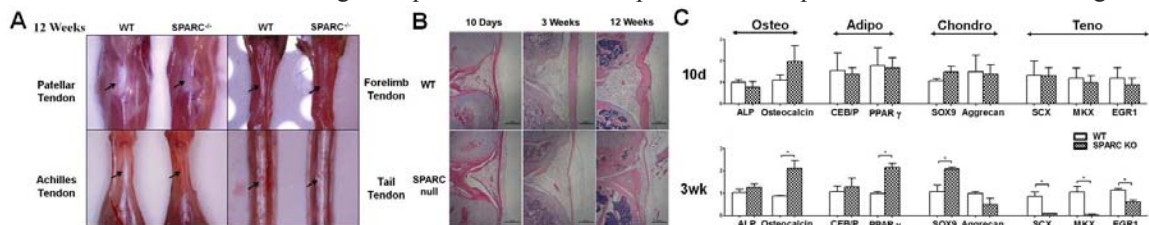


Fig. 1. (A) Tendon defects in adult SPARC null mice. (B) Impaired patellar tendon development in SPARC null mice is detectable by 3 weeks of age. (C) Differentiation marker gene profiles of Achilles tendon from WT and KO mice at 10 days and 3 weeks.

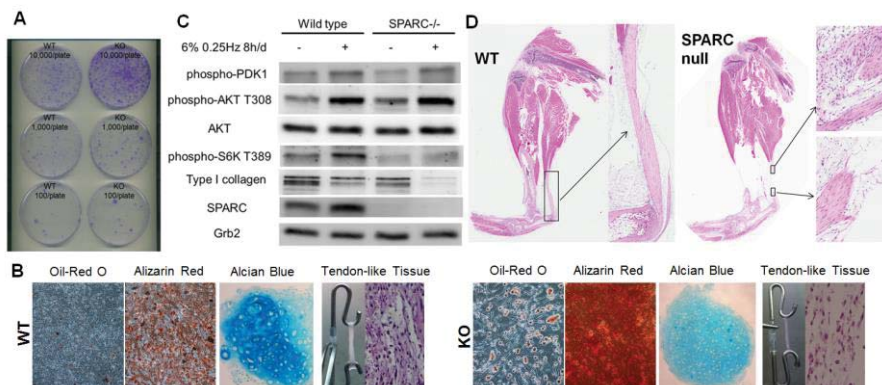


Fig 2. (A) Colony forming ability of TDSCs. (B) Adipogenic, osteogenic, chondrogenic and tendon-like tissue formation ability of WT and SPARC null TDSCs. (C) Collagen production and activation of the AKT-S6K pathway by mechanical stimulation is inhibited in SPARC^{-/-} tendon-like tissue. (D) Histology of Achilles tendon showing tendon rupture in the SPARC KO after 16 days of running.

ORIGIN OF CELLS THAT CONTRIBUTE TO MURINE ROTATOR CUFF TENDON HEALING

Ryu Yoshida¹, Nathaniel Dymant¹, Farhang Alaei¹, Augustus Mazzocca¹, David Rowe¹
¹University of Connecticut Health Center, Farmington, Connecticut, USA

INTRODUCTION

Little is known about the source and/or phenotype of cells that participate in rotator cuff healing. The purpose of this study was to elucidate the origin of cell populations that contribute to rotator cuff healing.

METHODS

Transgenic Mice: Three inducible Cre mice with gene promoters driving Cre recombinase with a modified estrogen receptor (ERT2) were crossed with Rosa26-tdTomato (Ai9) Cre reporter mice to label specific cell populations and their progeny: 1) PRG4-CreERT2 x Ai9 (PRG4-9) – the Prg4 gene which encodes for lubricin, 2) α SMA-CreERT2 x Ai9 (SMA-9) – Acta2 gene, which encodes for alpha smooth muscle actin, 3) AGC-CreERT2 x Ai9 (AGC-9) – Acan gene which encodes for aggrecan. **Surgery:** At 12 weeks of age, mice were injected with 80 μ g/g of tamoxifen intraperitoneally, and a full thickness, central defect was created in the supraspinatus tendon insertion with a 29G needle. **Histology** Frozen sections (8 μ m) of shoulders harvested at 1, 2, and 5 weeks (n = 5-6 per group) were made using cryofilm in both coronal and sagittal orientations. Each section was imaged twice consecutively; first for tdTomato fluorescence and DAPI and second for toluidine blue. Images from each section were aligned to correlate the fluorescence to cell morphology and anatomy.

RESULTS

Uninjured shoulder: In the PRG4-9 mice, a small population of Tomato+ cells in the body of the supraspinatus and the paratenon on the bursal side of the tendon were seen. Tomato+ cells were also seen in the articular cartilage. In the AGC-9 mice, Tomato+ cells in the articular cartilage as well as unmineralized fibrocartilage at the supraspinatus tendon enthesis were seen. No fluorescent cells were evident elsewhere in the tendon. SMA-9 mice showed Tomato+ cells in the paratenon, subacromial bursa, and blood vessels.

Injured shoulder: Three notable changes were seen consistently in shoulders of all three transgenic mice (Fig.1). First, a long thin layer of tissue formed over the bursal side of supraspinatus tendon (arrow 1). Second, the proximal region of the tendon adjacent to the injury site became more hypercellular and disorganized (arrow 2). Finally, the remaining distal stump of the supraspinatus insertion site became acellular (arrow 3).

In the PRG4-9 and SMA-9 mice, 56 \pm 14(SD)% and 44 \pm 11% of cells within the layer of healing tissue overlying the injured supraspinatus tendon were Tomato+ (p > 0.05). In contrast, only 1% of cells were Tomato+ in the AGC-9 mice (p < 0.05). There was significant expansion of Tomato+ cells in the hypercellular region of the tendon (arrow in Fig. 2D) in the PRG4-9 mice but not the SMA-9 and AGC-9 mice (p < 0.05).

DISCUSSION

PRG4-9 and SMA-9 labeled cells contributed to significantly larger proportions of supraspinatus healing than the AGC-9. Consistent with our previous study on patellar tendon healing [Dymant et al. PLoS One 2013], the main contributors to the healing response came from outside the tendon. While our patellar tendon studies indicated that these cells were from either a paratenon or perivascular origin, cells contributing to supraspinatus healing were from a paratenon and not the perivascular origin (perivascular cells were not Tomato+ in PRG4-9). However, the supraspinatus is covered by muscle (deltoid) unlike the patellar tendon. Cells within the inner lining of the deltoid perimysium are Tomato+ in both the PRG4-9 and SMA-9 models and could contribute to the new tissue on the bursal side. In the uninjured tendon, these cells reside predominantly on the bursal side of supraspinatus; this finding suggests the importance of bursal sided, extra-articular cells to rotator cuff tendon healing.

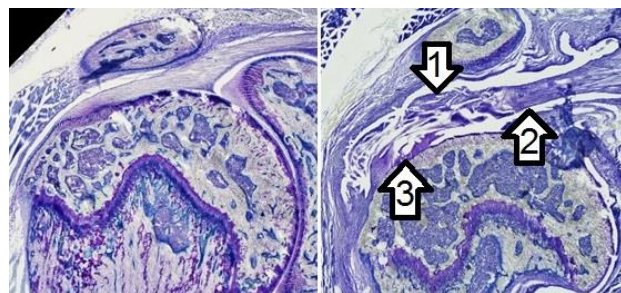


Fig. 1: Coronal sections of normal (left) and injured (right, 2 weeks post-op) shoulders stained with toluidine blue

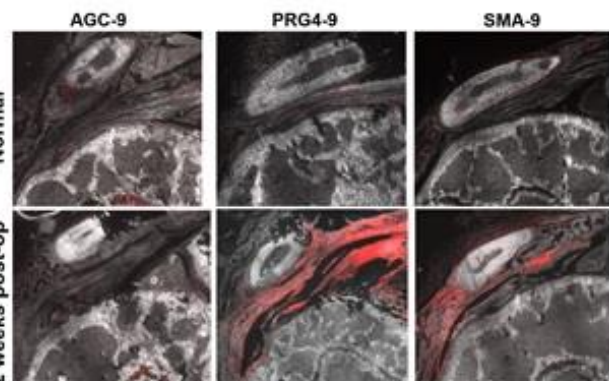


Fig. 2: Coronal sections of shoulder from 3 Cre transgenic mice

STEM/PROGENITOR CELL RECRUITMENT TO DETERIORATING TENDONS IN MICE WITH CONDITIONAL DELETION OF TGF-BETA TYPE II RECEPTOR

Guak-Kim Tan¹, Anna G. Stabio¹, Doug R. Keene¹, Brian A. Pryce¹, Ronen Schweitzer^{1,2}

¹Shriners Hospitals for Children, Portland, OR, ²Oregon Health and Science University, Portland, OR, USA.

INTRODUCTION

Recent studies have demonstrated that tendon stem/progenitor cells (TSPC) can be isolated from the tendon midsubstance and epitenon [1]. Nothing however is known about the possible fate and roles of TSPC in normal tendon growth and degenerative processes (e.g. tendinopathy). Using a scleraxis-Cre (ScxCre) tendon deleter, we have previously showed that targeted deletion of TGF- β type II receptor (T β R2) resulted in the loss of differentiation status of tenocytes in postnatal stages [2]. Here, we further investigated the consequences of the phenotype and observed a progressive deterioration of mutant tendons, accompanied by recruitment of new tenocytes with stem/progenitor cell-like characteristics, suggesting that this may be a useful model for studies of tendon degeneration as well as TSPC activation and recruitment in vivo.

RESULTS

At P0, tendons of T β R2;ScxCre mutants (CKO) were structurally intact but later exhibited varying degrees of tissue defects. While some tendons were septated and then ruptured within days, the other tendons persisted but appeared smaller than their wild-type counterparts (not shown). Despite these early defects, severe disruption of epitenon and disorganization of collagen matrix were observed only in older pups as revealed by transmission electron microscopy (TEM) (Fig.1). Strikingly, while the majority of cells in the deteriorating tendons lost expression of differentiation markers (Fig. 3a,b and [2]), from P3 onwards we observed the appearance of large and rounded cells that are positive for ScxGFP, Col1a1 and Tenomodulin (Fig. 2 and not shown). Moreover, most of these cells exhibited weak Rosa-tdTomato Cre reporter signal and still retained T β R2 expression ([2] and Fig. 3a), prompting us to ask if these cells are newly recruited. To more directly examine this possibility we utilized the mTmG dual Cre reporter that allows simultaneous visualization of both recombined and non-recombined cells [3]. In P7 het control, all tenocytes were recombined (Fig. 2b). On the other hand, in CKO some of the ScxGFP-positive cells have recombined whereas some did not (Fig. 2c), suggesting a very recent induction of Scx (and therefore ScxCre) expression. These findings suggest a tendon cell recruitment in response to the deterioration/degeneration in T β R2;ScxCre CKO tendons. Using immunohistochemistry we obtained further support for the stem/progenitor nature of these cells since they stained positively for the stem/progenitor cell markers Sox9 and nucleostemin (Fig.3b,c).

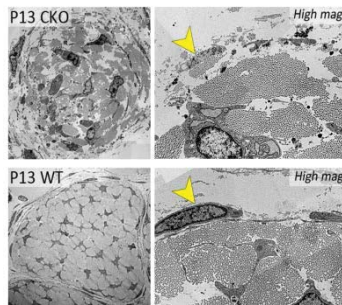


Fig.1: Tendon deterioration/degeneration in T β R2;ScxCre mutants. TEM analysis revealed that in comparison with the wild-type (WT) tendon the mutant (CKO) tendon showed disorganized collagen matrix and disrupted epitenon structures surrounding the tissue (yellow arrow).

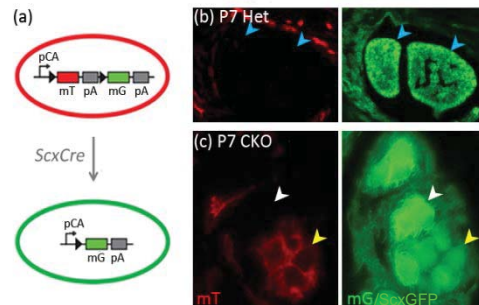


Fig.2: The cells that retained ScxGFP expression in T β R2;ScxCre CKO tendons are likely newly recruited cells. (a) In the mTmG dual-color reporter system [3], the membrane-tdTomato (mT) cassette is deleted in the ScxCre-expressing cells, allowing the expression of the GFP (mG), as shown here in the (b) het control (T β R2^{+/+};ScxCre) (blue arrow). (c) In CKOs, some of the ScxGFP-positive cells have lost mT expression, i.e. recombined (white arrow), whereas some did not recombine (yellow arrow), suggesting a very recent induction of Scx expression, i.e. newly recruited cells.

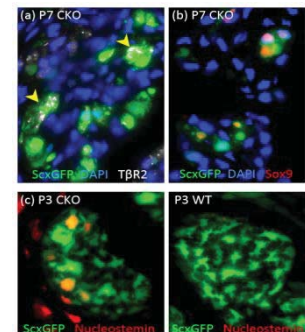


Fig.3: The recruited cells (ScxGFP-positive) in CKO tendons stained positively for (a) TGF- β type II receptor (T β R2; yellow arrows) and the stem/progenitor cell markers (b) Sox9 and (c) nucleostemin as demonstrated by immunohistochemistry. WT=wild-type.

DISCUSSION The present studies extend our previous observations where targeted disruption of TGF β signaling in tenocytes led to loss of tendon cell fate, and discover two significant findings. Firstly, the loss of tendon cell fate was accompanied by a progressive deterioration/degenerative process in the CKO tendons. Surprisingly, while TGF β signaling is strongly associated with extracellular matrix (ECM) production [4], we do not observe any ECM abnormalities in CKO tendons in the beginning, and when matrix damage emerges it seems to be related to the defective tenocyte differentiation. Secondly, we demonstrate for the first time a direct recruitment of stem/progenitor cells into the deteriorating tendons. Furthermore, findings from the Cre-lineage tracing indicate that these cells are not derived from the tendon midsubstance or epitenon (not shown), implying the existence of multiple sources of TSPC. Moreover, these cells displayed an aberrant morphology which might be associated with the unique tenocyte morphologies identified in tendinopathic tissues [5]. This scenario thus opens an opportunity to directly examine the origin of TSPC and the mechanisms of their activation.

REF: [1] Mienaltowski et al. TE Part A, 2013. [2] Tan et al. ORS Annual Meeting, Las Vegas, N, 2015. [3] Muzumdar et al. Genesis, 2007. [4] Roberts et al. Kidney Int. 1992. [5] Xu et al. Clin Orthop Relat Res, 2008.

A COMPARISON OF ADIPOSE- AND BONE MARROW- DERIVED MESENCHYMAL STEM CELL BEHAVIOR ON MICRO-PHOTOPATTERNED SURFACES

S. Meehan*, A. Allen*, A. Prakash, C.L. Gilchrist, F. Guilak and D. Little

Orthopaedic Research Laboratories, Departments of Orthopaedic Surgery and Biomedical Engineering, Duke University, Durham, NC. *Co-first Authors.

INTRODUCTION

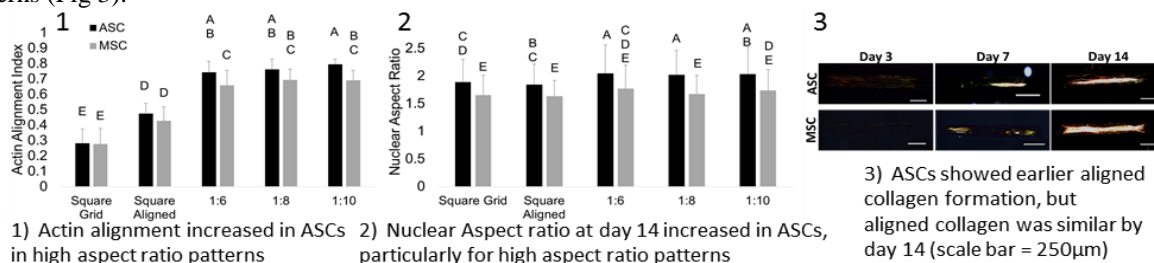
Tissue engineering approaches are being investigated for their potential to improve healing of the rotator cuff [1-3]. In particular, several studies have used electrospun nanofibers as scaffolds for rotator cuff repair[4-7]. However, the mechanism of engineered tendon development on nanofibrous scaffolds is not fully understood. A number of studies have evaluated the use of bone marrow-derived mesenchymal stem cells (MSCs) [1, 3, 8] or adipose-derived stem cells (ASCs) [9, 10], but there have been few studies that have directly compared these cell types under similar culture conditions. We have previously used microphotopatterned surfaces to evaluate the behavior of MSCs in response to different micro- and mesoscale architectural cues with respect to tendon-like differentiation [11]. The objective of this study was to compare the behavior of ASCs and MSCs under standardized culture conditions over time in response to different micro- and mesoscale architectural cues to gain improved understanding of differences in engineered tendon development between ASCs and MSCs.

METHODS

Glass-bottom dishes were spin-coated with polyvinyl alcohol to create a ~150 nm thick hydrogel layer. Sections of the gel were photoablated using a two-photon microscope to create cell-adhesive regions ($2.03 \pm 0.175 \mu\text{m}$ wide, spaced $5 \mu\text{m}$ on center). Dishes were functionalized with fibronectin and then blocked with BSA [12]. Five distinct patterns were created: $500 \times 500 \mu\text{m}$ (square grid) pattern, $500 \times 500 \mu\text{m}$ (square aligned), $125 \times 750 \mu\text{m}$ (1:6), $125 \times 1000 \mu\text{m}$ (1:8), and $125 \times 1250 \mu\text{m}$ (1:10) with aligned cell-adhesive regions [11]. Passage 5 human ASCs and MSCs were seeded onto patterns ($18,000 \text{ cells/cm}^2$). Cells were cultured for up to 14 days in low serum (2% FBS) media with no exogenous growth factors. Cells were labeled for actin and nuclei and imaged immediately above the substrate to determine actin and nucleus alignment. After confocal imaging, samples were stained with picosirius red then imaged using a polarized light microscope.

RESULTS

Actin alignment of ASCs was significantly greater than MSCs on high aspect ratio patterns (Fig. 1) and significantly increased to peak at day 7. Nuclear aspect ratio was also greater in ASCs than MSCs, across all types of pattern, but most noticeably in high aspect ratio patterns at day 14 ($>1:6$) (Fig 2). Additionally, ASCs showed increased nuclear alignment in high aspect ratio patterns. ASCs showed earlier evidence of aligned collagen on 1:10 patterns (Fig 3).



DISCUSSION

Compared to MSCs, ASCs showed increased actin and nuclear alignment, nuclear aspect ratio, and earlier aligned collagen deposition on microphotopatterned surfaces, particularly in high aspect ratio patterns. Additionally, both ASC and MSC actin alignment peaked at day 7, while nuclear alignment and aspect ratio for both cell types continued to increase until day 14. Actin alignment was also more sensitive than nuclear aspect ratio to high aspect ratio patterns ($>1:6$) as compared to square patterns, particularly for MSCs. These data also suggest that there may not be direct correlation between actin and nuclear orientation throughout early engineered tendon development and may reflect differences in responsiveness to micro- compared to mesoscale cues between ASCs and MSCs. This may be a result of cell-cell and cell-matrix interactions becoming more influential than cell-substrate interactions as matrix is built upon the patterns. Intracellular pre-stress on aligned nanofibers may play a critical mechanobiologic role in stem cell differentiation, and therefore these findings indicate that the differences between mechanoresponsive pathways and response to substrate micro-environment by different cells types used to engineer tendon warrant further study.

REFERENCES

- 1) Gulotta LV et al, *Am J Sports Med* (2009) 37:2126-33.
 - 2) Montgomery SR et al, *Curr Rev Musculoskelet Med*, (2011) 4: 221-30.
 - 3) Mora M et al, *World J Stem Cells* (2015) 7:691-9.
 - 4) Orr SB et al, *Acta Biomater* (2015) 24:117-26
 - 5) Chainani A et al, *Tissue Eng Part A* (2013) 19:2594-604.
 - 6) Moffat KL et al, *Tissue Eng Part A* (2009) 15:115-26.
 - 7) Beason DP et al, *J Shoulder Elbow Surg* (2012) 21:245-50.
 - 8) Omae H et al, *J Tissue Eng Regen Med* (2012) 6:238-44.
 - 9) Yang G et al, *Biomaterials* (2013) 34:9295-306.
 - 10) Im GI et al, *Osteoarthritis Cartilage* (2005) 13:845-53.
 - 11) Gilchrist CL et al, *Biomaterials* (2014) 35:10015-24.
 - 12) Doyle AD et al, *J Cell Biol* (2009) 184:481-90.
- Funding Sources: AR059784, AR065764

TENDON TISSUE DERIVED EXTRACELLULAR MATRIX ENHANCES TENOGENIC RESPONSE TO TGF-BETA OF MESENCHYMAL STEM CELLS VIA SMAD COMPLEX SIGNALING

Guang Yang, Benjamin B. Rothrauff, Yangzi Jiang, Rocky S. Tuan

Center for Cellular and Molecular Engineering, University of Pittsburgh, Pittsburgh, PA, USA

INTRODUCTION

Tendon and ligament (T&L) tissue repair after injuries continues to present a clinical challenge due to poor intrinsic healing capacity. The transforming growth factor- β (TGF- β) family is actively involved in tendon differentiation and healing, and the tissue-specific bioactivity of TGF- β is known to be dependent on additional cues provided by the extracellular microenvironment. We report here that a soluble, tendon tissue derived extracellular matrix (tECM) enhances TGF- β induced tenogenic differentiation of human mesenchymal stem cells (MSCs).

MATERIALS AND METHODS

MSCs were obtained from lipoaspirate-derived human fat tissue and treated with differentiation medium containing 10 ng/ml TGF- β with/without tECM as a medium supplement (10% v/v). The expression of tenogenic markers, including scleraxis (SCX) and tenomodulin (TNMD) was analyzed. Cellular response to TGF- β was also evaluated by Western blot assay for Smad2/3 complex, the downstream signal transducer of TGF- β ligands.

RESULTS

tECM displayed pro-tenogenic effect in the presence of TGF- β . Western blot analysis showed that treatment with tECM combined with TGF- β gave rise to significantly higher levels of SCX expression compared to other medium supplement groups in 2D culture (Fig. 1 A). Immunofluorescence staining revealed evidently higher density and intensity of staining for TNMD (Fig. 1 B, green) in the tECM-treated group.

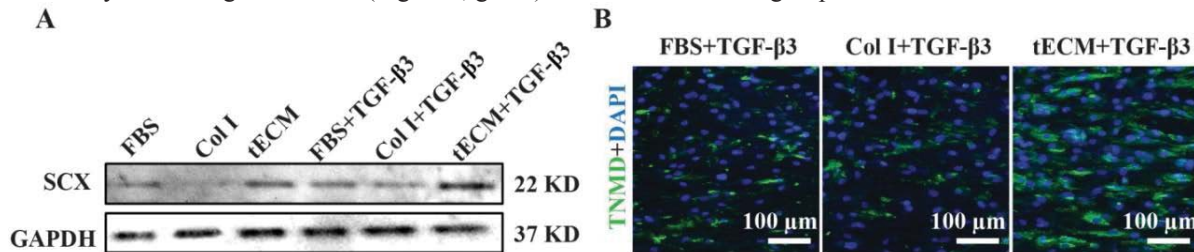


Figure 1. tECM enhanced the tenogenic differentiation of human MSCs induced by TGF- β 3.

Exposure to tECM substantially increased Smad phosphorylation in response to exogenous TGF- β 3 compared to ECM free group, while total amount of Smad2/3 complex remained comparable between groups (Fig. 2 A). The increase in SCX expression induced by tECM exposure was inhibited by treatment with the Smad2/3 specific inhibitor SB431542 (Fig. 2 B), suggesting that the pro-tenogenic effect of tECM is Smad-dependent.

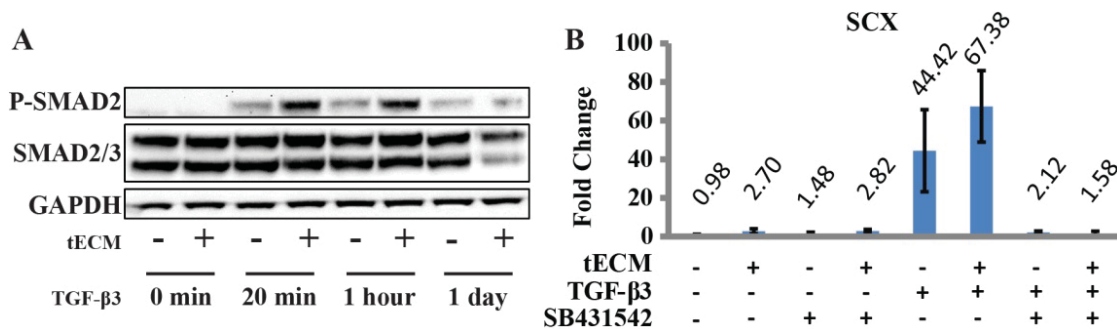


Figure 2. tECM enhanced TGF- β 3-induced tenogenesis via activation of Smad complex.

DISCUSSION

Our results demonstrate that tECM acts in concert with TGF- β to promote tenogenic differentiation of human MSCs, via Smad2/3 mediated signaling. In our ongoing research, we are focusing on the involvement of cell surface integrins-tECM interactions as initial steps of an outside-in tenogenic signal transduction pathway, to further evaluate the functional application of tECM in MSC-based tendon tissue engineering and regeneration. This study is supported by NIH, Commonwealth of Pennsylvania Dept. of Health, and U.S. Dept. of Defense.

FRESH AND FROZEN TISSUE ENGINEERED 3D BONE-LIGAMENT-BONE CONSTRUCTS FOR SHEEP ACL REPAIR FOLLOWING TWO-YEAR IMPLANTATION

Vasudevan D. Mahalingam, Edward M. Wojtys, Deneen M. Wellik, Ellen M. Arruda, Lisa M. Larkin
University of Michigan, Ann Arbor, MI

INTRODUCTION

Injuries to the anterior cruciate ligament (ACL) often require surgical reconstruction utilizing tendon grafts in order to restore knee function and stability. Current available graft options for ACL repair, however, are associated with reports of recurrent knee instability and failure to return to sport, and have continued risk for the development of early onset osteoarthritis. These may be attributed to stiffer biomechanical properties of available grafts compared to native ACLs as well as poor integration of the graft with the host. Our laboratory has fabricated tissue engineered bone-ligament-bone (BLB) constructs that demonstrate host integration and advancement toward native ligament mechanical properties and phenotype [1]. Previous studies investigating the use of frozen BLBs as a method of preservation have resulted in similar outcomes compared to fresh BLBs after six months implantation [2]. The purpose of this current study was to evaluate the long-term efficacy of fresh and frozen BLBs in our sheep ACL reconstruction model. We hypothesized that both fresh and frozen BLBs would show continued regeneration of structural and functional properties towards those of native ACL after two years implantation.

METHODS

All animal care and animal surgeries were performed in accordance with the *Guide for the Care and Use of Laboratory Animals: Eighth Edition* under an experimental protocol approved by the University of Michigan's Committee for the Utilization and Care of Animals. Fabrication of multiphasic BLB tissue-engineered constructs was performed using previously defined methods [1]. Fresh and frozen BLBs were implanted arthroscopically as ACL graft replacements following removal of the native ACL as previously described [1,2]. After two years of recovery following implantation, sheep were euthanized and both the experimental and contralateral limbs were surgically removed. Knees with ligaments intact were evaluated for joint laxity and were then further dissected for uniaxial tensile testing of the isolated ACL. Following mechanical testing, explanted contralateral ACL (C-ACL) and BLBs were harvested for histology.

RESULTS

Two years post-ACL reconstruction, fresh (n=2) and frozen (n=2) BLBs exhibited similar morphological and biomechanical properties as well as advanced regeneration toward measures found in C-ACL (n=4). Average joint laxity of the explanted fresh BLB knee was 2.8 ± 0.1 mm and 2.9 ± 0.4 mm for the frozen BLB knee with C-ACL knee laxity averaging 0.8 ± 0.1 mm. Mechanically, the average tangent modulus (slope of the stress-strain curve at strain range 0.04 – 0.10) of the explanted fresh BLBs was 59 ± 10 MPa and 66 ± 7 MPa for the frozen BLBs. Fresh and frozen BLB moduli showed no statistical difference and reached approximately 50-60% of the C-ACL, at 124 ± 20 MPa over a similar strain range. Staining for morphology with H&E revealed similar collagen fascicle formation and organization between fresh and frozen explanted BLBs.

DISCUSSION

We have previously reported that using our BLBs as replacement grafts for ACL reconstruction had improved outcomes compared to current graft options [1]. Furthermore, we have shown that the use of frozen BLBs resulted in outcomes indistinguishable from those of fresh BLBs following six months implantation [2]. The ability to use frozen BLB grafts that do not have live cells will help to facilitate regulatory approval and clinical translation of our technology. Our findings from this current study show that after long-term implantation of two years, morphological and biomechanical outcomes of both fresh and frozen BLBs remained similar. In addition, our results exhibited a continued advancement of the engineered tissue towards native ACL with an approximate 30% increase in restoration of contralateral modulus compared to our six-month recovery study [2]. Future work studying histological analyses will be conducted to further characterize the increased maturation of the BLBs. These data indicate that an additional 1.5-year regeneration period allows for the BLB to continue developing *in vivo*. In addition, we have confirmed that freezing the BLBs remains a viable option for the preservation of our graft after fabrication.

REFERENCES

1. Ma J, et al. Three-dimensional engineered bone-ligament-bone constructs for anterior cruciate ligament replacement. *Tissue Eng Part A*. 2012 Jan;18(1-2):103-16 PMID: 21902608; PMCID: PMC3246408.
2. Mahalingam VD, et al. Fresh versus frozen engineered bone-ligament-bone grafts for sheep anterior cruciate ligament repair. *Tissue Eng Part C Methods*. 2015 Jun;21(6):548-56 PMID: 25397990; PMCID: PMC4442592.

EFFECT OF TRIPEPTIDE COPPER COMPLEX GHK-CU ON CULTURED HEALING CELLS DERIVED FROM TENDON GRAFT IN ANTERIOR CRUCIATE LIGAMENT RECONSTRUCTION

Yuk-Wa Lee^{1,2}, Sai-Chuen Fu^{1,2}, Yau-Chuk Cheuk^{1,2}, Shu-Hang Yung^{1,2}, Christer G Rolf^{1,3}, Chih-Hwa Chen^{4,5}, Kai-Ming Chan^{1,2}

¹Department of Orthopaedics and Traumatology; ²Lui Che Woo Institute of Innovative Medicine, Faculty of Medicine, The Chinese University of Hong Kong, Hong Kong SAR, China.

³Department of Orthopaedic Surgery, Huddinge University Hospital, CLINTEC, Karolinska Institutet, Sweden

⁴Bone and Joint Research Center, Department of Orthopedics and Traumatology; ⁵Graduate Institute of Biomedical Materials and Tissue Engineering, College of Biomedical Engineering, Taipei Medical University Hospital, School of Medicine, College of Medicine, Taipei Medical University, Taiwan.

INTRODUCTION

Anterior cruciate ligament reconstruction (ACLR) is commonly performed but it creates an unusual biological response of “graft healing” which is less characterized. We investigated the temporal changes in cellular activities during graft healing by culturing the healing cells in the tendon grafts harvested at different time points post operation in a rat model of ACLR. This cell culture model is useful to test biologics that may promote graft healing with additional information about time of application. Previously we showed that multiple intra-articular injections of Glycyl-Histidyl-Lysine-copper complex (GHK-Cu), an activator of tissue remodelling, could transiently promote graft healing¹. In order to determine the best time of application of GHK-Cu, we studied the effects of GHK-Cu on the cells originally present in tendon grafts, as well as the healing cells from tendon grafts harvested at different time post-operation.

METHODS

(A) Culture of cells originally present in tendon graft. Hamstring tendon grafts were collected from ACL ruptured patients at time of ACLR surgery, and cells were isolated and cultured according to our previous protocol². Cells at P3 were treated with 0, 0.03, 0.3, or 3mg/ml GHK-Cu. Cell viability at 48 hr after treatment was measured by Alamar blue assay (n=6), and cell migration at 24, 48, and 60 hr after treatment was measured by *in vitro* wound closure assay (n=3). **(B) Culture of healing cells from tendon graft harvested after ACLR.** Male adult SD rats were operated at right knee to have ACLR using ipsilateral flexor tendon graft³. At day 7 and 14 post-operation, cells from tendon grafts were isolated for culture. Cells at P2 were treated with 0, 0.03, 0.3, or 3mg/ml GHK-Cu (n=6). At 48 hr after treatment, cell proliferation was measured by BrdU assay. At 72 hr after treatment, cells were collected for qPCR to measure gene expression related to matrix remodelling, including pro-col1A1, pro-col3, MMP1, MMP13, and TIMP1. Kruskal Wallis test followed by post-hoc Mann-Whitney U test were used to compare the treatment effects. Statistical significance was accepted at p<0.05.

RESULTS

The viability and migration of cells originated from human tendon graft were not affected by GHK-Cu at different doses. On the contrary, cultured healing cells from rat tendon graft collected at week 1 post-ACLR, in response to GHK-Cu treatment, exhibited a higher cell proliferation rate as compared to cells from week 2 post-ACLR in a dose-dependent manner (Fig.1). When treated with GHK-Cu, cells isolated from both week 1 and 2 post-ACLR had significantly higher expression of pro-col1A1, MMP13, and TIMP1 (p<0.05), whereas cells from week 1 post-ACLR showed increased pro-col3 and MMP1 expression (p<0.05).

DISCUSSION

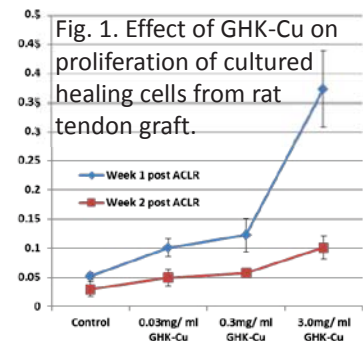
The results showed that cells isolated from tendon graft at first 2 weeks post-ACLR but not in the original tendon graft were responsive to GHK-Cu. As host cells repopulate to the grafted tendon at early healing phase⁴, GHK-Cu may act on the repopulated cells at week 1-2 following ACLR. Our previous work showed that GHK-Cu injection from week 2-5 post-ACLR led to transient improvement¹. With the current results, GHK-Cu targeted at the first 2 weeks post-ACLR may be more effective. In order to overcome the fast clearance of bioactive agents, a carrier system for sustained delivery of GHK-Cu for 2 weeks may be required to further promote graft healing.

ACKNOWLEDGEMENTS

The current work was supported by the General Research Fund (CUHK14100614).

REFERENCES

1. Fu *et al*, *J Orthop Res* 2015. 2. Rui *et al*, *Tissue Eng Part A* 2010. 3. Fu *et al*, *Knee Surg Sports Traumatol Arthrosc* 2012. 4. Kobayashi *et al*, *Am J Sports Med* 2005.



A NOVEL MAGNESIUM RING DEVICE COMBINED WITH ECM BIOSCAFFOLDS IMPROVES ACL HEALING COMPARED TO ECM TREATMENT ALONE

K. F. Farraro, A. Pastrone, J. R. Mau, S. L-Y. Woo

Musculoskeletal Research Center, University of Pittsburgh, Pittsburgh, PA, USA

INTRODUCTION Recently, there has been renewed interest in healing an injured anterior cruciate ligament (ACL) as an additional treatment choice to ACL reconstruction¹. In our research center, we have used biological augmentation with extracellular matrix (ECM) bioscaffolds to successfully heal a fully transected ACL in goats². However, due to the slow ACL healing process, mechanical augmentation is also needed to restore initial joint stability and load it and its insertion sites³. For this purpose, we designed a novel bioresorbable magnesium (Mg) ring device to connect the two ends of an injured ACL and facilitate healing^{4*}. Previously, we have found that this device could restore stifle joint stability and ACL function immediately after surgery. In this study, we hypothesized that this device, when used alongside an ECM bioscaffold, would improve ACL healing *in vivo* (Group 1) over our previous results using ECM treatment alone² (Group 2).

METHODS Skeletally-mature, female Spanish goats were used for this *in vivo* study (N = 4). After transection of the ACL, Mg ring repair was performed⁴, and an ECM bioscaffold was applied to the injury site. Animals were allowed free cage activity following surgery, and they were humanely sacrificed at 12 weeks of healing.

The gross morphology of the ACL was assessed, and its cross-sectional shape and area were obtained using a non-contact laser micrometer system. To assess stifle joint stability and ACL function, a robotic/UFS testing system was used⁵. The resulting 5 degree-of-freedom stifle joint kinematics and in-situ forces in the ACL of the healing and sham-operated stifle joints were measured under an externally-applied 67-N anterior-posterior tibial load at 30, 60, and 90° of joint flexion. Finally, the structural properties of the femur-ACL-tibia complex (FATC) were determined using load-to-failure uniaxial tensile testing. Independent t-tests were used to compare the data from the experimental groups. To reduce interspecimen variation, all data were normalized by those from the respective sham-operated controls.

RESULTS All of the treated ACLs healed by 12 weeks with continuous neo-tissue (Fig. 1). The cross-sectional areas of the healing ACLs were similar, and were $130 \pm 26\%$ and $127 \pm 90\%$ and of those of the sham-operated controls in Groups 1 and 2, respectively ($P > 0.05$).

The stifle joint stability and in-situ forces in the ACL under the 67-N anterior tibial load were also similar between treatment groups. At the tested joint flexion angles, the normalized anterior-posterior tibial translation (APTT) ranged from 2.9 – 3.2 in Group 1 and 2.5 – 3.5 in Group 2 ($P > 0.05$). The corresponding normalized in-situ

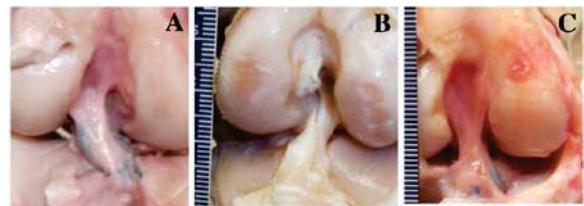


Figure 1: Gross morphology at 12 weeks of healing of Group 1 (A), sham-operated control (B), Group 2 (C)²

force in the ACL ranged from 0.3 – 1.0 in Group 1 and 0.6 – 1.0 in Group 2 ($P > 0.05$). Data on the structural properties of the FATC, however, revealed an increase in properties with the addition of the Mg ring device.

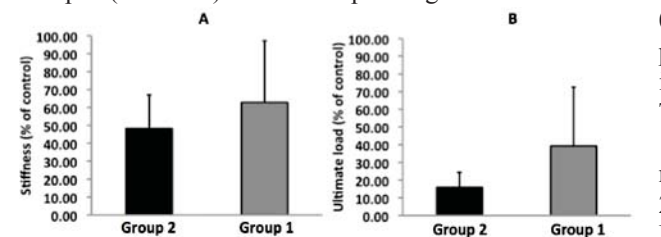


Figure 2: Normalized stiffness (A) and ultimate load (B) of the femur-ACL-tibia complex (FATC) in Groups 1 and 2²

The normalized stiffness in the healing FATC in Group 1 was 30% higher than that in Group 2, and the normalized ultimate load in the healing FATC in Group 2 was 2.5 times that in Group 2 (Fig. 2; $P > 0.05$).

DISCUSSION At 12 weeks, both Mg ring repair + ECM treatment (Group 1) and ECM treatment² (Group 2) led to successful healing of a fully transected goat ACL without significant hypertrophy. However, the

structural properties of the healing FATC in Group 1 were improved over Group 2, showing that the addition of Mg ring repair produced a stronger healing ACL; in support of our hypothesis. With these positive results, we are extending our pre-clinical studies to include a larger sample size and longer healing time points in order to evaluate whether these findings could persist and whether they could parallel or supersede those with ACL reconstruction.

ACKNOWLEDGEMENTS Support from an NSF Engineering Research Center Grant (#0812348) and the Commonwealth of Pennsylvania is gratefully acknowledged.

REFERENCES 1. Murray, et al. 2013. Am J Sports Med, 41(8):1762-70. 2. Fisher, et al. 2012, KSSTA, 20(7):1357-1365. 3. Fleming, et al., 2008. JOR, 26(11):1500-1505. 4. Farraro, et al. 2014. J Biomech, 47(9): 1979-86. 5. Sakane, et al. 1999, KSSTA, 7(2):93-7.

* Patent pending

THE IMMUNOMODULATION OF LIGAMENT HEALING

C.S. Chamberlain, E.M. Saether, E.M. Leiferman, and R. Vanderby
Department of Orthopedics and Rehabilitation, University of Wisconsin-Madison, Madison, WI

INTRODUCTION

Ligament repair ranges from months to years and results in scar tissue mechanically inferior to native tissue. Ligament healing involves the upregulation of macrophages, broadly classified as the M1 (classically activated) and M2 (alternatively activated) macrophages. The M1 macrophages secrete pro-inflammatory mediators, such as IL-1, and participate in the activation of various cytotoxic processes, which creates extensive collateral damage and aberrant inflammation. In contrast, the M2 macrophages secrete potent anti-inflammatory cytokines, such as interleukin-10 (IL-10) and interleukin-4 (IL4) and play important roles in wound healing and restoration of tissue homeostasis. Controlling these early inflammatory mediators and cell types may therefore modulate subsequent healing and diminish scar formation. The goal of this study is to therefore improve ligament repair by modulating the macrophage phenotypes.

METHODS

Experimental procedures were approved by the University of Wisconsin Institutional Animal Care and Use Committee. Male Wistar mice were subjected to medial collateral ligament injury and treated with clodronate, interleukin-4 (IL-4), interleukin-1 receptor antagonist (IL1RA), or mesenchymal stem cells (MSC). Tissue was collected and used for immunohistochemistry, multiplex analysis, and mechanical testing.

RESULTS AND DISCUSSION

Depletion of macrophages, using liposome encapsulated clodronate, resulted in a significant reduction of macrophages during the first 5 days of healing. Endothelial cells and myofibroblasts were also significantly decreased at day 5 while inflammatory cytokines, IL-12, IL-1 α , and IL-2 were upregulated (Fig. 1A). Although collagen production was significantly higher, ligament strength was significantly compromised (Fig. 1B). These results suggest that macrophage depletion, without regard to the specific phenotypes, significantly impedes the healing process via altered cytokine production and collagen organization. Based on these results, IL-4 and IL-1Ra were administered to the injured MCL to control macrophage phenotypic behavior and block inflammation. IL-1Ra treatment increased M2 macrophages (Fig. 1C), decreased inflammatory cytokines and increased anti-inflammatory cytokines (Fig. 1D). IL-4 treatment tended to reduce the number of M1 macrophages (Fig. 1E) and type III collagen while increasing type I procollagen (Fig. 1F). These findings indicate that modulation of the macrophage phenotypes by IL-1Ra and IL-4 improves some aspects of healing such as inflammation and collagen production. However, neither treatment significantly improved early, post-injury ligament strength. Instead of using a single cytokine to modulate the immune response and healing, MSCs were next administered to the injured MCL. Treatment of the injured MCL with 1×10^6 MSCs resulted in both improved ligament strength (Fig. 1G) and decreased M1 macrophages (Fig. 1H) 14 days post-injury. These findings further support our concept that modulation of inflammation is key to ligament healing and MSC treatment can accelerate these processes. Taken together, results strongly support the concept that the rate and extent of ligament healing, and ultimately, functional healing can be significantly enhanced by a treatment regimen that appropriately modulates the anti-inflammatory processes.

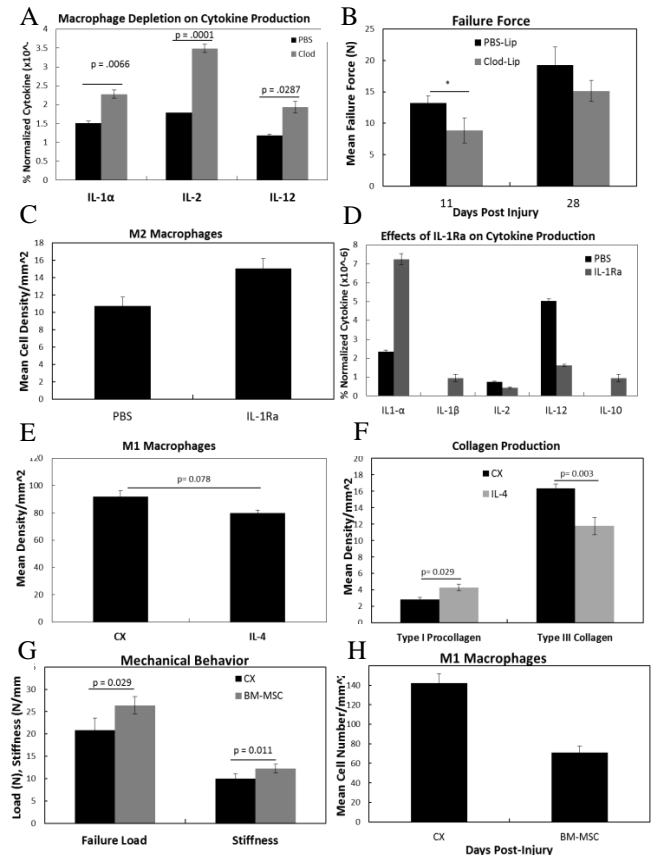


Figure 1. Treatment effects on ligament healing. A) Depletion of macrophages results in an increase in inflammatory cytokines and B) reduced ligament strength. C) IL-1Ra increased the number of M2 macrophages and D) modulated cytokine response. E) IL-4 reduced the number of M1 macrophages. E) IL4 also increased type I procollagen and decreased type III collagen. F) MSC treatment increased strength and stiffness and G) reduced the number of M1 macrophages. Data are expressed as mean \pm S.E.M.

CURCUMIN: DOES IT DECREASE INFLAMMATION IN TENDON HEALING?

Diana Zhu¹, Rohan Rao¹, Nathan Moroski¹, Thay Lee¹, Ranjan Gupta¹

¹Department of Orthopaedic Surgery, University of California, Irvine, USA

INTRODUCTION

Tendon injuries and ruptures occur commonly and present a challenging problem to practicing clinicians. Current non-surgical treatment modalities include NSAIDs, splinting, and activity modification; however, risks such as gastric bleeding and failure of treatment limit the efficacy of these modalities. As such, we propose the use of curcumin as an anti-inflammatory adjunct in treatment of tendon injury. Curcumin, a curcuminoid compound found in turmeric, has recently been shown to have anti-inflammatory effects against various types of cancer¹⁻³. There also appears to be suppression of inflammatory factor nuclear factor κ B, and attenuation of macrophage infiltration^{2,4}. Our hypothesis was that curcumin would decrease inflammation in an established animal model of tendon injury

METHODS

68 Sprague-Dawley rats (250g) were utilized in our animal model as approved by the UC Irvine institutional animal care and use committee, where the right Achilles tendon was transected and immediately repaired. Curcumin (Fusionary Formulas, USA) was prepared in pure arachis oil and administered in a daily high dose (500 mg/kg), low dose (50 mg/kg), with oil-only vehicle and no-treatment rats serving as controls. Bilateral Achilles tendons, the right being experimental and the left as an internal control, were harvested at 3 days, 7 days, and 21 days to correspond with the three stages of human tendon healing. Western blot, qRT-PCR, and immunohistochemistry were performed to assess levels of inflammatory markers TNF α , IL1 β , IL6, MMP-8, Collagen 1, and IL-10.

RESULTS

At the 21 day time point, the high-dose curcumin group (n=7) demonstrated marked differences in mRNA production from the control group (n=7) in TNF- α (0.544 versus 15.206), IL1 β (1.415 versus 3.813), IL6 (3.061 versus 6.810), IL-10 (7.111 versus 11.184), MMP8 (2.831 versus 59.511), and Collagen 1 (3.927 versus 0.480). Western blot showed 3.5-fold decrease in TNF alpha protein and 2.7-fold decrease in IL-1B protein in high-dose versus vehicle.

DISCUSSION

Our data suggests that curcumin is able to decrease anti-inflammatory markers at the level of tendon healing in proven animal model. Most significantly high-dose curcumin treated rats showed decreased TNF- α and IL1 β production at the site of injury, which appears to indicate a decrease in inflammation at 21 days. In addition, curcumin-treated rats showed increased collagen mRNA production, suggesting that its administration may play a role in earlier remodeling of scar and potentially earlier recovery. This initial study suggests significant possibilities for the use of curcumin in tendon rupture injuries as an anti-inflammatory adjunct to current treatment modalities.

REFERENCES

- 1) Osterman CD, Lynch JC, Leaf P, Gonda A, Bennit HRF, Griffiths D, Wall NR. Curcumin modulates pancreatic adenocarcinoma cell-derived exosomal function. PLOS One. 2015 Jul.
- 2) Dhillon N, Aggarwal BB, Newman RA, Wolff RA, Kunnumakkara AB, Abbruzzese JL, Ng CS, Badmaev V, Kurzrock R. Phase II trial of curcumin in patients with advanced pancreatic cancer. Clin Cancer Res. 2008
- 3) Shanmugam MK, Rane G, Kanchi MM, Arfuso F, Chinnathambi A, Zvaed ME, Alharbi SA, Tan BK, Kumar AP, Sethi G. The multifaceted role for curcumin in cancer prevention and treatment. Molecules 2015;20(2):2728-69
- 4) Li L, Aggarwal BB, Shishodia S, Abbruzzese JL, Kurzrock R. Nuclear factor κ B and I κ B kinase are constitutively active in human pancreatic cells, and their downregulation by curcumin (diferuloylmethane) is associated with the suppression of proliferation and the induction of apoptosis. Cancer 2004; 101:2351-62

THE DIFFERENTIAL EFFECTS OF PROTEASE-ACTIVATED RECEPTORS 1 AND 4 IN HUMAN PLATELET ACTIVATION AND INFLAMMATION

Jianying Zhang, , Jorge L. Rocha,, Melissa McLane, MaCalus V. Hogan, James H-C. Wang#
Department of Orthopaedic Surgery, University of Pittsburgh School of Medicine, PA. #wanghc@pitt.edu

INTRODUCTION

Tendon injuries occur frequently and cost billions of health care dollars annually. Recently, there has been an increase in the use of platelet-rich plasma (PRP) to treat tendon injuries. However, the efficacy of PRP treatment is controversial due to inconsistent results from human clinical trials. It is thought that variations in PRP preparation contribute to these inconsistencies. Specifically, platelets in PRP contain pro-angiogenic (e.g. VEGF) or anti-angiogenic (e.g. endostatin) factors [1], which may differentially affect the healing of tendon injuries. It is known that these factors are selectively released after platelet activation by specific receptors. Therefore, in this study we investigated the effect of protease activated receptors 1 and 4 (PAR1 and PAR4) in platelet activation and inflammation.

METHODS

Platelet preparation – Human blood was obtained from 12 healthy donors and 9 ml of blood was mixed with 1 ml of 3.8% sodium citrate and centrifuged at 500g for 10 min. Then, the supernatant (PRP) without the buffy coat was centrifuged at 1000g for 10 min and the resulting pellet was washed in Tyrodes-HEPES buffer and centrifuged for 10 min at 1000g. Finally, platelets in the pellet was suspended in Tyrodes-HEPES buffer and used in experiments.

Platelet activation – About 100 μ l of platelet from above was activated with 5 μ l 1 mM PAR1-activating peptide (PAR1-AP) or PAR4-activating peptide (PAR4-AP) at 25°C for 10 min. Then, the mixture was centrifuged at 1000g for 10 min, and the levels of VEGF, endostatin, IL-1RA and HMGB-1 in the supernatant was determined by ELISA. Platelets without activators were used as controls.

RESULTS

PAR1 induced angiogenic effects in human platelets. PAR1 activated platelets released 3 times more VEGF than when activated with PAR4 (**Fig. 1A**). However, PAR4 activated platelets released 7 times more endostatin than the PAR1 activated platelets (**Fig. 1B**). Further, PAR1 induced anti-inflammatory effects in human platelets; it did not change IL-1R-A (**Fig. 2A**) but decreased HMGB-1 levels (**Fig. 2B**). In contrast, PAR4 stimulated inflammatory effects in human platelets by lowering IL-1-RA and increasing HMGB-1 levels.

DISCUSSION

Our findings indicate that PAR1 induces angiogenic and anti-inflammatory effects in human platelets, while PAR4 has anti-angiogenic and inflammatory effects. Of significance is HMGB-1, which is constitutively expressed in the nuclei of most mammalian cells. Under cellular stress, HMGB1 is released into the extracellular matrix and activates the immune response thus acting as a danger-signal [2]. Both PAR1 and PAR4 selectively regulated the release of VEGF and endostatin, and IL-1RA and HMGB-1 from human platelets. Therefore, role of PAR1 and PAR4 on human platelet activation and inflammation should be considered prior to the use of PRP to treat tendon injuries.

REFERENCES

- [1] Ma L, Perini R, McKnight W, et al. Proteinase-activated receptors 1 and 4 counter-regulate endostatin and VEGF release from human platelets. PNAS, 102:216-220, 2005.
- [2] Erlandsson Harris H, Andersson U. The nuclear protein HMGB1 as a proinflammatory mediator. Eur J Immunol 34, 1503-1512, 2004.

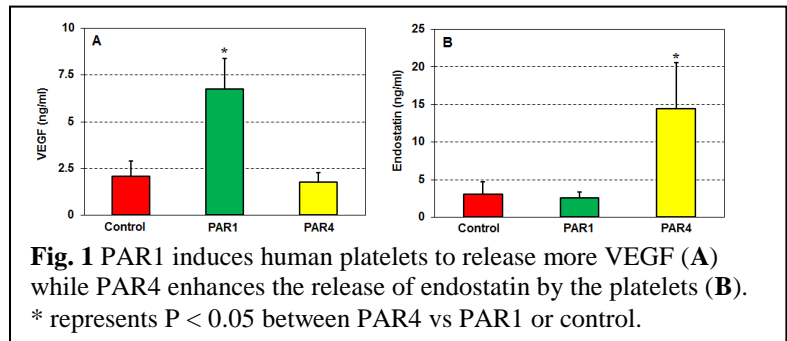


Fig. 1 PAR1 induces human platelets to release more VEGF (A) while PAR4 enhances the release of endostatin by the platelets (B). * represents P < 0.05 between PAR4 vs PAR1 or control.

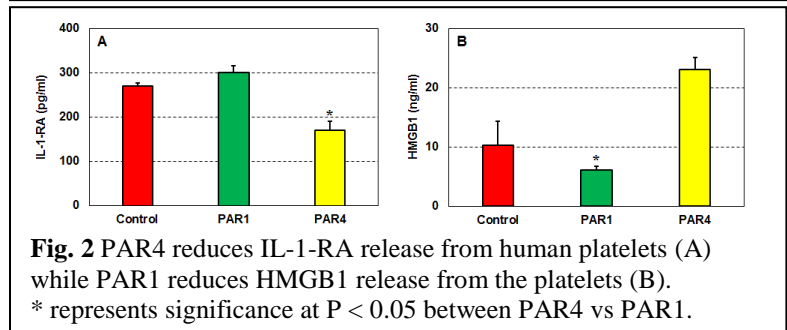


Fig. 2 PAR4 reduces IL-1-RA release from human platelets (A) while PAR1 reduces HMGB1 release from the platelets (B). * represents significance at P < 0.05 between PAR4 vs PAR1.

THE ROLE OF INTERLEUKIN-13 IN TENDINOPATHY

Moeed Akbar¹, Susan M Kitson¹, James H Reilly¹, Shauna C Kerr¹, Lindsay A N Crowe¹, George A C Murrell², Iain B McInnes¹, Derek S Gilchrist¹, Neal L Millar¹

1. *Institute of Infection, Immunity and Inflammation, College of Medicine, Veterinary and Life Sciences University of Glasgow, UK*

2. *Department of Orthopaedic Surgery, St. Georges Hospital Campus, University of New South Wales, Australia*

INTRODUCTION

Inflammatory mediators are increasingly implicated as key mediators driving matrix remodelling in tendinopathy. We previously established Interleukin-33 (IL-33) as a pivotal cytokine in the transition from type I collagen (Col1) to type III collagen (Col3) synthesis¹. Interleukin-13 (IL-13) is synonymous with aberrant tissue remodelling in many pathologies including liver and lung fibrosis and rheumatoid arthritis. Based on our previous investigations we sought evidence of IL-13 expression in human tendinopathy and thereafter, to explore mechanisms whereby IL-13 may regulate inflammatory mediators and matrix regulation in human tenocytes.

METHODS

Torn supraspinatus tendon (established pathology) and matched intact subscapularis tendon (representing 'early pathology') biopsies were collected from patients undergoing arthroscopic shoulder surgery. Control samples of subscapularis tendon were collected from patients undergoing arthroscopic stabilisation surgery. Primary human tenocytes were cultured from hamstring tendon tissue obtained during hamstring tendon ACL reconstruction. The *in vitro* effect of recombinant human IL-13 on primary human tenocytes was measured using proliferation assays and quantitative RT-PCR.

RESULTS

Immunohistochemistry of tendinopathic tissue indicated the presence of IL-13 to be localised around an influx of leukocytes that stained positive for mast cell and macrophages. In addition, recombinant human IL-13 led to a dose dependent increase in tenocyte proliferation, *in vitro*. Furthermore, analysis via quantitative RT-PCR demonstrated recombinant IL-13 treatment on tenocytes, *in vitro*, resulted in increased expression of genes involved in matrix remodelling. Significant increases were observed in Col1, Tenascin-C and Periostin. However, no significant increase in Col3 expression was measured.

CONCLUSIONS

The role of inflammatory mediators in tendinopathy continues to prompt much debate. The current study has identified the presence of IL-13 in tendinopathy. The close localisation of IL-13 with infiltrating leukocytes suggests these cells as a potential source of this cytokine. Furthermore, the results from the current study indicate that IL-13 increases expression of Col1 (as well as other matrix proteins) but has no effect on Col3 expression. We propose that IL-13 is a central inflammatory mediator driving the early tendinopathy processes which may offer novel therapeutic approaches in the management of tendon disorders.

REFERENCES

1. Millar, N. L. *et al.* MicroRNA29a regulates IL-33-mediated tissue remodelling in tendon disease. *Nat Commun* **6**, 6774 (2015).

RESEARCH IN ORTHOPAEDICS- WHAT HAVE I LEARNED IN 40 YEARS?

Kai-Ming Chan, MD, PhD

Department of Orthopaedics and Traumatology, The Chinese University of Hong Kong, Hong Kong, P.R.C.

Leading the Sports Medicine and Regenerative Technology team, my team has a particular interest in treating patients with tendinopathy, anterior cruciate ligament injuries, and osteoarthritis; however, current treatments remain frustrating, as they do not return patients to pre-injury functionality. However, we as clinicians and researchers cannot be complacent in searching for novel treatment options. The growing population has led to increased strain on the healthcare industry; motivating researchers to continually seek innovative ways to reduce costs, produce treatments that quickly return individuals to preinjury functionality, and prevent injuries.

My team and I have worked throughout the years with a common goal of bringing all research from bench-to-bedside. Our study on tendinopathy needed to first address the basics of the disease and what is currently understood. This began successfully by coining the term 'failed healing' to propose a process through which tendinopathy may occur, and while this remains a theory, it forms a solid foundation on which to study the aetiopathogenesis of tendinopathy. With this model in mind, a suitable rat model was developed that is now a well-established model to study tendinopathy. In more recent years we have established a project to determine the microbial influence on the development of tendinopathy, with the ultimate goal of creating injectable products to treat the disease. Anterior cruciate ligament (ACL) injuries are a common occurrence, yet there is a gap between surgical ACL reconstruction (ACLR) and graft healing, and incorporation. It is this uncertainty that makes clinicians unconfident in assessing whether patients are ready to return to regular activity. An intra-operative vitamin C irrigation solution was developed to promote graft healing, post-surgery based on promising results in tendon healing models. Graft incorporation is essential for successful ACLR, thus our project to determine the effect of GHK-Cu incorporated into a novel coating hydrogel was initiated. It is our eventual goal to combine these products with current surgical procedures to promote graft healing. In order to improve research output in these areas, we have formed collaborations with academic and industry partners.

The International Symposium on Ligaments and Tendons (ISL&T) provides the foremost platform for specialised research on these topics to be presented. It has been my honour to be a part of its development for the past eight years, as well as chairing certain meetings. ISL&T is particularly important for students and young investigators to gain experience in defending their work and networking with established researchers. It was through meetings such as ISL&T that I created my own network and sought to connect the dots within it. Thus, the Musculoskeletal Regeneration Research Network (MRN) was established in 2013, with a shift towards a central goal of being a strong advocate for stem cell and regenerative medicine in orthopaedics. It aims to build an extensive network with like-minded individuals, who are leaders in the field. Collaborations between members are encouraged to produce breakthroughs in the field, and become an opinion leader in orthopaedic research.

Research is a long, often difficult process, but it is ultimately a very rewarding experience. Looking back on my progress, I still feel that there is more to be done. Novel products are yet to be produced that will become a mainstay in tendon and ACL healing, as well as methods to prevent these injuries from occurring. With more resources and novel technology these goals will become a reality, but this relies heavily on clinicians and researchers working closely together. It is my hope that over the last 40 years, I have inspired young researchers to reach new heights and push the boundaries in orthopaedic research.

WHAT DO ORTHOPAEDIC SURGEONS NEED FOR RESEARCH?

Mahmut Nedim Doral
Gurhan Donmez, Gazi Huri, Egemen Turhan, Onur Bilge*
Hacettepe University/Ankara, *NE University/Konya-Turkey

Advances in orthopaedic research can improve people's lives in many ways and there's so much still to learn about the human body. It's known that the prevalence of musculoskeletal procedures has increased in different countries, from 18% to 25% of all operating room procedures performed during hospital stays in the last 10 years. Despite the difficult working conditions and heavy work load of orthopaedic surgeons in their daily practice, basic research is another mission of especially academical individuals and should be progressed to develop new technologies and surgical methods. In order to find better ways to relieve pain and improve quality of life of our patients, developments in specific fields, including molecular and stem-cell biology, biomaterials, biomechanics, bioengineering, developmental biology, and molecular genetics, have all contributed to advancements in orthopaedic research. On one hand, improvements and refinements in laboratory techniques may hasten the pace of progress in research and open new gates for future directions. On the other hand, basic science and translational researches have revealed important potential applications for nanotechnology in orthopaedic surgery, particularly with regard to improving the interaction between implants and host bone. These investigations often require multidisciplinary approaches ranging from basic cellular and molecular biology, bioengineering, biomechanics, and clinical research. It is clear that collaboration between disciplines and centers with expertise in biology, mechanics, and clinical research is essential to continue to advance ameliorate the field.

The greatest barriers to the development of new basic research facilities include available technical expertise, space, infrastructure, equipments, multi-disciplinary clinical collaboration, and finances. This lecture will focus on the basic infrastructure and equipment needs for the development of orthopedic research laboratories, as well as some of the financial considerations required to develop these facilities.

CELL THERAPIES FOR TENDON SURGERY

Ming H Zheng, MD, PhD, FRCPath

Centre for Orthopaedic Research, School of Surgery, University of Western Australia, Perth, Western Australia, 6009, Australia

Tendons and ligaments are frequently damaged during rigorous activities such as sport or the process of aging. Despite their relatively high prevalence and morbidity of tendon and ligament injury in sport, most treatments have been proven to provide no, or only modest short-term benefits. Traditional first-line treatments might include rest and activity modification, exercises such as eccentric strengthening and bracing. Topical or oral non-steroidal anti-inflammatory drugs (NSAIDs) and local glucocorticoid injections may provide modest short-term benefits for pain. More recently, novel treatments including extracorporeal shock wave therapy, and injectable autologous blood products and botulinum have been studied but have either been proven to be ineffective or remain unproven. Current surgical and therapeutic treatment options include prosthetic devices, autografts, allografts, or xenografts [7], however these exhibit only limited success. Over the past 15 years, we focus exclusively on the translational medicine program of tendon repair and regeneration. We have observed that depletion of the functional tenocyte pool in the region of the tear may account for fatigue of the normal healing response. On the basis of the pathology studies and pre-clinical animal work, we have developed cell therapy strategies for tendon and ligament repair in human. These include the development of ultrasound guided autologous tendon cell injection (ATI) for tendon tear and the Matrix argument autologous tendon cell implantation (MATT) for surgical repair of tendon and ligament. To date, a series of clinical trials on ATI were conducted in patients with different anatomical sites of tendinopathy including chronic lateral epicondylitis, rotator cuff tendon tear, gluteal tendinopathy. We have showed that ATI, the first homologous cell therapy technique developed for the treatment of tendinopathy, has the potential to address this unmet clinical need by replenishing the pool of functional tenocytes in the site of tendinopathy. We have also developed sensor controlled bioreactor for the generation of neo-tendon tissue using autologous tendon cells from a needle biopsy and collagen based ligament for ACL reconstruction. Here we will provide an overview of the translational program of tendon and ligament regeneration with a strong focus on the clinical data of ATI, MATT and human neo-tendon implant.

LEARN FROM TENDON STEM CELLS - POTENTIAL CLINICAL USE

Hongwei Ouyang, MD, PhD

School of Medicine, Zhejiang University, Hangzhou, China

Tendon injuries are common especially in sports activities, but tendon is a unique connective tissue with poor self-repair capability. Although tendon stem cells hold promise for treating tendon injuries by repopulating injured tendons, the regenerative capacity of tendon stem cells is influenced by regulatory networks orchestrated by local

Growing evidence supports the contribution of inflammation to the development of tendinopathy. But the crosstalk between inflammatory response and regenerative process in tendinopathy have not been fully characterized. In human and mice tendinopathy model, we found that a subpopulation of Scx/Sox9 double positive tendon stem/progenitor cells (TSPCs) presented in the local proinflammatory microenvironment around calcific sites. Scleraxis (Scx), an essential tendon specific transcription factor, was suppressed upon proinflammatory cytokine treatment and loss of Scx lead to more severe calcification in mice models. Notably, we observed an inversed relationship between Scx expression and HIF-2alpha (encoded by EPAS1) signaling, activated by proinflammatory cytokines, at calcified sites. And abnormal upregulation of HIF-2alpha served as a key transcriptional switch to direct TSPCs differentiation

Using both natural decellularized matrices and synthetic scaffolds which mimic the native tendon ECM, we found that tendon specific topographic ultrastructure induced tendon lineage commitment of stem cells. Tendon stem/progenitor cells (TSPCs) and Human-induced pluripotent stem cells (hiPSCs) were spindle-shaped and well orientated on tendon-like aligned nanofibers and expressed higher tendon-specific genes than on randomly-oriented nanofibers. Interestingly, tendon-derived decellularized matrix promoted the tendinous phenotype in hTSPCs and inhibited their osteogenesis, even under osteogenic induction conditions. Mechanistic studies suggested that tendon specific ECM regulates teno- and osteolineage-specific transcription factors Scleraxis and Runx2 of stem cells

These findings indicate that the manipulation of local mechanical and biochemical microenvironment can be adopted to develop new pharmaceutical or biomaterial therapeutics of targeting TSPC regulation in tendon diseases as well as clinical application of stem cell-based therapies for tendon tissue regeneration.

OUT OF ACADEMICS: PRODUCT DEVELOPMENT FROM CONCEPT, PATENT PROCESS, R&D, PROTOTYPING, TESTING, TO THE MARKET

Albert J. Banes^{1,2}, Michelle Wall¹, Aisley Amegashie¹, Jon Volmer¹, and Elizabeth Banes¹
Flexcell Intl. Corp., Burlington, NC, BME, NCSU, UNC, Raleigh, NC.

In this scientific and economic climate, we all gauge the importance of our research questions in terms of market, whether it is the NIH “market”, pharma or medical and scientific devices. Universities take a broader view of patents and company structure for faculty members today than occurred 35 years ago when the biotech company, Flexcell was started. There is a contrast in approach between how academic institutions deal with potentially patentable ideas vs industry. Many universities take all faculty or student patent disclosures and move towards a provisional application, without a serious merit review. Moreover, most university patent applications are written by the attorneys with insufficient input from the inventor. Once a concept or process is published as a provisional or an application, the clock and revenue stream are ticking until a patent is issued and validation and quality control problems are solved and a roll-out occurs. Academicians take a scientific view of where their idea should go, whereas, industry takes a more pragmatic view toward a market “need”, wanting a block buster drug, “killer” application or device for the market. Once the R&D has matured into a device for instance, then applications must be developed and the market educated as to use. Devices are notoriously easy to work around in the patent world, however, first to market makes a huge difference. As an 11 year consultant for Marian Labs Inc, from 1981-1992, I worked on the development of the first synthetic dermis, called “Integra”. The technology was licensed from MIT and Harvard, as the brainchild of John Burke and Ioannas Yannas. Marian Labs’ scientists and engineers, by agreement, could not change the formulation. As with the then novel Biobrane material by Aubrey Woodruff, I discovered that cells would not adhere and multiply in the material. This finding was confirmed, leading to research on why cells did not like the material in vitro. Being involved in collagen chemistry at the time, I took a look at the raw material, bovine dermis, and realized that it had a considerable bioburden. I suggested that the company switch its primary source from dermis to tendon. That switch was done and the industry moved forward with a purchase of then Integra assets by Integra Life Science in 1989 and the subsequent development of a usable dermis. For the record, the original patent and others in the industry at that time noted that both dermis and tendon could be used as a collagen source. However, no one was actually using tendon as the starting material until I emphasized its virtues, as a cleaner starting material, free of bioburden, higher % of type 1 collagen, with a lessor amount of type 3. The original price in 1985-88 was to be \$2k/sq ft for Integra, synthetic dermis. The market was to be burn patients. The problem was that most burn patients were indigent and reimbursements would not cover these charges. Others stepped into the R&D world in synthetic and biological wound dressings, including Advanced Tissue Sciences, BF Goodrich, Smith Nephew. Even in the 80s, one company produced a wound cover that looked like Naugahyde but sold \$25M in its first year! The take home is, know your market, do not get caught having to educate the market to buy your product, and be first with a winner!

The authors are employees of Flexcell Intl. Corp and are compensated as such.

References: 1. **Out of Academics: Education, Entrepreneurship and Enterprise.** Banes,A.J. ABE 2013, 41: 1926-1938.

PRP MYTHS

Ramon Cugat, M.D, Ph.D.

Orthopaedic Surgical Department, Hospital Quiron Barcelona, Barcelona, Spain
Medical School at University of Barcelona, Barcelona, Spain

PRP MYTHS

Platelet Rich Plasma is a substance that contains Growth Factors and in order to talk about its Myths, it is better to talk about the truths with a clear understanding that it's one thing to talk about PRP and it's another to talk about Growth Factors.

The **TRUTH** about Growth Factors is:

Growth factors are a set of substances that carry out an important function in intercellular communication. They carry out a large number of biological functions among which cellular proliferation is important, though they also decisively affect cellular survival, migration, differentiation and even apoptosis. Growth factors carry out their function at very low concentrations in body fluids and tissues, in the region of pico or nanograms. They act by binding to receptors located on the cell membrane that transmit the signal from the exterior to the interior of the cell, through the coupling of different protein kinases that are phosphorylated and which regulate a signaling cascade that ends up with the activation of one or more genes.

MECHANISM OF ACTION

The process of tissue regeneration includes a complex set of biological events controlled by the action and synergy of a cocktail of growth factors. There are three agents involved in tissue regeneration: the cellular component, a combination of multiple biological mediators that include growth factors and cytokines among others and a matrix or "scaffold" that gives the new tissue under construction support. The truth here is that Platelet-rich plasma has an anti-inflammatory and anabolic effect and the growth factors responsible for this are as follows:

HGF, which inhibits MMPs and ADAMTS (a disintegrin and metalloproteinase with thrombospondin) enzymes; has an antagonistic effect on IL-1, tumor necrosis factor, and nitric oxide; and induces the synthesis of TIMPs VEGF and HGF, which through synergistic and pleiotropic actions stimulate reparative angiogenesis.

FACT

Currently, there are a variety of systems for obtaining substances that contain growth factors and other elements like leukocytes, fibrin etc. Because of this variety, the products obtained have different chemical and cellular compositions.

This explains why the results are not always similar: Activation and inhibition do not occur at the same times and under the same circumstances. It is therefore important to know the composition of the product that is administered.

CONCLUSIONS

In clinical practice Growth Factors shorten Tissue Regeneration/Repair Time in conservative treatment. When the injury requires surgery GF's also help Tissue Regeneration/Repair.

IS THERE ANY SUBSTANCE IN THE PRP TREATMENT OF TENDINOPATHY?

James H-C. Wang, PhD

MechanoBiology Laboratory, Department of Orthopaedic Surgery
University of Pittsburgh School of Medicine
Pittsburgh, PA, USA E-mail: wanghc@pitt.edu

Tendinopathies are debilitating tendon conditions that affect millions of people every year in the United States alone and cause significant financial burden to a society. In recent years, platelet-rich plasma (PRP) is widely used as a promising treatment option for tendinopathy patients in orthopaedic/sports medicine. Because of its widespread use, the market value of PRP is expected to reach \$126 million by 2016. It is well known that PRP is rich in platelets that are natural reservoirs of growth factors, which stimulate the healing of injured tissues by inducing proper differentiation of tissue specific stem cells. Further, PRP forms a gel also called as fibrin gel after platelet activation by thrombin, Ca^{2+} or collagen. This fibrin gel itself is believed to contribute to tendon healing by providing a conductive scaffold for cell migration and new matrix formation. However, the efficacy of PRP treatment for tendinopathy is controversial mainly due to inconsistent results from human clinical trials, which is highly complex because factors such as age, gender, disease history, and treatment history can influence the outcome of PRP treatment.

To address this controversy in the PRP efficacy, my group investigated the effect of PRP in several studies performed *in vitro* and *in vivo*. In the first study, we showed that treating TSCs with PRP-releasate induces TSC differentiation into active tenocytes, which proliferate quickly and produced abundant collagen, indicating the potential of PRP to enhance the repair of injured tendons. Additionally, PRP did not induce non-tenocyte differentiation of TSCs into chondrocytes, adipocytes, or osteocytes, suggesting that PRP treatment does not increase the risk of non-tendinous tissue formation in treated tendons. In the second study, we used a cell culture model to demonstrate that PRP's anti-inflammatory function is mediated via HGF contained in PRP. HGF acts by suppressing the levels of the prostaglandin biosynthetic pathway components (COX-1, COX-2 and mPGES-1 expression) and PGE₂ production. Our animal model studies also corroborated these results; PRP injections reduced COX-1 and COX-2 protein expression and lowered PGE₂ levels in wounded mice Achilles tendons. Since PGE₂ is an inflammation mediator, PRP's beneficial outcomes reported in human clinical trials is likely due to a reduction in PGE₂ production. Finally in the third study, we examined the differential effects of leukocyte-containing PRP (L-PRP) and pure PRP (P-PRP, or PRP without leukocytes) on tendon stem/progenitor cells. We found that both L-PRP and P-PRP induce the differentiation of TSCs into active tenocytes and increase their proliferation. More importantly, however, L-PRP induces inflammatory and catabolic responses in differentiated tenocytes while P-PRP mostly augmented anabolic responses.

In addition to presenting our base science findings on PRP, in this presentation I will also discuss the barriers to the current clinical applications of PRP in the treatment of tendinopathy and suggest new approaches to PRP treatments in clinics.

HEALING AND REGENERATION AFTER ANTERIOR CRUCIATE LIGAMENT INJURY

Chih-Hwa Chen, MD

Department of Orthopaedic Surgery, Taipei Medical University Hospital, Taipei Medical University, Taipei, Taiwan

Novel treatment methods for repair and regeneration of ACL injury with biological approaches have been developed. ACL repair with biological agents have been an option for future treatment of acute ACL injuries. Identification of obstacles to native ACL healing is crucial for developments of potentially solutions using biological strategies. Understanding the mechanisms of this healing process and the nature and potential of stem cells and progenitor cells for treating ACL injury and the cells involved may lead the way for novel and biology-based techniques for treatment of ACL injury. Several biological factors influence the healing after ACL injury process that mainly through the local growth factors and ACL cell repair mechanisms controlled by stem cells or progenitor cells. Growth factors have demonstrated their roles in the healing process of ACL injury. These growth factors, including transforming growth factor (TGF), epidermal growth factor (EGF), vascular endothelial growth factor (VEGF), insulin like growth factor (IGF), basic fibroblast growth factor (bFGF), and platelet derived growth factor (PDGF), were proved to potentially regulate the ligament cell activities, promote cell proliferation and anabolic state of ligamentous cells, induce extracellular matrix (ECM) deposition , and influence the differentiation of mesenchymal stem cells into fibroblasts to achieve the repair of ACL tears. The use of platelet rich plasma (PRP) was considered for potentially effective agent for improving the healing of ACL injury. Mesenchymal stem cells (MSCs) can be considered a possible solution to regenerate injured ligaments. The MSCs demonstrated the capacity to secrete the ECM and regenerate ligamentous tissue when injuries occurred. Mesenchymal stems cell have demonstrated their roles in the healing process of ACL injury. These stem cells, including adipose derived stem cells and ACL derived stem cells for the repair and regeneration of torn ACL. MSCs injection in ACL tears promotes the ability to differentiate into fibroblasts and secrete the ECM, the capacity to regenerate a ligamentous tissue in partial ACL tears. The application of growth factors and MSCs for the treatment of ACL tears required to clarify the effectiveness of growth factors and MSCs for the management of ACL tears.

BIOMECHANICS AND KINEMATIC STUDIES OF THE ACL

Guoan Li, PhD; Ali Hosseini, PhD

Orthopaedic Bioengineering Lab, Massachusetts General Hospital
Boston, MA

INTRODUCTION

ACL reconstruction is routinely performed to restore stability of the knee after traumatic rupture of the ACL. Although clinically successful, on average, 50% of ACL reconstructed knees develop OA within 10 years after the surgery. We performed a series of in vitro and in vivo studies to investigate the forces inside the knee joint to explore the possible mechanisms of post-operative OA.

IN-VITRO STUDY: ACL GRAFT FORCES AND ATT IN ACL RECONSTRUCTED KNEES

Using 19 cadaveric knees tested on a robotic system, we examined the knee anterior tibial translation (ATT) under a 130 N anterior tibial load before and after ACL reconstruction using an anteromedial portal technique and a BPTB graft. The correlation between the changes of ACL graft forces and the changes of knee motion (residual laxity) compared to the intact knee condition was analyzed (**Fig. 1**). The data showed a significant negative correlation between the increases of ACL graft forces and the increases of knee motion ($r=0.61$, $p<0.05$). A zero change of knee motion (or restoration of anterior laxity of the intact knee) corresponded to a 20 N increase of the graft force compared to the native ACL force, indicating that contemporary ACL reconstruction had ACL graft forces higher than the intact ACL forces in order to restore normal knee stability.

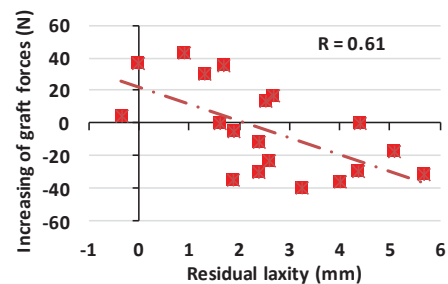


Fig.1 Correlation of the changes of ACL graft forces and the residual laxity of the knee under an anterior tibial load of 130 N.

IN-VIVO STUDY: CARTILAGE DEFORMATION AND ATT OF ACL RECONSTRUCTED KNEES

Using 9 ACL patients, we determined the increases of peak cartilage contact deformation and the changes of anterior knee motion (residual laxity) during a weightbearing single leg lunge after ACL reconstruction by comparing with the uninjured contralateral knees at post-operation of 1 year (**Fig. 2**). The changes of peak cartilage contact deformation were between 3.3% and 12.4%, and the changes of knee motion were between -0.7 mm to 5.0 mm at weightbearing full extension position of the knee of this group of patients. The data showed a significant negative correlation between the increasing cartilage contact deformation and decreasing of the knee motion ($r=0.68$, $p<0.05$). A zero change of knee motion (i.e., the functional knee laxity was restored) corresponds to a 9.5% increase of the peak cartilage contact deformation compared to the uninjured contralateral knee.

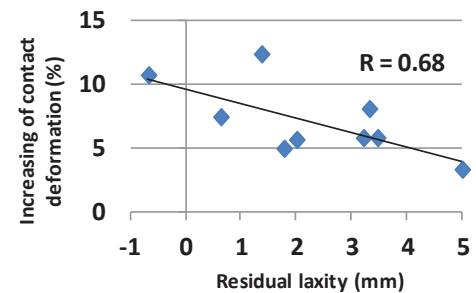


Fig. 2 Correlation of the changes of peak cartilage contact deformation and the residual laxity of the knee during the single-leg lunge.

SUMMARY

We found from these studies that with contemporary ACL reconstruction techniques, the ACL graft forces need to be higher than the native ACL forces in order to restore the anterior knee joint stability in an anterior drawer test, and there is a relationship between the increasing changes of cartilage contact deformation and the decreasing changes of knee motion in ACL reconstruction patients.

These data implied that in a clinically successful ACL reconstruction, a balance in controlling functional knee motion after ACL reconstruction might be critical, since over-constraint of knee motion during functional activities could result in increased cartilage deformation. There is a need to determine what changes of functional knee motion would be beneficial in maintaining cartilage contact deformation after ACL reconstruction surgery.

PREDICTING TENDON ECM COMPOSITION FROM TENOCYTE STRAIN AND FIBER DAMAGE

Arash Mehdizadeh, Bruce Gardiner and David Smith

Faculty of Engineering, Computing and Mathematics, University of Western Australia, Crawley, Western Australia, Australia

INTRODUCTION

Tendon is a fibrous tissue connecting muscle with bone. Cyclic loading damages collagen fibres, which need to be repaired to maintain tendon tissue integrity. While the details of the molecular repair processes are not all known, it is clear that the concentrations of the various molecules in the interstitial fluid are crucially important in regulating tendon homeostasis and repair process. The composition of extracellular matrix in tendon depends on the secretion profile of resident cells known as tenocytes. For mechanical tissues like tendon, it is well known that mechanical strain plays an important role in determining the secretion profile of cells. In this study we present a mathematical method to predict concentrations of various key molecules in the extracellular matrix (ECM) of tendon tissue as a function of tendon activity level and damage.

METHODS

To develop our theoretical model of ECM composition for tendon, we first provide a mathematical framework for upscaling or relating cell scale processes to tissue level observations. Based on experimentally available data on the variation in the secretion profile with respect to strain, we then propose that reference secretion profiles exist as a functions of local strain. These secretion profiles as functions of strain are referred to here as elementary cell responses (or ECRs). When we apply loading to the whole tendon, the ECRs together with a model of tendon fatigue damage enables us to theoretically calculate changes in the average tissue concentration profiles for various signalling and structural molecules with increasing levels of cyclic tissue strain.

RESULTS AND CONCLUSIONS

Figure 1, below, presents the ECR and average tissue level concentrations (tissue level response) of TGF- β in tendon as functions strain and number of cycles (N). As shown, our model predicts U-shape tissue level TGF- β concentration profiles as tendon strain is increased from zero up to damaging levels. Similar profiles are obtained for other key ECM molecules (particularly IL-1 β , MMP-1, ADAMTS-5, GAG and Collagen type I). Our findings are consistent with the experimental observations in numerous studies of loaded tendon. Particularly, our results clearly capture the similarities in tendon ECM composition that are reported for both under-used and over-used tendons.

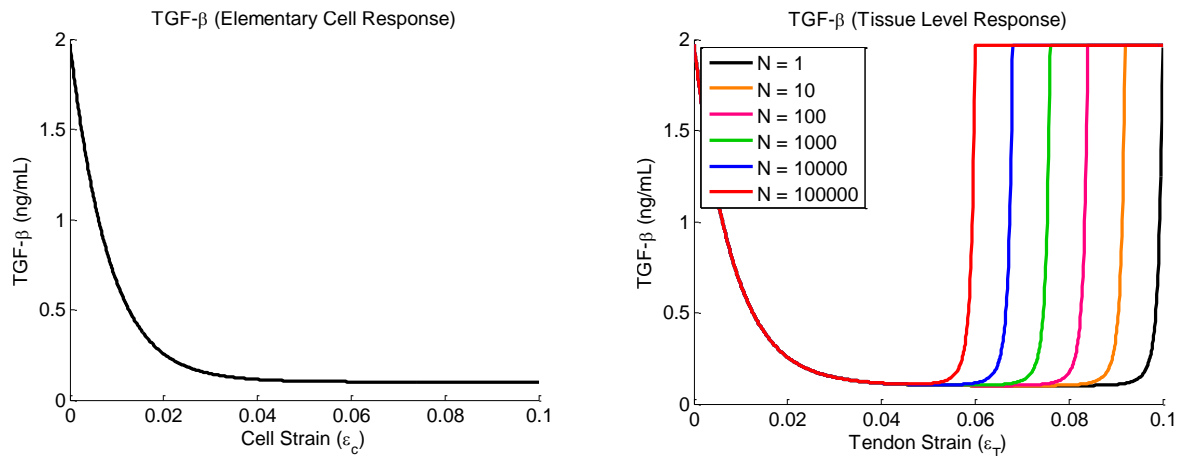


Figure 1. TGF- β Cell and tissue level response at equilibrium. ECR is reported as a function of local cell strain, TLR is reported as a function of tendon tissue strain and number of cycles (N).

DEVELOPMENT AND VALIDATION OF A COMPUTATIONAL FOOT AND ANKLE MODEL TO INVESTIGATE LATERAL LIGAMENTOUS STRAIN

Sophia Chui-Wai HA¹, Daniel Tik-Pui FONG², Feng WEI³, Defeng WANG⁴, Kai-Ming CHAN¹

¹ Department of Orthopaedics and Traumatology, Prince of Wales Hospital, Faculty of Medicine, The Chinese University of Hong Kong, Hong Kong

² National Centre for Sport and Exercise Medicine, School of Sport, Exercise and Health Sciences, Loughborough University, Loughborough, Leicestershire, United Kingdom

³ Orthopaedic Biomechanics Laboratories, Departments of Radiology and Mechanical Engineering, Michigan State University, East Lansing, Michigan, United States of America

⁴ Department of Imaging and Interventional Radiology, Prince of Wales Hospital, Faculty of Medicine, The Chinese University of Hong Kong, Hong Kong

INTRODUCTION

Ankle inversion sprain is one of the most frequent injuries sustained in sports [1]. Understanding the injury mechanisms is a key component of preventing sports injuries [2]. Computational models of musculoskeletal joints and limbs can provide useful information about joint mechanics [3]. Validated models can be predictive tools to understand normal joint function and serve as clinical tools for predicting and helping to prevent sports injuries [4]. This study aims to develop and validate a computational model of the foot and ankle to investigate lateral ligamentous strain in various joint motions.

METHODS

A male athlete was invited to participate in this extended study [5]. His mid-femur to the foot segments were CT scanned to obtain detailed joint anatomy. The CT images were imported to MIMICS and meshed as individual solid bodies. These bones were computationally separated and being assembled in SolidWorks according to the anatomical position. Ligaments were represented as linear springs. Ligamentous restraints and motion constraint were applied to the model. Since toe involvement in inversion sprain is minimal, the phalanges were neglected in this model.

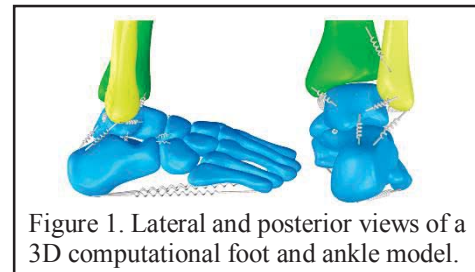


Figure 1. Lateral and posterior views of a 3D computational foot and ankle model.

Ligament strain of the model was validated against a cadaveric study done by our laboratory. In the cadaver study, specimens were moved from neutral position to a variety of motions: 30° inversion, 20° eversion, 50° plantarflexion, 20° dorsiflexion, 30° internal rotation, and 40° external rotation. Ligament length of the anterior talofibular ligament, calcaneofibular ligament, and posterior talofibular ligament were measured continuously at every 10° by a digital caliper. Sensitivity tests were performed using the computational model by modifying all ligament stiffness values by either increasing 25% or decreasing 25%. Continuous motions in three planes were then simulated with the computational model. Ligament strains in anterior talofibular ligament, calcaneofibular ligament, and posterior talofibular ligament were calculated and compared to those measured in the cadaver tests.

RESULTS

The ligament strains of the model followed similar trends as those of the cadaver study. The strain of anterior talofibular ligament increased during plantarflexion, inversion, and internal rotation. The calcaneofibular ligament strain was under stress in dorsiflexion, inversion, and internal rotation. The posterior talofibular ligament strain was elongated in dorsiflexion, eversion, and external rotation.

DISCUSSION

The computational model was successfully developed and validated against a cadaver study. This computational model will be further used to simulate the subject-specific injury profile in order to estimate the ligament strain during a Grade 1 injury [5]. Additionally, this model can also be used in evaluation of an intelligent anti-sprain system to determine if it is effective in preventing this particular injury, and thus to further optimize the anti-sprain system.

REFERENCES

1. Fong, D.T.P., et al., Sports Med, 2007. **37**(1): p. 73-94.
2. Bahr, R. and T. Krosshaug. Br J Sports Med, 2005. **39**(6): p. 324-9.
3. Liacouras, P.C. and J.S. Wayne. J of Biomech Eng, 2007. **129**(6): p. 811-817.
4. Wei, F., et al., Ann Biomed Eng, 2011. **39**(2): p. 756-765.
5. Fong, D.T.P., et al., Am J Sports Med, 2009. **37**(4): p. 822-827.

ADAPTIVE REMODELING OF ACHILLES TENDON: A MULTI-SCALE COMPUTATIONAL MODEL

Stuart Young, Bruce Gardiner, Arash Mehdizadeh, Jonas Rubenson, Brian Umberger, David Smith
 Faculty of Engineering, Computing and Mathematics, University of Western Australia, Crawley,
 Western Australia, Australia

INTRODUCTION

It is known that musculotendon units adapt to changing loading requirements, but there is only a limited understanding of how tendon adaptation actually occurs *in vivo*. To date, it is unclear how the muscle-tendon unit's mechanical and energetic function is affected by tendon damage and repair. We addressed this by developing a predictive multiscale computational tendon model that combines both mechanical and biochemical processes.

METHODS

The central hypothesis is that known damage and repair processes occurring within tendon modify the distribution of collagen fiber lengths in Achilles tendon. Through a computational model of the damage and repair processes we show that these physiological processes enable tendon to adapt to its environmental conditions and improve muscle efficiency for locomotion. To do this, we first developed a discrete 'string model' of tendon that can reproduce (human) Achilles tendon stress-strain behavior. Then using known information about mechanical and proteolytic damage and repair of collagen fibers in tendon, we propose a method for functionally integrating these basic processes. To demonstrate tendon adaptation over time, we implement the tendon-remodeling model within a three-component Hill type model of the (human) Achilles-soleus musculotendon unit.

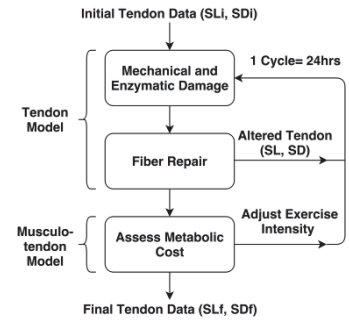


Figure 1. Tendon remodeling flowchart, SL and SD represent tendon fiber slack length and standard deviations.

RESULTS AND CONCLUSIONS

With appropriate parameter selection the tendon remodeling model is able to predict changes to the tendon length and mechanical properties due to its loading environment. Furthermore it is shown to independently predict rates of collagen fiber turnover that are in general agreement with previously puzzling experimental data. Inclusion of a muscle-model to the system allows tracking of energetic changes to the entire musculotendon unit providing further insight to the effects of tendon remodeling. While the basic tendon remodeling model demonstrated here represents only the first steps in this new approach to tendon remodeling, it appears likely that the structure of the proposed remodeling model may itself provide a theoretical foundation for valuable qualitative and quantitative insights into both normal physiological and pathological tendon states.

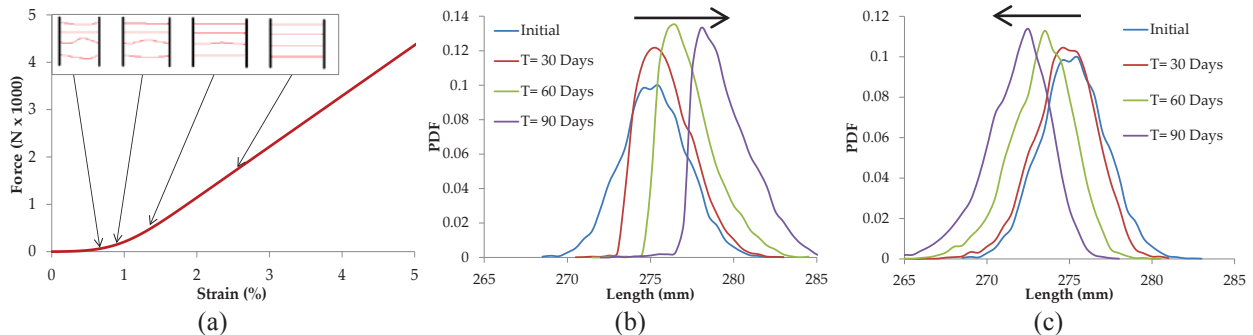


Figure 2. a) Typical tendon force-strain curve response from tendon model. b) Lengthening of the tendon fiber length distribution as a result of mechanical damage and repair. c) Shortening of the tendon fiber length distribution as a result of proteolytic degradation damage and repair. Note the shifting mean in b) and c) and their directions.

HISTOLOGY-INSPIRED MECHANICAL ANALYSIS OF ANTERIOR CRUCIATE LIGAMENT INJURY

Callan M. Luetkemeyer, James A. Ashton-Miller, Ellen M. Arruda

University of Michigan, Ann Arbor, MI, USA

INTRODUCTION

The anterior cruciate ligament (ACL) is the most common knee ligament injured, and recent studies by Lipps et al. and Beaulieu et al. have examined the fatigue life of the human ACL. However, the mechanisms involved in ligament fatigue remain unknown and many risk factors for ACL injury are unidentified or unexplained. For example, it is well-known that women are 2-7 times more likely to sustain an ACL injury than men, smaller intercondylar notch width is correlated with greater injury risk, and most ACL tears occur at the femoral enthesis, but the rationale for these findings is lacking. Histological analysis by Beaulieu and colleagues lead to the identification of six main shapes of the human femoral enthesis by the profile of their tidemarks, as well as quantification of the attachment angle of the ACL as it arises from the femur. These findings were used to create models to investigate the effects of femoral enthesal shape and attachment angle on the strain field in the ACL.

METHODS

Strain fields were computed using both an analytical 2D model and a 3D finite element model. ABAQUS 6.13 (Abaqus Inc.) was used with a Holzapfel-Gasser-Odgen (HGO) constitutive model. Material constants were found using the average of previously published uniaxial experimental data for both bundles. These strain fields will inform a micromechanical model to investigate the ACL fatigue process. Fracture properties were measured using T-peel and simple lap shear tests in conjunction with digital image correlation (DIC).

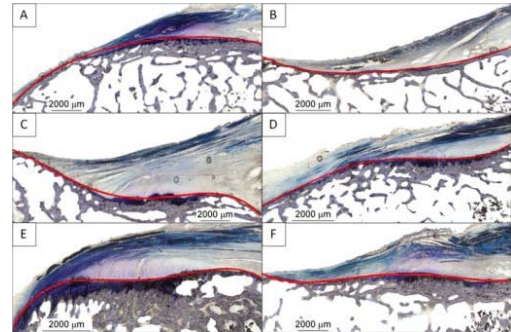


Fig. 1. Human ACL femoral enthesis profiles, adapted from Fig. 3 in Beaulieu et al. 2015.

RESULTS

Enthesal shapes A (convex), C and E reduced the maximum von Mises strain compared to a flat (linear) shape, while shapes B (concave), D and F increased von Mises strain in comparison to the linear (no curvature) shape. Not surprisingly, a smaller attachment angle increased shear strain, thus increasing the maximum von Mises strain for all shapes.

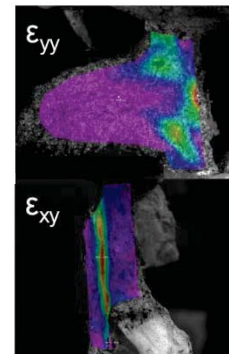
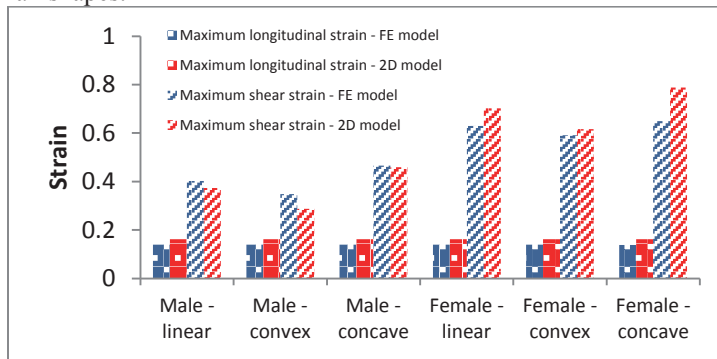


Fig. 2. (Left) Comparison of 2D and 3D model results. (Right) Preliminary fracture testing data.

DISCUSSION

These results lend insight into why most ACL failures occur at the femoral enthesis, and most importantly, why women are more susceptible to ACL injury. Not only do women, on average, have a more acute angle of attachment, but they are also more likely to have one of the less advantageous enthesal shapes. Grouping the shape data by gender, we found that nearly half of all female sections in the Beaulieu et al. study (43%) had shapes B, D or E, while less than 20% of the male sections possessed one of these less advantageous shapes. Additionally, we have shown that ductile fracture tests of the ACL are feasible, the results of which have the potential to model the ACL fatigue failure process.

PRE-OPERATIVE INTRAMUSCULAR FAT FRACTIONS ARE SIGNIFICANTLY HIGHER IN PATIENTS WITH EVENTUAL FAILED ROTATOR CUFF REPAIR

Drew A. Lansdown¹, Sonia Lee², Craig Sam², Roland Krug², Brian T. Feeley¹, C. Benjamin Ma¹
(1) Department of Orthopaedic Surgery; (2) Department of Radiology & Biomedical Imaging
University of California, San Francisco

INTRODUCTION

Worsening fatty infiltration has been correlated with failure of surgical repair and poor surgical outcomes, though prior efforts may have been limited by the variability of the Goutallier classification.¹ A quantitative MRI-based method using IDEAL can accurately determine the intramuscular fat fraction.² The purpose of this study is to evaluate fatty infiltration before and after surgical treatment using IDEAL MRI. We hypothesized that patients with failed rotator cuff repairs would have increased intramuscular fat fractions.

METHODS

A total of 23 patients (61.2±10.1 years, 8 female) underwent baseline MRI with IDEAL fat imaging before surgery and 6 months after rotator cuff repair. The supraspinatus (SS), infraspinatus (IS), subscapularis (SC), and teres minor (TM) muscles were segmented manually on four consecutive slices centered at the scapular Y. The intramuscular fat fraction was calculated for each muscle. Pre-operative tear size and post-operative repair integrity were recorded. Tear size was categorized as involving one tendon (13 patients) or multiple tendons (10 patients) based on intra-operative findings. Patients were divided into two groups based on repair integrity on MRI appearance at 6 months follow up. Student's t-tests were used to compare fat fractions, and chi-squared tests were used to compare frequency variables. Statistical significance was defined as $p < 0.05$.

RESULTS

The intramuscular fat fractions were significantly higher in patients with tears involving multiple tendons relative to single-tendon tears in SS, IS, and SC muscles at baseline and follow up. There were 7 patients with a failed repair based on MRI appearance. Two patients with a single tendon tear had a failed repair and 4 patients with a multiple tendon tear had a repair failure ($p=0.18$). The baseline SS fat fraction was significantly higher ($p=0.012$) in patients with eventual failure at 6 month follow up (Figure 1). The post-operative fat fractions for SS ($p=0.021$) and IS ($p=0.022$) were also higher at 6 months for the failed repair group relative to the intact group (Figure 1). For patients with an eventual failed repair, the IS fat fraction increased from 5.61% at baseline to 10.5% at 6-month follow-up ($p=0.10$).

DISCUSSION

The intramuscular fat fractions were significantly higher in patients with tears involving multiple tendons. This observation is consistent with prior observations in a larger groups of patient where tear size and tendon retraction were strong predictors of worsening fat content.² This finding is also unchanged at 6 months after rotator cuff repair. Patients with imaging evidence of a failed repair had significantly higher fat fractions in SS, and these patients had significantly higher fat fractions in SS and IS muscles at 6 month follow up. In those patients with a failed repair, the IS fat fraction showed a trend towards a significant progression between baseline and follow-up. Quantitative MRI may have the ability to help surgeons and patients understand the potential risks of post-operative failure after rotator cuff repair.

REFERENCES

1. Gladstone JN, Bishop JY, Lo IKY, Flatow EL. Fatty infiltration and atrophy of the rotator cuff do not improve after rotator cuff repair and correlate with poor functional outcome. *Am J Sports Med.* 2007;35(5).
2. Lee S, Lucas RM, Lansdown DA, Nardo L, Lai A, Link TM, Krug R, Ma CB. Magnetic resonance rotator cuff fat fraction and its relationship with tendon tear severity and subject characteristics. *J Shoulder Elbow Surg.* 2015;24(9).

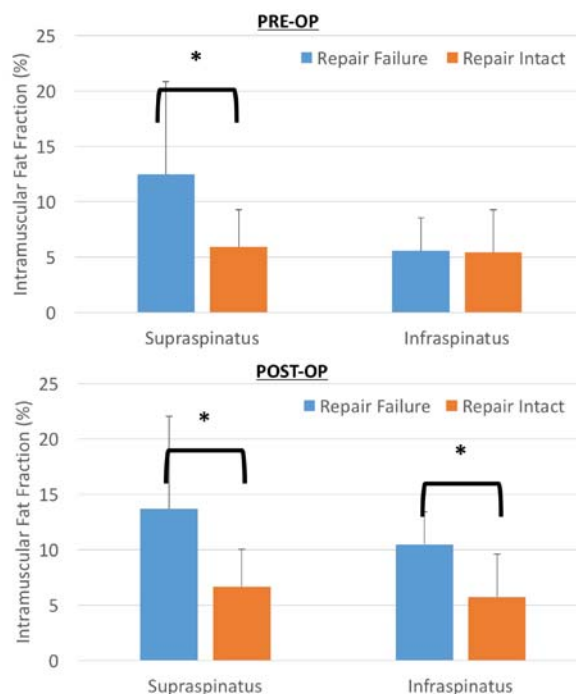


Figure 1. Intramuscular fat fractions for the supraspinatus and infraspinatus muscles shown for patients with failed rotator cuff repairs and intact repairs both before (top) and after (bottom) surgical repair. * signifies $p < 0.05$.

MICRO-CT EVALUATION OF CARTILAGE DEGENERATION IN TWO RODENT MODELS OF ROTATOR CUFF INJURY

McFaline-Figueroa, Jennifer¹; Parks, Akia¹; Guldborg, Robert^{2,3}; Platt, Manu^{1,3}; Temenoff, Johnna^{1,3}

1. Coulter Dept. of Biomedical Engineering, Georgia Tech and Emory University, Atlanta, GA 2. George W. Woodruff School of Mechanical Engineering 3. Petit Institute for Bioengineering and Bioscience, Georgia Institute of Technology, Atlanta, GA, US.

INTRODUCTION There has been increasing interest in recent years in the effect of rotator cuff tendon injuries on the integrity of other tissues within the glenohumeral joint. Previous work has shown a relationship between rotator cuff injuries and degeneration of the articular cartilage 12 weeks after a full-thickness supraspinatus tear in rodents [1], and in postmortem analysis of shoulder joints in humans with partial and full-thickness rotator cuff tears [2]. Therefore, this study sought to better understand the changes in the humeral articular cartilage in rat models of two different stages of rotator cuff tendon injury: 1) an overuse injury induced by downhill running; and 2) a surgically-induced full thickness rotator cuff tear. It is hypothesized that both overuse and full thickness tear injuries will cause degenerative changes in the cartilage of the humeral head, as compared to non-injured controls. For these studies Equilibrium Partitioning Ionic Contrast-microcomputed tomography (EPIC- μ CT) was used to quantify cartilage and subchondral bone morphology and cartilage GAG content.

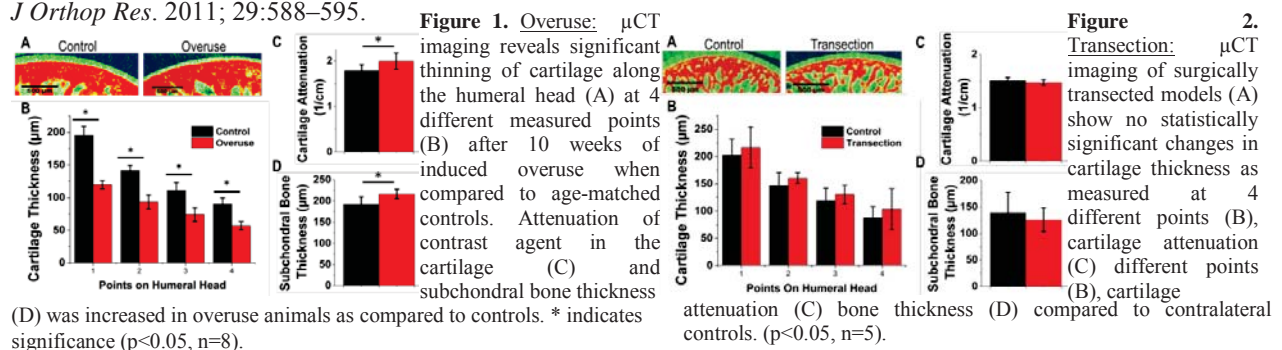
METHODS Procedures were approved by the IACUC at Georgia Tech. In the overuse injury, male Dahl-Salt Resistant rats were subjected to a daily downhill running regime described previously [3] for 10 weeks (n=8 humeral heads), compared to age-matched controls with only cage activity (n=8 humeral heads). In the tendon transection injury, male Sprague Dawley rats were subjected to a unilateral surgery described previously [4] where the supraspinatus and infraspinatus tendon were sharply dissected from the insertion region at the humeral head and 2mm of the suprascapular nerve was resected. Joints were evaluated 6 weeks after tendon transection (n=5 humeral heads), compared to their non-operated shoulder (n=5 humeral heads).

For both injury models, humeral bones were treated with 10% Hexabrix (Covidien) for 30 minutes in a 37° bath. The humeral heads were scanned using the μ CT50 (Scanco Medical) at 45 kVp, 200 μ A, 600ms integration time, and a 9 μ m voxel size, and analyzed for cartilage thickness at 4 measured points along the humeral head. Subchondral bone thickness was measured along the whole surface and contrast agent attenuation was evaluated. Individual pairs of data (between injury vs. control at a specific location) were analyzed by t-tests (p<0.05). Values are reported as mean \pm standard deviation.

RESULTS The quantification of μ CT imaging on 10 week overuse animals show a decrease in cartilage thickness in running animals as compared to their controls. Values for cartilage contrast agent attenuation and subchondral bone thickness were increased in running animals (Fig 1). In animals 6 weeks after full thickness tears, there was no significant difference in cartilage thickness, cartilage attenuation or subchondral bone thickness (Fig 2).

DISCUSSION Significant differences in cartilage thickness as well as increased contrast agent attenuation following 10 weeks of running suggest degeneration of the cartilage due to the overuse protocol, including a loss of proteoglycan content. To the best of our knowledge, this is the first time cartilage thickness has been evaluated in an overuse model. In contrast, although previous work has demonstrated cartilage degeneration using a transection model at 12 weeks after tendon injury [1], there were no appreciable differences at the 6 week time point evaluated here. Overall, these results demonstrate that, at least in tendon overuse scenarios, humeral cartilage degeneration also occurs, and suggests that further study is needed to better understand how various mechanisms of tendon injury affect the local catabolic environment within the glenohumeral joint.

REFERENCES [1] Kramer, E. et al. *J Shoulder Elbow Surg.* 2013; 22, 1702-1709. [2] Feeney, et al. *J Shoulder Elbow Surg.* 2003; 12(1), 20-23. [3] Soslowsky, L.J. et al. *J Shoulder Elbow Surg.* 2000; 9(2), 79-84. [4] Liu, X. et al. *J Orthop Res.* 2011; 29:588–595.



EFFECT OF HYPERCHOLESTEROLEMIA ON FATTY INFILTRATION AND ROTATOR CUFF HEALING IN A CHRONIC ROTATOR CUFF TEAR MODEL OF RABBIT

Seok Won Chung*, Sae Hoon Kim, Hae Bong Park†, Ji Eun Kwon‡, and Joo Han Oh

Department of Orthopaedic Surgery, Seoul National University College of Medicine, *Konkuk University School of Medicine, †CM Chungmu Hospital, ‡National Police Hospital, Seoul, Korea

INTRODUCTION

The purpose of this study is to verify the effect of hypercholesterolemia on fatty infiltration and rotator cuff healing in chronic rotator cuff tear model using a rabbit supraspinatus. We also aimed to investigate whether the control of hypercholesterolemia can help the improvement of fatty infiltration and healing after rotator cuff repair.

METHODS

Forty-eight rabbits were randomly allocated into 4 groups (12 rabbits per each group, 8 for the electromyographic (EMG) and mechanical tests in right shoulder and the histological test of fat proportion in both shoulders; additional 4 (bilateral shoulder) for the histology of tendon-to-bone healing): Group A (high-chol.+repair), Group B (high-chol.+statin+repair), Group C (repair), and Group D (control). Initial hypercholesterolemia was made by feeding rabbits of Group A and B with a high-cholesterol meal for 4 weeks, then the supraspinatus tendon was detached in Group A, B, and C. Six weeks after detachment, the supraspinatus tendon was repaired in a transosseous manner. Group A got the high-cholesterol diet persistently until final evaluation (6 weeks after repair), however, Group B changed the diet to general diet with an administration of cholesterol lowering agent (simvastatin) from the time of repair. The EMG test, mechanical test, and histological test of tendon-to-bone healing was performed at final evaluation, and the histological evaluation for the fat-to-muscle proportion was performed at two times at the time of repair and at final evaluation.

RESULTS

For EMG test, Group A showed significantly smaller area in compound muscle action potential (6.69 ± 2.23 ms·mV) compared with Group C and D (10.50 ± 2.96 ms·mV and 14.40 ± 2.79 ms·mV, $p=0.008$ and <0.001). Group B (9.05 ± 3.23 ms·mV) showed larger area than group A without statistical significance ($p=0.112$), almost to the level of group C. For mechanical test, Group A showed significantly lower load-to-failure and stiffness (42.01 ± 13.80 N and 36.32 ± 14.70 N/mm) compared with Group C (65.12 ± 22.81 N and 65.31 ± 23.21 N/mm, $p=0.020$ and 0.006 , respectively). The load-to-failure and stiffness of Group B (58.23 ± 22.39 N and 47.22 ± 14.14 N/mm) was higher than Group A without statistical differences ($p=0.103$ and 0.153 , respectively), but the stiffness of group B was still much less than group C ($p=0.065$). The Group D (normal control) showed much higher load-to-failure (148.01 ± 26.12 N) than any other groups (all $p<0.001$), however, the stiffness of Group D (62.51 ± 14.29 N/mm) was between that of Group B and C. For the histological test, Group A and B showed significantly higher fat-to-muscle proportion ($59.26 \pm 17.80\%$ and $64.02 \pm 11.87\%$) compared with Group C ($44.26 \pm 7.85\%$, $p=0.044$ and 0.004 , respectively) or D ($8.02 \pm 5.29\%$, all $p<0.001$) at 6 weeks after detachment. At the final evaluation, the fat-to-muscle proportion (Figure 1) of Group A was more increased to $78.23 \pm 10.87\%$ ($p=0.015$), but that of Group B was decreased to $54.68 \pm 10.47\%$ ($p=0.146$). Group A showed coarse and poorly organized collagen fibers with fat interposition in tendon-to-bone insertion area, but Group B and C showed better collagen fiber continuity and orientation with higher collagen density than group A. (Figure 2)

Figure 1.

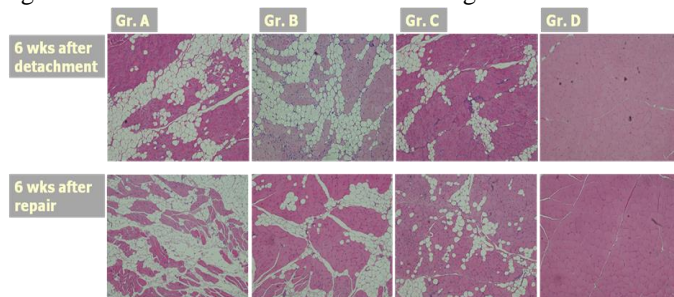
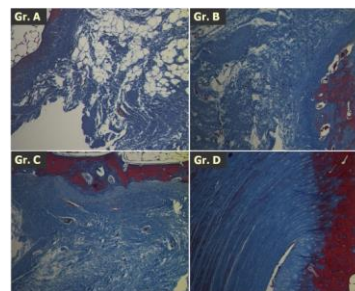


Fig.2



DISCUSSION

The hypercholesterolemia resulted in the deleterious effect on the fatty infiltration and tendon-to-bone healing assessed by electromyographic, mechanical, and histological evaluation, and the control of hypercholesterolemia seemed to be able to reverse these harmful effects to some degree even after rotator cuff repair surgery.

REFERENCES

1. Abboud JA et al. Clin Orthop Relat Res. 2010
2. Beason DP et al. J Orthop Res. 2011.
3. Cavallini DC et al. Lipids Health Dis. 2009.
4. Dolkart O et al. Am J Sports Med. 2014.
5. Esenkaya I et al. Muscles Ligaments Tendons J. 2011.
6. Gladstone JN et al. Am J Sports Med. 2007.
7. Kertesz A et al. Int J Mol Sci. 2013.
8. Longo UG et al. Br J Sports Med. 2010.
9. Oh JH et al. J Shoulder Elbow Surg. 2014.

TISSUE ENGINEERED TENDON CONSTRUCTS FOR ROTATOR CUFF REPAIR IN A SHEEP MODEL

Stoyna S. Novakova, Vasudevan D. Mahalingam, Delta L. Leeper, Ellen M. Arruda, Answorth Allen, Asheesh Bedi, and Lisa M. Larkin

University of Michigan, Ann Arbor, MI Hospital for Special Surgery, New York, NY

INTRODUCTION

Rotator cuff (RC) tears are a common orthopaedic disorder in the US with 70,000 repairs performed annually at an estimated health care cost of 474M [1]. Thus, the need for technologies to improve structural healing after rotator cuff repair is of paramount importance. Repair of RC with suture techniques fails 20-57% of the time due to a lack of native tendon to bone interface or “enthesis” regeneration [2-3]. Therefore, many of RC repairs (30,000/year) are mechanically reinforced with biological or synthetic patches. The efficacy of the commonly used biological patches, however, is modest, with re-tear rates as high as 91% [4]. Our lab has previously demonstrated entheses regeneration using our cell-generated graft approach in a sheep ACL repair model [5]. Our hypothesis is that our cell-generated graft will also be effective for RC repair.

METHODS

Bone marrow stromal cells were harvested from an iliac crest marrow aspiration of an adult male sheep and were used to fabricate engineered tendon constructs using methods described previously [5]. Following fabrication, the tendon constructs were used as an underlay in combination with a double row suture repair (N=12) and compared to a double row suture repair only (N=11) in female sheep. PCR analysis was used to track cell migration of male DNA out of the construct, and host female DNA into the repair site. Following a 4-month recovery, the grafted and contralateral shoulders were removed from one animal and imaged using x-ray, and with the tendon of the infraspinatus muscle still attached to the humerus, the entire graft was tested for biomechanical integrity using an MTS system. Following biomechanical measures, the muscle, myotendinous junction, entheses, and humeral head were preserved for histological analysis of tendon and entheses structure.

RESULTS

Following a 4-month recovery, the entheses of the grafted tendon showed healing of the bone tunnel and entheses. However, the tendon fibrils of the graft were still highly cellular and not as well organized as those of the native control tendon. Assessment of the biomechanical integrity of the tendon showed a recovery of 80.1 % of the geometric stiffness and 11.6% of the tangent modulus in the grafted tendon compared to the control.

DISCUSSION

We have previously reported that using our cell-generated graft as a replacement graft for ACL reconstruction we had improved outcomes compared to current graft options [5]. Thus, we decided to test the efficacy of our cell-generated graft in a rotator cuff tear model in sheep and compare this novel graft technology to the commonly used double row suture repair technique. While the geometric stiffness indicates the regeneration of tissue in the graft with similar mechanical properties to control, the tangent modulus of the graft suggests that, at the tissue level, the graft is much more compliant than native tissue. The histological analysis indicates that while the entheses has regenerated by 4 months, the tendon structure in the graft is not as well developed compared to control. Similar results were observed in our sheep ACL model, in that, at 4 months the ligament was still very compliant but it continued to remodel and become stiffer with time and by 6 months the ligament structure was indistinguishable from native ligament. Thus, we are continuing our recovery of the remaining animals to 6 months for reassessment.

REFERENCES

1. Vitale, M.A., et. al., *Rotator cuff repair: an analysis of utility scores and cost-effectiveness*. J Shoulder Elbow Surg, 2007. **16**(2): p. 181-7.
2. Montgomery, S.R., et. al., *Failed rotator cuff surgery, evaluation and decision making*. Clin Sports Med, 2012. **31**(4): p. 693-712.
3. Zhang, A.L., et. al., *Arthroscopic versus open shoulder stabilization: current practice patterns in the US*. Arthroscopy, 2014. **30**(4): p. 436-4.
4. Ratcliffe, A., D. et. al., *Scaffolds for Tendon and Ligament Repair and Regeneration*. Annals of biomedical engineering, 2015. **e**. pub.
5. Ma, J., et. al., *Morphological and functional characteristics of engineered bone-ligament-bone constructs*. JBE, 2009. **131**(10): p. 101017.

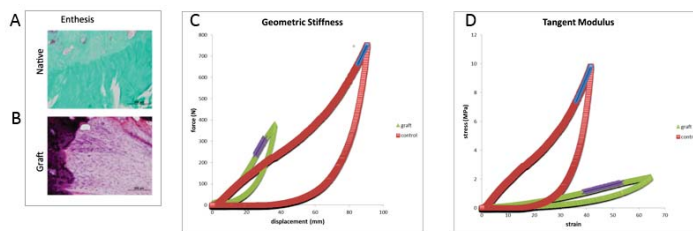


Figure 1. Histology and Biomechanics of Tendon-Bone Interface Following 4-month Recovery from a Rotator Cuff Repair. At 4 months, compared to control (A) the entheses of the grafted tendon (B) has regenerated, however, the tendon fibrils of the graft are still very cellular and not as organized as adult native tendon. Assessment of the biomechanical integrity of the tendon showed a recovery of 80.1 % geometric (C) and 11.6% tangent modulus (D) stiffness in the graft compared to native control tendon.

POSTER PRESENTATION ABSTRACTS

HYPOXIA INHIBITS PRIMARY CILIA FORMATION AND REDUCES CELL-MEDIATED CONTRACTION IN STRESS-DEPRIVED RAT TAIL TENDON FASCICLES

Oslapas, A.N., Gardner, K., Lavagnino, M., +Arnoczky, S.P.

Laboratory for Comparative Orthopaedic Research, Michigan State University, East Lansing, MI

INTRODUCTION

Hypoxia has been implicated in the progression of chronic tendinopathy (1-4). Hypoxia has also been shown to negatively regulate skeletal mechanotransduction by decreasing the sensitivity of bone cells to mechanical signals (5). The inability of some tendinopathy patients to respond to therapies designed to stimulate a mechanotransduction response (i.e. eccentric loading) may reflect a decrease in the mechanosensitivity of tendon cells secondary to a hypoxic environment. Therefore, the purpose of the current study was to determine the effect of hypoxia on the formation of primary cilia (a mechanosensing organelle of tendon cells) *in vitro* and to determine the effect of hypoxia on cell-mediated contraction of stress-deprived rat tail tendon fascicles (RTTfs). *We hypothesize that hypoxia will decrease the number of tendon cells expressing elongated primary cilia in vitro. In addition, we hypothesize that hypoxia will decrease the normal cell-induced tendon contraction that occurs with the loss of cytoskeletal tension.*

MATERIALS AND METHODS

Following institutional animal care and use approval, tendon cells isolated from RTTfs of adult rats were cultured in the presence of normoxia (21% O₂) or hypoxia (1% O₂) for 24 hrs (40,000 cells/well; n=7 plates [42 wells]/condition). The cells were then stained for tubulin and 200 cells per well counted for the presence or absence of elongated cilia and hypoxic versus normoxic conditions compared using a paired *t*-test. To investigate the effect of hypoxia on cell-mediated tendon contraction RTTfs from 1-month-old male Sprague-Dawley rats (n=6) were cultured under hypoxic and normoxic conditions (20 RTTfs/condition/rat) for 3 days. Changes in length were measured daily and compared using corrected paired *t*-tests

RESULTS

A significant (p=0.002) decrease in the percent of elongated cilia 18.2% ± 9.34 was found in cells maintained in hypoxic conditions (54.1% ± 12.2) when compared to cells in normoxic conditions (71.7% ± 6.32) (Fig 1).

RTTfs in both normoxia and hypoxia demonstrated a decrease in their length by Day 1. RTTfs in hypoxia showed a significant decrease in the amount of contraction compared to RTTfs in normoxia at Day 2 (p=0.007), at Day 3 (p=0.001) (Figure 2). RTTfs transferred from hypoxia to normoxia at day 3 demonstrated significantly more contraction at day 6 than those that remained in hypoxia (p=0.008) confirming that the decrease in contraction after 3 days in hypoxia was not due to cell death.

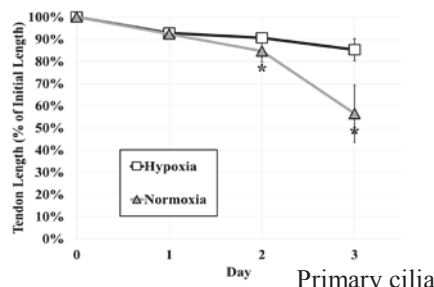


Figure 2: Graph showing the decreased contraction of tendons in hypoxia compared to normoxia over time.

* normoxia vs hypoxia. p<0.05

REFERENCES

1. Benson RT+ *J Bone Joint Surg Br* 2010; 2. Millar N+ *Ann Rheum Dis* 2012; 3. Skovgaard D+ *J Nucl Med* 2009
4. Jozsa L+ *Arch Orthop Trauma Surg* 1982 6. Riddle RC+ *J Biol Chem* 2011 6. Gardner K+ *J Orthop Res* 2011.
7. Gardner K+ *J Orthop Res* 2012.

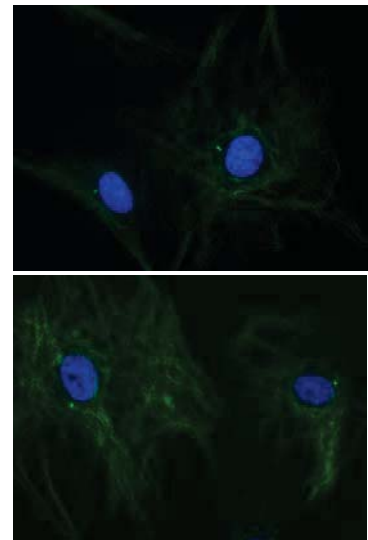


Figure 1: Photomicrograph showing the presence or absence of elongated primary cilia on tendon cells under normoxic (A) and hypoxic (B) conditions.

DISCUSSION

Primary cilia are important mechanosensing organelles in tendon cells and are thought to play a key role in maintaining tendon cell homeostasis (6). The decrease incidence of elongated primary cilia in a hypoxic environment, as well as the decreased mechanoresponsiveness of tendon cells under these conditions may relate to the inability of some cases of chronic tendinopathy to respond to strain-based rehabilitation modalities (i.e. eccentric loading).

HYPERELASTIC AND VISCOELASTIC CHARACTERIZATION OF ANTERIOR CRUCIATE LIGAMENT BIOMECHANICS

Kaitlyn Mallett¹, Ellen M. Arruda^{1,2,3}

Department of Mechanical Engineering¹, Department of Biomedical Engineering², Program in Macromolecular Science and Engineering³, University of Michigan, Ann Arbor, MI, USA

INTRODUCTION

Anterior cruciate ligament (ACL) replacements are among the most common knee ligament invasive procedures. It is estimated that the combination of ACL and meniscal injuries can lead to the development of osteoarthritis in up to 48% of patients with replacements [1]. Within the dynamic model of the knee, the ACL is primarily responsible for preventing anterior translation of the tibia with respect to the femur, and is particularly challenging to experimentally characterize. In its anatomically relevant state, it is twisted and partially extended regardless of knee flexion angle [2-5]. The tissue structures that make up the ACL also exhibit mechanical heterogeneity. The ACL is primarily comprised of two sections of tissue, the anteromedial and the posterolateral bundles (AMB and PLB respectively). These bundles are not simultaneously unloaded under any configuration, and are oriented so that regardless of the angle of extension of the knee, one bundle is always in a state of tension, further complicating characterization efforts [6,7]. These complications pose a major challenge to health care professionals, and there is a pressing need to understand the mechanics of the ACL in physiologically relevant loading states in order to develop accurate constitutive models and select appropriate replacement options.

METHODS

We have performed experiments on the individual bundles of the ACL in uniaxial tension, as well as tests of the full ACL in physiologically relevant loading conditions. Using digital image correlation (DIC) and traditional tension testing techniques, we are able to obtain quantitative global stress and time data, as well as average and region-specific strain information over the surface of the test specimens. DIC is a non-contact and non-intrusive measurement technique that offers many advantages to traditional characterization testing, however, many biological tissues require the application of an artificial pattern, and the generation of innocuous patterns containing the required high density and contrast for correlation poses a challenge to researchers. In this work, a novel approach is utilized for DIC pattern generation, fabrication, and application. Using this technique, the pattern speckle size is controlled within the constraints of camera resolution and specimen size. The use of a new patterning medium that is non-soluble in water allows for continual tissue hydration without loss of pattern integrity. The medium is also removable, making reapplication of the pattern possible.

RESULTS AND DISCUSSION

This technique is capable of generating the pseudo-random, high density and high-contrast pattern necessary for obtaining accurate high resolution strain data of the surface strains of soft biological tissue. The hyperelastic data of the AM and PL bundles demonstrate the diversity of the bundle response. The viscoelastic response of the tissue has been quantified by performing stress relaxation tests and load-unload tests at several strain rates. We demonstrate that the posterolateral bundle of the ACL is linear viscoelastic up to 10% initial strain, whereas the anteromedial bundle is functionally graded in uniaxial tension. We also perform anterior tibial translation loading experiments; this motion is relevant to ACL injury as the ACL tears when the tibia anteriorly translates excessively relative to the femur. We have analyzed the failure response of the AM and PL bundles. We have developed a non-linear viscoelastic constitutive model of the ACL and implemented it into a finite element framework for computational analysis of the ACL during physiologically relevant loading conditions. In the computational environment we can transition from the uniaxial loading state to the anatomically correct loading state and predict the strain fields in the ACL during an anterior tibial translation. Our computational model is able to predict the location of ACL tears in the proximal third of the tissue and simulate the ACL tissue response to diverse knee injury situations.

REFERENCES

- [1] Øiestad B. E., Engebretsen L., Storheim K., and Risberg M. A., 2009, "Knee osteoarthritis after anterior cruciate ligament injury: a systematic review.," *Am. J. Sports Med.*, **37**(7), pp. 1434–43.
- [2] Butler D. L., Kay M. D., and Stouffer D. C., 1988, "Comparison of material properties in fascicle-bone units from human patellar tendon and knee ligaments," *J. Biomech.*, **19**(6), pp. 425–432.
- [3] Butler D. L., 1989, "Anterior cruciate ligament: its normal response and replacement," *J. Orthop. Res.*, **7**(6), pp. 910–21.
- [4] Norwood L. A., and Cross M. J., 1979, "Anterior cruciate ligament: functional anatomy of its bundles in rotatory instabilities," *Am. J. Sports Med.*, **7**(1), pp. 23–26.
- [5] Girgis F., Marshall J., and Al Monajem A. R. S., 1975, "The cruciate ligaments of the knee joint: anatomical, functional and experimental analysis," *Clin. Orthop. Relat. Res.*, **106**, pp. 216–231.
- [6] Arnoczky S. P., Warren R. F., and Ashlock M. A., 1986, "Replacement of the anterior cruciate ligament using a patellar tendon allograft. An experimental study," *J Bone Jt. Surg [Am]*, **68**(3), pp. 376–385.
- [7] Odensten M., and Gillquist J., 1985, "Functional anatomy of the anterior cruciate ligament and a rationale for reconstruction," *J-Bone-Joint-Surg-Am*, **67**(2), pp. 257–9355.

INHIBITION OF RETINOIC ACID SIGNALING AND STIMULATION OF WNT SIGNALING ALLOWS EFFICIENT PARAXIAL MESODERM FORMATION FROM HUMAN EMBRYONIC STEM CELLS

Ryan P. Russell, Yaling Liu, Peter Maye

University of Connecticut Health, Department of Reconstructive Sciences, School of Dental Medicine

INTRODUCTION

Embryonic stem cell (ESC) technologies are continually advancing research and development of treatment strategies for various human diseases, including those that impact the human skeleton. However, a more comprehensive understanding of how to direct ESCs into mature, functional skeletal cell types remains a necessity¹. Studying the axial skeletal lineage is advantageous as its derivatives are capable of forming multiple skeletal cell types including chondrocytes, osteoblasts and tenocytes². We have focused on a stepwise, embryonic differentiation program to generate paraxial mesoderm, sclerotome and eventually skeletal progenitor populations. We have directed human ESCs into paraxial mesoderm through activation of Wnt signaling and inhibition of the retinoic acid pathway. This approach, coupled with the use of transgenic reporter cell lines, including that for TBX6, a key paraxial mesoderm specification gene, demonstrates the first stage in our axial skeletal differentiation protocol.

METHODS

In-vitro differentiation was performed using a *TBX6-mCherry/UbiquitinC-Citrine* human H9 ESC reporter line derived in our lab. ESCs were plated on Matrigel at low density, then switched to a base differentiation media containing N2, B27, MTG, and ascorbic acid the following day. On day 2, cultures were treated with combinations of Wnt3a (50ng/ml), CHIR99021 (3uM), AGN193109 (1uM), and Noggin (100ng/ml) over 4 days. After 4 days of treatment, cultures were imaged, FACS sorted for TBX6⁺ reporter populations, and analyzed via RT-PCR.

RESULTS

Wnt pathway stimulation with Wnt3a and CHIR99021 for 4 days resulted in nominal TBX6 reporter expression in comparison to untreated cells, however treated colonies were more robust and showed stronger Ubiquitin reporter expression. Addition of the retinoic acid receptor antagonist AGN193109 along with Wnt3a and CHIR99021 resulted in a strong increase in TBX6 reporter expression confirmed by FACS analysis, 26.9% TBX6⁺ compared to <1% without AGN. Addition of the BMP antagonist Noggin resulted in a more limited TBX6 reporter expression pattern (9.9% TBX6⁺) compared to Wnt3a, CHIR, AGN without Noggin. FACS sorting of the Wnt3a, CHIR, AGN treated samples resulted in a TBX6⁺ population of 22.8% of viable cells. RT-PCR was performed to compare gene expression between the sorted and unsorted populations. For the paraxial mesoderm markers MEOX1 and Mesogenin, the TBX6⁺ population showed an 18- and 30-fold increase over the unsorted population, respectively. There was a 26-fold difference in endogenous TBX6 expression between the positive and negative sorted populations, confirming the accuracy of the reporter construct in matching endogenous gene expression. Expression of the chemokine receptor CXCR4 (CD184) was also 25-fold higher in the TBX6⁺ population.

DISCUSSION

Wnt pathway stimulation combined with retinoic acid inhibition strongly promotes ESC differentiation into paraxial mesoderm. Key paraxial mesoderm regulatory genes are significantly upregulated in our reporter positive populations, indicating efficient paraxial mesoderm induction as well as reliable reporter function, as are several cell surface marker genes that may be useful for future progenitor cell isolation. Obtaining a uniform population from this primary differentiation stage will allow for more effective generation of sclerotome populations and eventually, functional skeletal progenitors for therapeutic use. By following a differentiation scheme comparable to embryonic development, our ultimate goal is to generate skeletal progenitor cells that are able to persist within repaired tissue and thus maintain their therapeutic function beyond any initial transient effects.

REFERENCES

1. Docheva, D., Müller, S. A., Majewski, M. & Evans, C. H. Biologics for tendon repair. *Adv. Drug Deliv. Rev.* **84**, 222–39 (2015).
2. Scaal, M. Early development of the vertebral column. *Semin. Cell Dev. Biol.* (2015).

HIGH THROUGHPUT, MULTI-IMAGE CRYOHISTOLOGY OF JOINT TISSUES

¹Nathaniel A Dymant, ¹Xi Jiang, ²Yusuke Hagiwara, ¹David W Rowe

¹University of Connecticut Health Center, Farmington, CT; ²Nippon Medical School Hospital, Tokyo, Japan

INTRODUCTION High-quality histological assessment of tendon/ligament research is becoming more prominent with the advent of animal models containing fluorescent proteins such as GFP. Maintaining GFP fluorescence through paraffin processing is challenging, therefore frozen sectioning is the preferred method in these animal models. However, producing frozen sections with minimal sectioning artifact is difficult, especially in adult tissues. Our lab has developed a cryosectioning method using a unique cryotape that adheres to the tissue during sectioning, maintaining the tissue morphology. Consequently, this method can be used to produce high-quality sections with minimal artifact in adult, mineralized tissues of GFP animals. These sections can then be adhered to microscope slides and subsequently taken through multiple rounds of staining and imaging on the same section. As a result, the multiple rounds can be aligned allowing for colocalization measurements of several response measures. This abstract will outline the general workflow for this technique and provide examples from previous tendon/ligament development and repair studies.

METHODS Experimental Design. *Normal Growth.* The Achilles tendon from triple transgenic reporter mice containing Col2a1-CFP, Col1a1(3.6kb)-GFPTpz, and Col10a1-mcherry transgenes were assessed at 2 weeks of age (n=4). *Joint Destabilization.* The ACL was transected (ACLT) in 10-week-old Col1a1(3.6kb)-CFP and Col10a1-mcherry mice. Mineralization labels were delivered on the day before surgery (demeclocycline), 2 weeks post-surgery (calcein), and 4 weeks post-surgery (alizarin complexone). MCL entheses were assessed at 4 weeks post-surgery and compared to intact or sham controls. Sample Preparation. Following CO₂ asphyxiation, limbs were fixed in 10% neutral buffered formalin for 1-3 days at 4°C and then transferred to 30% sucrose for 12-24 hours at 4°C. The limbs were then oriented in either sagittal or coronal planes and embedded in cryomatrix. Sections (7-8µm) were made using cryofilm type-2C [1] and temporarily stored on plastic microscope slides at 4°C. The captured sections were adhered to glass microscope slides using UV-activated glue. The slides were hydrated in 1X PBS and then processed through several rounds of imaging, staining, re-imaging, re-staining, etc. These rounds included 1) endogenous fluorescent signals (fluorescent proteins and/or mineralization labels), 2) collagen structure (two photon second harmonic generation), 3) immunostaining (anti-IHH), 4) enzyme activity staining (tartrate-resistant acid phosphatase and alkaline phosphatase), and 5) chromogenic staining (toluidine blue O). Imaging. Two photon SHG for collagen was imaged on the Prairie Ultima IV multiphoton microscope while all other images were acquired using the Zeiss Axio Scan.Z1 digital slide scanner. Images from each round were aligned and constructed into multi-layer composites in Photoshop.

RESULTS Postnatal Growth [2]. Mineralized fibrocartilage begins to form at 2 weeks of age in the Achilles tendon. The nucleation of mineral coincides with expression of Col10a1-mcherry, IHH, and alkaline phosphatase by fibrocartilage cells at the base of the collagen fibers of the enthesis (Fig. 1). All of these measures from four rounds of staining/imaging were colocalized to the same cells on the same section using this method. Joint Destabilization [3]. Unmineralized fibrochondrocytes adjacent to the original tidemark (demeclocycline) displayed increased Col1a1-CFP and Col10a1-mcherry with a strong calcein label, indicating active mineral deposition. These cells were also AP⁺ and a subset was TRAP⁺. There was continued mineral apposition at 4 weeks, demonstrated by the alizarin complexone label that was advanced from the prior calcein label. All of these measures were colocalized to the same cells on the same section using this method.

DISCUSSION Using the cryotape sectioning in combination with multiple rounds of high-throughput staining and imaging, several response measures were acquired in high-quality sections of mineralized joint tissues. Not only does this method produce high quality sections and images, but the entire process from initial fixation through several rounds of imaging can be conducted in the time (<1 week) it takes to decalcify a specimen prior to paraffin embedding.

ACKNOWLEDGEMENTS NIH T90-DE021989, R01-AR54713, R01-AR052374, and K99-AR067283.

REFERENCES 1. Kawamoto et al Arch Histol Cytol, 2003; 2. Dymant et al, Osteoarthr Cartil, 2015; 3. Dymant et al, Dev Biol, 2015.

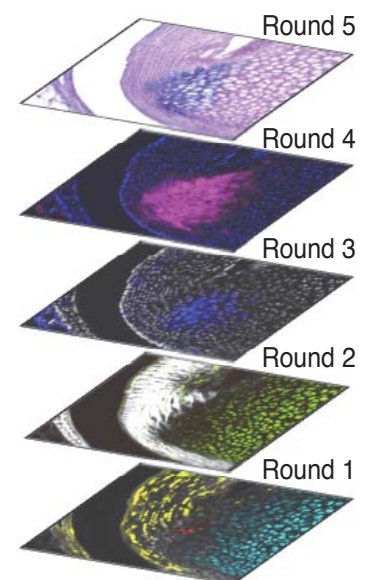


Figure 1. Imaging rounds. Round 1: endogenous fluorescent signals, Round 2: collagen SHG, Round 3: anti-IHH immunostaining, Round 4: enzyme activity, and Round 5: toluidine blue.

DYSFUNCTION OF CFTR IMPAIRS TENDON DIFFERENTIATION THROUGH ACTIVATION OF pERK1/2 IN MICE

LIU Yang, XU Liangliang, WU Tianyi, SUN Yuxin, JIANG Xiaohua, CHAN Kaiming, CHAN Hsiaochang, ZHANG Jinfang, LI Gang

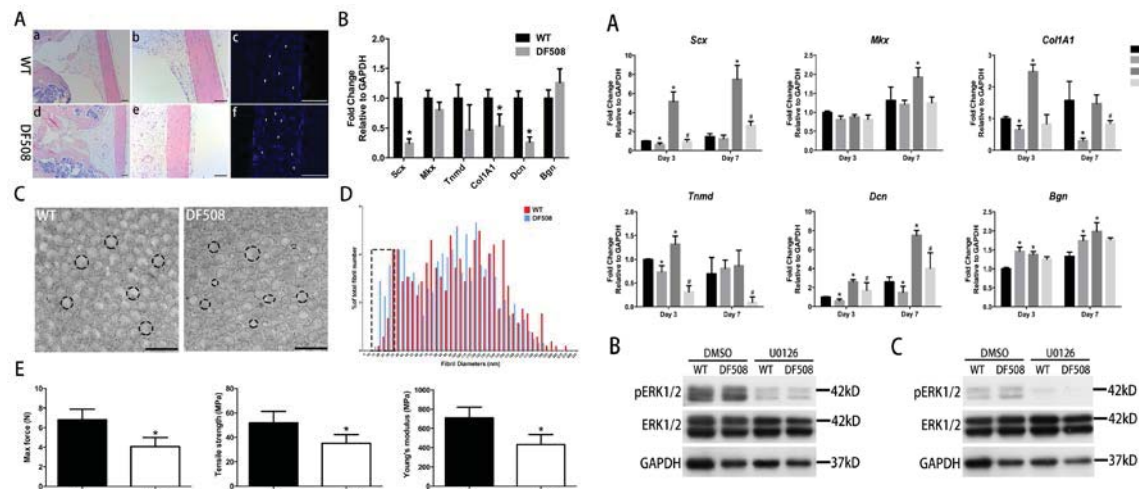
Department of Orthopaedics and Traumatology, Li Ka Shing Institute of Health Sciences, Prince of Wales Hospital, The Chinese University of Hong Kong, Shatin, Hong Kong, SAR, PR China. (gangli@cuhk.edu.hk)

INTRODUCTION

The repair of tendon injuries remains a big challenge due to less of specific transcription factor and limited understanding of tendon biology. The Cystic fibrosis transmembrane conductance regulator (CFTR), which is found in multiple tissues and involved in transport of chloride ions across cell membrane, can also be a stretch-mediated activation channel. Patients with dysfunction of CFTR can cause the disease of cystic fibrosis (CF). Low bone mineral density and muscle wasting can be found in the CF patients apart from the main syndrome of lung infection. In our study, we hypothesize that CFTR may play a function role on tendon differentiation due to its mechanosensitive gating properties and essential roles on musculoskeletal.

METHODS AND RESULTS

We first stretched the mouse isolated tendon derived stem cell with small magnitude for half hour. CFTR expression was increased after stretch, together with the high expression of tendon and extracellular matrix markers of Mohawk (Mxk), Tenomodulin (Tnmd) and Dcn. We then confirmed the expression of CFTR on wild-type (WT) mouse tendon tissue and tendon derived stem cells (TDSCs). Furthermore, we found tendon tissues in CFTR Δ F508 mice (DF508) showed irregular cell arrangement, uneven fibril diameters, weaker mechanical properties and delayed tendon healing. At molecular level, tendons in DF508 mice showed significantly lower mRNA expression of Scx, Col1A1, and Dcn compared with WT. Finally, we found mTDSCs in DF508 mice showed high expression of phosphorylation ERK1/2 (pERK1/2), compared with mTDSCs in WT. Interestingly, the expression of Scx, Col1A1 and Dcn can be reversed in mTDSCs of DF508 mice with using the specific ERK1/2 inhibitor U0126. The overall data indicate that dysfunction of CFTR can impair the tendon differentiation through activation of ERK signaling pathway.



Comparison of tendon tissues in WT and DF508 mice (A) H&E staining of patellar tendon tissue in WT (a-b) and DF508 (d-e); cells in patellar tendon staining with DAPI in WT (c) and DF508 (f), scale bar=100 μ m, white arrow: orientation of cells in patellar tendon. (B) mRNA expression of tendon and ECM markers in tail tendon tissue in 10-week-old DF508 and WT mice (n=6). (C) Microstructure of tendon fibrils in 8-week-old DF508 and WT mice by TEM (scale bar=500nm). (D) Histogram of tendon fibrils in DF508 and WT (n=4). (E) Mechanical properties of Achilles tendon in 10-week-old DF508 and WT mice (n=5). The error bar represents the SD. * <math>p<0.05</math>.

mTDSCs in WT and DF508 mice treated with U0126 (A) mRNA expression of tendon and ECM markers in mTDSCs of WT and DF508 treated with U0126 (10 μ M) for 3 days and 7 days. (B-C) Western blot of lysates in mTDSCs of WT and DF508 using a polyclonal mouse anti-pERK1/2, mouse anti-ERK1/2 at day 3 (B) and day 7 (C). GAPDH was regarded as internal control. The error bar represents the SD. * $p<0.05$.

DISCUSSION

Our study showed that CFTR may play a critical role in regulating the tendon development and repair. Dysfunction of CFTR can impaired the tendon differentiation both in vivo and in vitro. And inhibition of ERK MAPK can reverse the expression of Scx, Col1A1 and Dcn in mTDSCs of DF508 mice, as well as promoting tendon healing in DF508 mice in vivo. Inhibition of ERK MAPK can be a potential therapeutic target for promoting tendon injuries healing.

PROCOLLAGEN BIOMARKERS OF HEALING IN MICRODIALYSATE PREDICT PATIENT-REPORTED OUTCOME AFTER ACHILLES TENDON RUPTURE

Alim MD Abdul¹, Simon Svedman¹, Gunnar Edman, P. W. Ackermann, MD, PhD^{1,2}.

¹Integrative Orthopedic Laboratory, Department of Molecular Medicine and Surgery, Karolinska Institutet, 171 76 Stockholm, Sweden, ²Department of Orthopedic Surgery, Karolinska University Hospital, 171 76 Stockholm, Sweden.

INTRODUCTION

Patients with acute Achilles tendon rupture (ATR) exhibit a variable and mostly impaired long-term functional and patient-related outcome measures (PROMS). Still, however, there is a lack of early predictive markers of long-term outcome, which could facilitate the development of improved treatment methods. The aim of this study was to assess markers of tendon callus production in relation to outcome in ATR patients.

METHOD

This was a prospective cohort study. A total of 65 patients (57 men, 8 women; mean age 41, SD \pm 7) with ATR were prospectively assessed. All were operated on using a standardized operating method and thereafter randomized to post-operative treatment using either orthosis treatment or standardized plaster cast. At 2 weeks post-operatively markers of collagen metabolism, procollagen type I (PINP) and III (PIIINP) N-Terminal propeptide, and total protein content were assessed using microdialysis on the Achilles tendon, followed by enzymatic quantification techniques. At 1 year PROMS was assessed using reliable questionnaires, ATRS; FAOS; EQ-5D and functional outcome was measured using heel-rise test.

RESULTS

The qualitative, normalized procollagen levels in the injured leg, i.e. PINP/PIIINP concentration divided by protein content, were significantly, positively correlated with PROMS, while PINP and PIIINP levels exhibited significant negative correlations with PROMS and functional outcome. Linear multiple regression corroborated that increased normalized PIIINP was associated with improved EQ-VAS of perceived health ($R=0.50$, $p=.046$) and less ATRS pain ($R=0.33$, $p=.046$). These results were substantiated by higher PIIINP resulting in less ATRS subscales strength ($R=0.55$, $p=.003$) and less ability to walk on uneven surface ($R=0.34$, $p=0.039$) as well as PINP relating to more limb tiredness ($R=0.469$, $p=0.003$).

CONCLUSION

Assessment of procollagen markers in microdialysate from the healing Achilles tendon can moderately predict patient-related outcome after ATR. These findings suggest that these markers could be used for facilitating the development of improved treatment methods for patients with ATR.

RECOVERY OF VISCOELASTIC PROPERTIES OF ACHILLES TENDON FOLLOWING RUPTURE

J.A. Zellers¹, D.H. Cortes², L. Pontiggia³, J. Fish¹ and K. Grävare Silbernagel¹

¹University of Delaware, Newark, DE

²Penn State University, State College, PA

³University of the Sciences, Philadelphia, PA

INTRODUCTION

Functional performance of the calf musculature in individuals post-Achilles tendon rupture has been found to relate to tendon length and elastic modulus (Schepull et al., 2012; Silbernagel et al., 2012). Continuous shear wave elastography (cSWE) is a non-invasive method for measuring shear modulus and viscosity and has been described for use in assessment of the Achilles tendon (Cortes et al, 2015). The purpose of this study was to observe recovery of shear modulus and viscosity in the Achilles tendon and their relationship to performance on the heel-rise test in individuals following Achilles tendon rupture.

METHODS

Six subjects (4 male, 2 female) with a history of Achilles tendon rupture (n=7 tendons) were included in this study. Viscoelastic tendon properties, including shear modulus and viscosity, were measured via cSWE. Subjects performed the heel-rise test, and total work performed on the test was used for the data analysis. Subjects were reassessed at 2 month intervals for 6 months. At the time of this abstract, three subjects have completed all timepoints. For data analysis, the average of measurements for each subject over all completed timepoints was used.

RESULTS

At the time the subjects entered the study, they were a mean(SD) age of 38.2(15.6) years and were 79.7(87.3) months (range: 2-231 months) post acute Achilles tendon rupture. Six tendons had been surgically repaired. Subjects performed a Mean(SD) of 898.8(498.4) J of work on the heel-rise test on their ruptured side. The mean (SD) Achilles tendon length (calcaneus to gastrocnemius) was 23.56(3.21) cm, shear modulus was 93.17(10.98) kPa and viscosity was 35.89(11.57) Pa*s for all ruptured tendons. Comparison to the non-rupture side was limited due to one subject having bilateral ruptures and a second subject having calf muscle impairment on the non-rupture side.

Shear modulus (Fig. 1) was significantly related to time from injury based on a second-order model ($p=0.0266$), with a R^2 value of 0.837. Viscosity was not significantly related to time from injury based on a second-order model ($p=0.4334$), with a R^2 value of 0.342. Total work on the heel-rise test was not significantly related to time from injury, shear modulus, or viscosity.

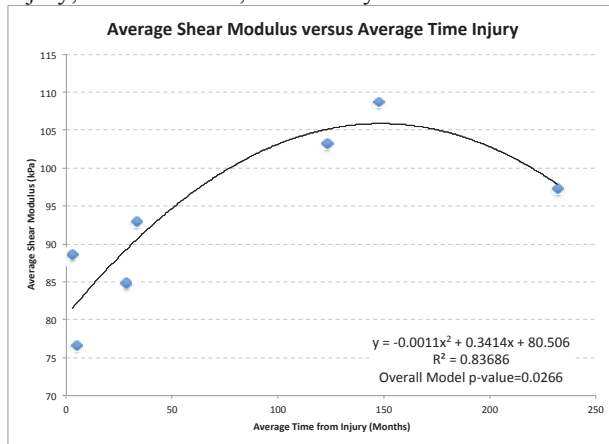


Figure 1: Average shear modulus (kPa) versus average time from injury in months for ruptured Achilles tendons.

DISCUSSION

Achilles tendon shear modulus measured by cSWE was found to improve significantly with time post-injury. Elastic modulus has been reported to relate to heel-rise test performance, however, shear modulus and viscosity were not found to be related to total work on the heel-rise test in the current study. This is likely due to significant methodological differences, including differences in length of time post-injury. These properties may be more strongly related to heel-rise performance in individuals under two years post-injury and should be the focus of future studies. This study is limited by small sample size, but provides preliminary support for the use of cSWE as a biomarker of tendon health in individuals with post-Achilles tendon rupture.

REFERENCES

- Cortes et al., *Ultrasound Med and Biol*, 2015.
- Schepull et al., *Scand J Med and Sci in Sports*, 2012.
- Silbernagel et al., *AJSM*, 2012.

COMPARISON OF THE CELLULAR COMPOSITION AND CYTOKINE-RELEASE KINETICS OF VARIOUS PLATELET-RICH PLASMA (PRP) PREPARATIONS

Joo Han Oh and Young Hak Roh*
Department of Orthopaedic Surgery

Seoul National University Bundang Hospital, *Gil Medical Center, Gachon University School of Medicine, Korea

INTRODUCTION

Variations in formulations used to prepare platelet-rich plasmas (PRPs) result in differences in the cellular composition and bio-molecular characteristics. The purpose of this study was to evaluate the cellular composition and the cytokine-release kinetics of PRP according to differences in the preparation protocols.

METHODS

Five preparation procedures were performed for 14 healthy subjects including two manual procedures [single-spin (SS) at 900 g for 5 min; double-spin (DS) at 900 g for 5 min and then 1500 g for 15 min] and three methods with commercial kits (Arthrex ACP[®], Biomet GPS[®], and Prodizen Prosys[®]). After evaluation of cellular composition, each preparation was divided into four aliquots and was incubated for 1 h, 24 h, 72 h, and 7 days for the assessments of cytokine release over time. The cytokine-release kinetics were evaluated by assessing platelet-derived growth factor (PDGF), transforming growth factor (TGF), vascular endothelial growth factor (VEGF), fibroblast growth factor (FGF), interleukin-1 (IL-1), and matrix metalloproteinase-9 (MMP-9) concentrations of each aliquot with bead-based sandwich immunoassay.

RESULTS

The DS PRP had a higher concentration of platelets and leukocytes than the SS PRP. Every PRP preparations exhibited an increase in PDGF, TGF, VEGF, and FGF release when compared to whole-blood samples. The FGF and the TGF release occurred quickly and decreased over time, while PDGF and VEGF release was constant and was sustained over 7 days. The PDGF and VEGF concentrations were higher in the DS PRP than in the SS PRP, whereas the TGF and FGF concentrations were higher in the SS PRP than in the DS PRP. Biomet GPS[®] had the highest VEGF and MMP-9 concentrations but the lowest TGF concentration. Arthrex ACP[®] had the highest FGF concentration but the lowest PDGF concentration. Prodizen Prosys[®] had the highest IL-1 concentration and higher PDGF concentration than Arthrex ACP[®].

DISCUSSION

The double spin method generally led to a higher concentration of platelet relative to the SS method. However, the cytokine content was not necessarily proportional to the cellular composition of the PRPs since a greater content could be different between the SS or DS method depending on the type of cytokine. Physician should select proper PRP preparations considering their bio-molecular characteristics and patient indications.

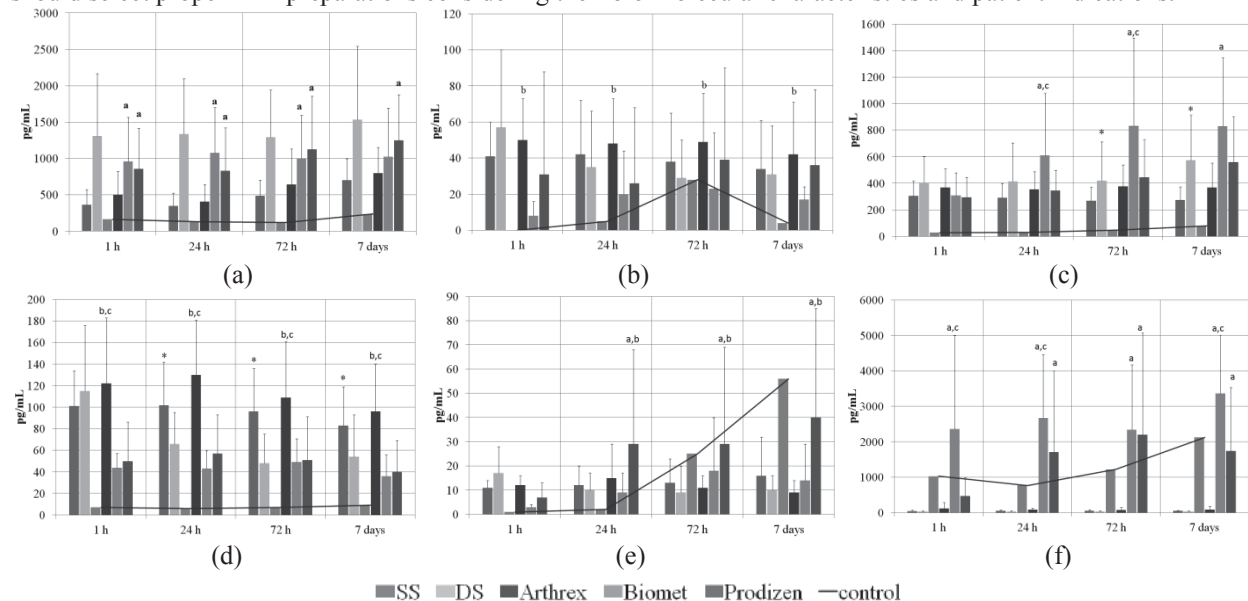


Figure 1. Cytokine-release kinetics of various PRP preparations. (a) PDGF, (b) TGF-b, (c) VEGF, (d) FGF, (e) IL-1, (f) MMP-9.

HEAT SHOCK INDUCES THE EXPRESSION OF PRO-INFLAMMATORY CYTOKINES IN HUMAN TENOCYTES

D'Addona A.¹, Somma D.², Formisano S.², Rosa D.¹, Maffulli N.³

(1) Department of Public Health, Section of Orthopaedics and Trauma Surgery, Federico II University of Naples, Naples, Italy

(2) Department of Molecular Biology and Medical Biotechnology, Federico II University of Naples, Naples, Italy.

(3) Department of Musculoskeletal disorders, University of Salerno, Salerno, Italy.

INTRODUCTION

The aetiology of tendinopathy remains unclear, and many causes have been hypothesised. Several models have recently implicated pro-inflammatory cytokines, especially in the earlier phases of the process. Without initial inflammation, the healing process can not take place. The purpose of the study is to evaluate the molecular mechanisms and the behaviour that characterise human tenocytes during stress condition.

METHODS

Tendinopathic and healthy tendon samples were harvested from patients who underwent surgery to treat chronic tendon disorders. Tendon samples were digested with Collagenase type I solution and cultured for 24-48 hours. A heat shock was performed at the temperature of 42 °C for 1 hour. Total mRNA was extracted and retrotranscribed into cDNA. The target genes were analysed using a quantitative Real Time PCR.

RESULTS

IL-1 β and IL-6 expression were significantly increased in tendinopathic samples after heat shock compared with not stimulated healthy samples ($p < 0.01$), with a peak at 4 hours post-heating (Fig. 1a-1b). IL-10 was increased in tendinopathic samples at 4 hours post-heating and in healthy samples after 20 hours post-heating ($p < 0.01$) (Fig. 1c). COL-I and COL-III expression were increased in tendinopathic not stimulated cells but their levels significantly decreased after heat shock ($p < 0.01$). COL-III levels increased in healthy samples after 20 hours post-heating ($p < 0.01$) (Fig. 2a-2b).

DISCUSSION

Tendinopathic tendon samples showed high levels of cytokines such as IL-1 β , IL-6 and IL-10, indicating that inflammation plays a role in tendon damage. COL-I and COL-III are increased in not stimulated tendinopathic tenocytes, as an attempt to repair themselves. Their levels decreased after heat shock as a sign of the failure of repair mechanisms in tendinopathic tendons. COL-III levels are increased in healthy samples after 20 hours post-heating showing an early attempt to induce healing after a stress condition. Heat shock in *in vitro* models is insufficient to trigger pro-inflammatory cytokines in healthy human tenocytes and further studies with combined stressors are required.

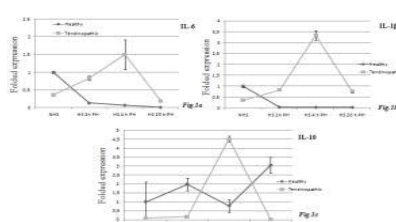


Fig.1

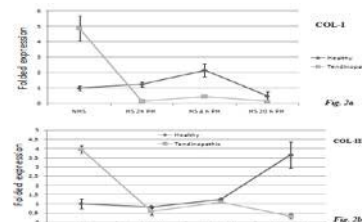


Fig. 2

Fig. 1. IL-1 β and IL-6 levels were increased in tendinopathic samples after heat shock compared to healthy samples, reaching a peak at 4 hours post-heating ($p < 0.01$). IL-10 levels showed a peak at 4 hours after heat shock in tendinopathic samples too ($p < 0.01$), while their levels are increased in shocked healthy sample at 20 hours post-heating compared to the healthy not shocked sample ($p < 0.05$).

Fig. 2. COL-III levels were increased in the healthy sample after 20 hours post-heating compared to tendinopathic ($p < 0.01$). COL-I and COL-III levels were increased in not stimulated tendinopathic samples in comparison with tendinopathic samples after heat shock ($p < 0.01$). COL-I levels decreased drastically after heat shock in tendinopathic cells ($p < 0.01$).

REFERENCES

- Karousou E., Ronga M., Vigetti D., Passi A, Maffulli N. Collagens, Proteoglycans, MMP-2, MMP-9 and TIMPs in human Achilles tendon rupture. Clin Orthop 2008; 466: 1577-1582.
- Ackermann PW, Domeij-Arverud E, Leclerc P, Amoudrouz P, Nader GA. Anti-inflammatory cytokine profile in early human tendon repair. Knee Surgery Sports Traumatol Arthrosc 2013; 21: 1801-1806.
- Maffulli N, Ewen SWB, Waterston SW et al. Tenocytes from ruptured and tendinopathic Achilles tendon produce greater quantities of type III collagen than tenocytes from normal Achilles tendon: An In vitro model of human tendon healing. Am J Sports Med 2000; 28: 499
- Hui B, Sun, Yonghui Li, David T, Fung, Robert J, Majeska, Mitchell B, Schaffler, Evan L, Flatow. Coordinate Regulation of IL-1 β and MMP-13 in Rat Tendons Following Subrupture Fatigue Damage. Clin Orthop (2008) 466:1555–1561.

ADVERSE EFFECTS OF SYNOVIAL FLUID ON ENDOGENOUS TENDON CELLS – IMPLICATIONS FOR INTRASYNOVIAL TENDON REPAIR

E.R. Garvican, J. Dudhia, R.K.W. Smith

Clinical Sciences and Services, The Royal Veterinary College, Hawkshead Lane, North Mymms, Hertfordshire

INTRODUCTION

Rotator cuff disease is the third most common orthopaedic complaint in general practice. Current medical and surgical treatment modalities carry a high rate of failure. Striking similarities exist between the naturally-occurring intra-synovial tears of the human rotator cuff and the equine deep digital flexor tendon (DDFT). Surgical debridement of the tendon damage does not generate acceptable success rates with approx 60% of horses unable to return to their previous level of work. The intra-synovial location of both tendons provides different treatment challenges to that of extra-synovial tendon injury where adverse effects of synovial fluid has been implicated in these clinical failures. This study aimed to investigate these effects *in vitro* with the aim of improving outcome of intra-synovial soft tissue healing.

METHODS

Explants from equine superficial digital flexor tendon (SDFT; extra-synovial) and the DDFT from both intra-synovial compressed (C-DDFT) and extra-synovial tensile (T-DDFT) and the epitenon regions were cultured in allogeneic or autologous synovial fluid (SF) or in DMEM (control). Human hamstring explants were cultured in allogeneic SF. Explant viability was assessed by viability staining and fluorescent imaging. Freeze-thawed equine explants (no viable cells) were re-populated with mesenchymal stem cells (MSCs) or tenocytes and cultured in SF.

RESULTS

Approximately 95% of epitenon cells and 50% of tenocytes in control explants remained viable throughout 24 h of the experiment. Cells of the epitenon exposed to SF remained viable (>95% viability after 24 h). In contrast, the viability of SDFT, C-DDFT and T-DDFT explants exposed to SF dropped rapidly. Within 30 minutes, explant viability was less than 10% and after 1 h no living cells could be detected. There was no significant difference between allogeneic and autologous SF (Figure 1). MSC and tenocyte monolayers cultured in SF remained viable. When freeze-thawed explants re-populated with equine MSCs or tenocytes were cultured in SF, all cells adhered to the matrix died. Cells within human hamstring remained viable when cultured in control media (>90% viability at 6 hours post-surgery). Human hamstring explants exposed to allogeneic SF for 1 h contained no living tenocytes, however vasculature cells remained viable.

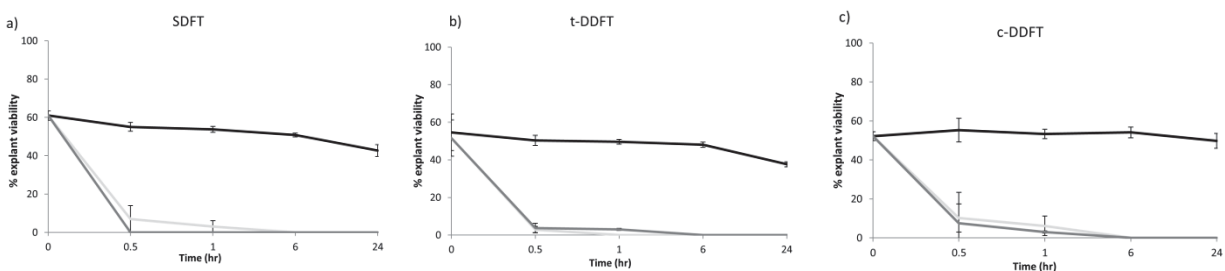


Figure 1: Viability of tenocytes in equine tendon explants (n=3). Percentage cell viability in a) SDFT; b) tensile and c) compressed (intra-synovial) regions of DDFT cultured for up to 24 h in control culture media (DMEM), autologous or allogeneic synovial fluid culture media (SF). — DMEM — autologous SF — allogeneic SF

DISCUSSION

Damage to an intra-synovial tendon, such as the human rotator cuff or the equine DDFT results in exposure of core tendon tissue to the cytotoxic effects of SF. This finding may explain the poor clinical prognosis for both the horse and human and why current treatment modalities in both species lack success. Future therapy should investigate methods by which the tendon defect can be sealed. Without a physical barrier separating synovial fluid from implanted MSCs, cell therapy is unlikely to deliver effective healing.

NOTES

NOTES

NOTES

International Symposium on Ligaments and Tendons (ISL&T-XV)

Program at a Glance

Time	Topic
7:30	Registration and Light Breakfast
8:00	Welcome Zong-Ming Li, Ph.D. and David T. Corr, Ph.D.
8:15	Clinical Keynote Lecture: <i>Innovation in Hip Arthroscopy Over the Past 10 Years</i> Marc Philippon, M.D.
8:30	Podium Session I: Biomechanics I – Healing Ligament and Tendon/In Vivo Assessment
9:50	Coffee Break/ Poster Session I (even numbers)
10:20	Podium Session II: Tendon Mechanobiology and Stem Cells
11:25	Podium Session III: Tissue Engineering in ACL Repair
12:15	Flash Presentations of Posters
12:30	Lunch (Group Photo and Poster Viewing)
13:30	Podium Session IV: Inflammation and Tendon Healing
14:15	Special Session: Translational Tendon and Ligament Research – In Honor of Professor Kai-Ming Chan
15:55	Coffee Break/ Poster Session II (odd numbers)
16:25	Podium Session V: Biomechanics II – Theoretical and Computational Modeling
17:00	Podium Session VI: Rotator Cuff Injury and Repair
17:50	Closing Remarks Savio L-Y. Woo, Ph.D., D.Sc., D. Eng. and Patrick Yung, M.D.
18:30	Banquet Dinner and Award Ceremony (Location: Ming Court Restaurant, <i>Transportation Provided</i>)